KU LEUVEN

ARENBERG DOCTORAL SCHOOL
Faculty of Engineering

Dynamic Resource Allocation and Self-Organizing Signalling Optimisation in LTE-A Downlink

Alessandro Chiumento

Supervisor:
Prof. dr. ir. Sofie Pollin
Prof. dr. ir. Liesbet Van der Perre, co-supervisor

Dissertation presented in partial fulfillment of the requirements for the degree of Doctor in Engineering

October 2015

Dynamic Resource Allocation and Self-Organizing Signalling Optimisation in LTE-A Downlink

Alessandro CHIUMENTO

Examination committee:
Prof. dr. ir. Yves Willems, chair
Prof. dr. ir. Sofie Pollin, supervisor
Prof. dr. ir. Liesbet Van der Perre, co-supervisor
Prof. dr. ir. Guy Vandenbosch
Prof. dr. ir. Emanuel Van Lil
Prof. dr. ir. Marc Moonen
Dr. ir. Wannes Meert
Prof. dr. ir. Przemek Pawelczak
(TU Delft)

Dissertation presented in partial fulfillment of the requirements for the degree of Doctor in Engineering

October 2015

Uitgegeven in eigen beheer, Alessandro Chiumento, Kasteelpark Arenberg 10 Box 2440, B-3001 Leuven (Belgium)

Acknowledgments

It is always a difficult and awkward task to determine the persons who have contributed, in minor and major ways to the completion of a work, any kind of work. The final results of one's efforts are, after all, the sum of the inputs received over the years from colleagues, friends, family and even strangers who might have provided insight in passing or, and very frequently, by pure coincidence. Most of the help and support received is also non technical and shares much more with the mental state of the author rather than with the content itself.

I will, then, attempt to find a way to describe my appreciation for all the big and little things that have played a role in bringing me, first, to the mental state in which pursuing a doctorate made even sense and, then, to actually compiling this manuscript I like to call a dissertation.

For the guidance received over the years as a student and for the effort they have put into my personal and professional development as a researcher I have to be particularly grateful to my promoters Sofie and Liesbet.

Liesbet, you have shown me how a dedication and passion can shape one's life and how to implement that drive into my daily life. Thank you for your support over the years and the much appreciated honesty.
Sofie, you have inspired me with both your relentless drive to find challenging and innovative solutions to problems we didn't know we had and for the constant research of a bottom line in the chaotic avenue of our research field. You have been of great support and understanding over the years and, for this especially, I'll always be grateful. I am looking forward to a long collaboration between us. But support and inspiration, although certainly fundamental, don't get you very far without a structured view of the problems at hand and a good step-by-step approach in handling them. It is the time to acknowledge the most structured person I know. Claude, over the years, your friendship, honesty, helpfulness and awe inspiring mechanistic approach to every facet of the human condition

have been quite some help and food for thought, so thanks for the company, the guidance and the fact that your help can be counted upon like the greenness of your lunch box.

For the amusing and challenging times in imec I have to be thankful to the green radio group in all its name changes and its friendly inhabitants. To all, thanks for the ride and good luck. Even though the imec environment has been hospitable, a few friends played a bigger role in enjoying the shared experience. Special mention goes then to Yann, Ubaid, Chunshu for the fun office times and Andre, Wim, Carolina, Olalla for the nice discussions and lunch breaks. To Mathias, Prashant and Roelof, where some bond, build from the office connection, became friendship: it is not often, not just lucky and extremely appreciated: thank you.

An appreciation goes to the new group of rascals at the Networked Systems Group in ESAT, who have welcomed me and been as helpful as they could.

Many people have contributed in making my stay in Leuven enjoyable and interesting. Definitely a big reason for my deciding to stay here was due to the international community and their meeting point Pangaea, which has allowed me to build solid and lasting friendships with so many. Particularly, a single group has played a major role over the years, because of shared interests, compatible personalities, challenging view points and, not in the least, a common ground with good food and cookery. For the good times spent together and the better ones to share in the future, thank you Tim, John, Maike, Sam, Sol and Lynn.

Un ringraziamento è sicuramente dovuto alla mia famiglia. Nonstante la lontananza da molti anni, mi sento comunque vicino e sono consapevole del fatto che per qualsiasi problema o preoccupazione io possa rivolgermi a voi senza problemi. È un pensiero confortante e non da poco sapere di essere amati e pensati ed è impossibile ricambiare pienamente. Quindi grazie Mamma, Papà e Marco.

At last Anna, the love of my life. It is so very fortunate to be loved and understood in life and so difficult to express that few people have successfully managed to put their emotions in words without sounding trite. I do not have the gift of poetry and I will say only this: this dissertation would not have been possible without you, simply because I would not be the person I am now had I not married you. Sharing my life with you has shown to be the most satisfying undertaking I could have ever chosen and I wait with excited trepidation the times to come with you and our little one.

Abstract

Modern cellular networks present many interesting challenges to the telecommunication engineers of today. The idea of a static configuration with clearly defined borders of older networks is no longer representative of the current situations, and most certainly, will not be for the next generations of communication technologies. Future mobile networks will involve a high number of base stations with various capabilities and make use of a plethora of communication technologies and access media; they will be able to recognize the dynamically shifting network conditions and requirements. The first real step towards an ubiquitous, high performance network, is represented by the 3GPP LTE technology, now widespread as 4G in many countries. The successive iterations of such technology, such as LTE-A, have permitted (and will bring) an additional increase in performance by increasing the network density and allowing self-organisation and self-healing.
The two main challenges addressed in this work, for the modern and future network, are represented by, firstly,the interference management and self-organisation of heterogeneous networks and, secondly, the minimisation of all the signalling control information necessary for the correct functioning of the network.

First, a **heterogeneous LTE-A downlink** network is analysed. The various components of the downlink network are discussed and the effects of resource allocation within each cell are analysed. Novel proposed scheduling methods show that there is still improvement possible compared to the state of the art and, by taking into consideration the practical limitations of a real network, additional gains can be achieved.

Second, a low-complexity, distributed and cooperative interference mitigation method, which is aware of network load and propagation conditions, is conceived and discussed. The proposed method is fully scalable and addresses the interference received by the different layers composing the network separately.

Finally, the impact that the **channel state information** has on the network's performance is studied. The channel state information of the users' channels is necessary in order for the base station to assign frequency resources. On the other hand, this feedback information comes at a cost of uplink bandwidth which is traditionally not considered. The impact that reduced user feedback information has on an LTE network, in time and frequency is studied. A model which considers the trade-off between downlink performance and uplink overhead is presented and novel feedback allocation strategies, which follow the same structure as the ones in the LTE standard, are presented in order to improve the overall performance. Intelligent **machine learning solutions** are proposed to adapt the base station feedback choice based on the users conditions and requirements. This way, the network can choose how much information it requires from its users, in both the time and the frequency domains, to minimise the control information overhead.

Beknopte samenvatting

Hedendaagse cellulaire netwerken bieden een groot aantal interessante uitdagingen voor telecommunicatie ingenieurs. Het paradigma van statische configuraties met duidelijk afgebakende cellen is niet langer bruikbaar bij het ontwerpen en optimaliseren van deze netwerken. Toekomstige mobiele netwerken voor breedbandcommunicatie zullen bestaan uit een groot aantal basisstations, met verschillende eigenschappen die bovendien gebruik maken van een brede waaier aan mogelijke communicatietechnologieën. Deze basisstations zullen echter ook in staat zijn om de dynamisch veranderende toestand van het netwerk te herkennen. De eerste stap naar een alomtegenwoordig netwerk met hoge bandbreedte wordt gekenmerkt door de 3GPP LTE technologie, nu in veel landen gekend onder de 4G vlag. De opeenvolgende iteraties van deze technologie, zoals LTE-A, maken een nog grotere verbetering van de bandbreedte mogelijk, door de densiteit van de basisstations verder op te drijven en deze basisstations steeds meer uit te rusten met algoritmes voor zelf-optimalisatie van het dichte netwerk.
The twee belangrijkste uitdagingen die aan bod komen in dit doctoraatswerk, relevant voor hedendaagse en toekomstige cellulaire netwerken, zijn eerst het beheersen van de interferentie tussen de vele heterogene basisstations door ze hun configuratie te laten zelf-optimaliseren. Ten tweede bekijken we hoe de controle informatie die uitgewisseld wordt tussen de verschillende gebruikers van het zelf-optimaliserende netwerk kan geminimaliseerd worden.

Eerst analyseren we een LTE-A netwerk in de downlink. De verschillende componenten in de downlink worden besproken en het effect van transmissieconfiguraties binnen elke cel geanalyseerd. Nieuwe methodes om deze configuraties te bepalen voor de verschillende gebruikers worden voorgesteld, die aantonen dat het mogelijk is om de bestaande technieken te verbeteren. Door praktische beperkingen van een echt netwerk in rekening te brengen kan onze oplossing zelfs nog bijkomende winsten halen.

Ten tweede wordt een gedistribueerde methode om interferentie te minimiseren

voorgesteld, die bewust is van propagatiecondities en netwerkbelasting. De voorgestelde methode is volledig schaalbaar en behandelt de interferentie veroorzaakt door de verschillende heterogene cellen in het netwerk apart.

Ten slotte wordt de impact die de kanaalstaatinformatie heeft op de netwerkprestatie bestudeerd. Het basisstation heeft de kanaalstaatinformatie van de verschillende gebruikers nodig om de transmissieconfiguraties op de verschillende frequentiebanden te bepalen. Het versturen van deze kanaalstaatinformatie kost echter belangrijke bandbreedte in de uplink. In dit werk wordt de impact van het beperken van de feedbackinformatie bekeken. A model dat de afweging tussen downlink prestatie en uplink overhead wordt voorgesteld en nieuwe optimalisatiestrategieën voor het optimaliseren van deze feedback in functie van netwerk parameters worden voorgesteld. Deze strategieën zijn gebaseerd op technieken uit het domain van de machine learning, die een model van de situatie leren en op basis daarvan de feedback informatie optimaliseren.

List of Acronyms

3GPP	3rd Generation Partnership Project
AFE	Analog Front-end
AGRAC	Automatic Gain and Resource Activity Controller
AMC	Advanced Modulation and Coding
BC	Best CQI scheduler
BLER	Block Error Rate
BPU	Baseband Processing Unit
CA	Carrier Aggregation
CQI	Channel Quality Indicator
CSI	Channel State Information
DCO	DC Offset
DFE	Digital Front-end
DIFFS	Digital Front-end For Sensing and Synchronization
E-UTRAN	Evolved - Universal Terrestrial Universal Radio Access Network
EESM	Effective Exponential Signal-to-noise-ratio Mapping
eNode-B or eNB	Evolved Node B
EPC	Evolved Packet Core
FB	CSI Feedback
FDD	Frequency Division Duplex
FFR	Fractional Frequency Reuse
GP	Gaussian Process
GPR	Gaussian Process Regression
HA	Hungarian Algorithm
HetNet	Heterogeneous Network
ICI	Inter-Cell Interference
ICIC	Inter-Cell Interference Coordination
IHA	Iterative Hungarian Algorithm
IHS	Iterative Hungarian Scheduler
LTE	Long Term Evolution
LTE-A	LTE- Advanced

M2M	Machine to machine
MAC	Medium Access Control
MCS	Modulation and Coding Scheme
MIMO	Multiple Input Multiple Output
MM	Max-Min scheduler
MPD	Markov Decision Process
OFDM	Orthogonal Frequency Division Multiplexing
OFDMA	Orthogonal Frequency Division Multiple Access
OSI	Open Systems Interconnection model
P-SCH	Primary Synchronization Channel
PD	Probability of Detection
PF	Proportional Fair scheduler
PFA	Probability of False Alarm
PFR	Partial Frequency Reuse
PDCCH	Primary Downlink Control Channel
PDSCH	Primary Downlink Shared Channel
PHY	Physical layer
QAM	Quadrature Amplitude Modulation
QL	Q-learning
QPSK	Quadrature Phase- Shift Key modulation
RB	Resource Block
RE	Resource Element
RF	Resource Fair scheduler
RL	Reinforcement Learning
RMSE	Root Mean Square Error
RNC	Radio Network Controller
RR	Round Robin scheduler
RRM	Radio Resource Management
SC-FDMA	Single Carrier Frequency Division Multiple Access
SFR	Soft Frequency Reuse
SINR	Signal to Interference and Noise Ratio
TB	Transport Block
TDD	Time Division Multiplexing
UE	User Equipment

List of Symbols

This section contains the symbol lists for all the equations used in this work. Because some symbols repeat, with different meaning, from chapter to chapter, 4 different lists have been included. Each list is relative to a different chapter.

γ	SINR
P	Transmit Power
G	Channel Gain
N	Noise
N_{RB}^{DL}	Resource Blocks in Downlink Bandwidth
k	subband size
P_{FB}	Bits of information for subbands positions
x	User connected to base station
$r_{i,k}$	Downlink throughput for user x_i on RB k
R_i	Average throughput for user x_i
F	Jain's fairness index
y_{eff}	Effective SINR computed via EESM

Symbol list for Chapter 2

C	Macro base stations in considered LTE-A downlink network
S	Sectors per macro base station
M	Total number of macro sectors in considered LTE-A downlink network
P	Pico base stations in considered LTE-A downlink network
F	Femto base stations in considered LTE-A downlink network
X_m	Users served by each macro sector
X_p	Users served by each pico sector
X_f	Users served by each femto sector
$r_{x_i,k}$	Downlink throughput for user x_i on RB k
P_k	Transmit power on RB k
P_{max}	Maximum transmit power
$a_{x_i,k}$	binary control variable to determine assignment of RB k to user x_i
$\boldsymbol{y}^1_{x_i}$	SINR vector of user x_i on all RBs with interference present
$\boldsymbol{y}^2_{x_i}$	SINR vector of user x_i on all RBs with interference removed
$\boldsymbol{r}^1_{x_i}$	Datarate vector of user x_i on all RBs with SINR $\boldsymbol{y}^1_{x_i}$
$\boldsymbol{r}^2_{x_i}$	Datarate vector of user x_i on all RBs with SINR $\boldsymbol{y}^2_{x_i}$
d_{x_i}	Throughput demand for user x_i
$\boldsymbol{u}^1_{x_i}$	Utility vector of user x_i on all RBs with rate $\boldsymbol{r}^1_{x_i}$
$\boldsymbol{u}^2_{x_i}$	Utility vector of user x_i on all RBs with rate $\boldsymbol{r}^2_{x_i}$
$\boldsymbol{U}^1$	Utility matrix for all the users in a cell built from $\boldsymbol{u}^1_{x_i}$
$\boldsymbol{U}^2$	Utility matrix for all the users in a cell built from $\boldsymbol{u}^2_{x_i}$
$\boldsymbol{R}$	Restriction list
th_{x_i}	Datarate threshold for user x_i
$\hat{k}_h$	Set of RBs assigned by IHA at each iteration h
$\boldsymbol{Z}$	Cluster Utility matrix
$\boldsymbol{A}$	Base station final assignment matrix
$\gamma^{dif}_{s,k}$	Difference between interfered and not-interfered SINR on RB k in sector s

Symbol list for Chapter 3

N_u	Number of served users in a cell
q	Number of subbands in higher layer selected feedback method
M	Number of subbands in in Best-M feedback method
S	Total modulation symbol rate in uplink and downlink
N_{RB}^{DL}	Resource Blocks in Downlink Bandwidth
S_{dl}	Downlink modulation symbol rate
S_{ul}	Uplink modulation symbol rate
S_{fb}	Symbol rate due to feedback
T_{tot}	Total uplink and downlink throughput
T_{dl}	Downlink throughput
T_{ul}	Uplink throughput
$T_{ul,data}$	Uplink throughput associated with payload data
$T_{ul,fb}$	Uplink throughput associated with control information
γ_{dl}	Downlink transmission efficiency coefficient
γ_{ul}	Uplink transmission efficiency coefficient
γ_{fb}	Transmission efficiency coefficient for the control information
T_p	Payload throughput
$\boldsymbol{S}$	Possible states for QL solution
$s^i(t)$	i-th state of the system at time t
$\boldsymbol{A}$	Set of actions possible to QL agent
$a(t)$	Action chosen by the QL agent at time t
$\boldsymbol{R}$	Reward function
$r(t+1)$	Reward given by QL agent for having performed and action at time t
$P_{\boldsymbol{S}(t),\boldsymbol{S}(t+1)}(a)$	State transition function given action a has been chosen
$\pi^*_{\boldsymbol{S}}$	Optimal policy for QL agent
$\boldsymbol{V}^*_{\boldsymbol{S(t)}}$	Sum of discounted rewards
$\gamma(t)$	Discount factor for QL agent
q^{π^*}	Action-value function obtained with optimal policy
β	Learning factor for QL agent
CQI_{avg}	Average CQI between all the served users
N_{UE}	Number of served users
S_{CQI}	Number of CQI values available for the CQI state CQI_{avg}
$\boldsymbol{I}$	Impact Matrix
$\boldsymbol{QT}$	Q-Table
CQI^u_{rel}	Difference between the CQI of user u and the average cell CQI CQI_{avg}
$Q_{channel}$	Quality indicator for presence of users of specific categories
T_Q	Throughput associated with each user category Q
N_{U_Q}	Numbers of users belonging to category Q
RR_Q	Normalised rate for each category Q

Symbol list for Chapter 4

D	Input-output dataset
x_i	i-th input sample
y_i	i-th output sample
$f(\boldsymbol{f})$	Dynamic function of the input states
n	Zero mean Gaussian noise
σ^2	Variance of noise n
$m(\boldsymbol{x})$	Mean function of the GP
$k(\boldsymbol{x}, \tilde{\boldsymbol{x}})$	Covariance function of the GP
$\boldsymbol{x}$ or $\boldsymbol{X}$	Input vector
$\boldsymbol{Y}$	Output vector
x^*	Future input point
$\hat{y}$	Future estimate relative to point x^*
$K(\boldsymbol{X}, \boldsymbol{X})$	Covariance matrix of the input samples
$K(\boldsymbol{X}, x_*)$	Covariance matrix of the overall input dataset
$k(x_*, x_*)$	Autocorrelation of the future data point
$m(\hat{\boldsymbol{Y}})$	Estimate for the GP given the future estimate $\hat{y}$
$Var(\hat{\boldsymbol{Y}})$	Variance of the estimated model
θ	Set of the covariance function's hyperparameters
v	Smoothness hyperparameter
t_{samp}	Time sampling window for the CSI information
t_{wu}	Prediction window for user u
$\boldsymbol{cqi_{samp}}$	Vector of the previously sampled CQI values
$\boldsymbol{cqi_{hist}}$	Vector containing the history of the CQI values
$\boldsymbol{cqi_{pred}}$	Vector of the predicted CQI values
$h(\cdot)$	Dynamic function modelling the system's behaviour
$h(\cdot)$ given the past $c(t)$	Control function
$r(t)$	Reference signal
$\mu(t)$	Best control strategy
$\mathfrak{I}$	Shannon information
w_a	Exploitation weight
w_e	Exploration weight
$\hat{L_u}$	Predicted packet loss due to poor CSI estimation

Symbol list for Chapter 5

Contents

List of Figures

List of Tables

To my families, the leaning
the standing and, most certainly
the crawling one.

Alessandro

Chapter 1

Introduction

1.1 Motivation: The Challenge of Sharing Resources

The concept of mobile device has changed considerably in recent years. The call-only cellular phone of the past has become a device able to communicate with a plethora of different standards and to perform advanced computations. This has brought the mobile networks providers to design new infrastructures able to carry the large quantity of data required by the modern user. The concept of Long Term Evolution (LTE) was first introduced in 2008 and is now the *de facto* standard for 4^{th} generation cellular network [1]. The network was designed with the idea to improve over the previous generations by increasing spectral efficiency at the physical layer and exploit multi-user and spacial diversity. These objectives have brought the realization of a network where every cell is able to use the whole frequency spectrum at a great improvement in spectral efficiency but at an enormous increase in interference. Consecutive iterations on the LTE standard (Rel10 in 2010 and Rel11 in 2012) have generated the LTE Advanced (LTE-A) project [5]. LTE-A includes the presence of heterogeneous cells in order to guarantee optimal service also in areas normally difficult to serve, such as heavily trafficked junctions or inside buildings. These heterogeneous networks are composed of base stations, with different sizes and capabilities, sharing coverage areas and frequency spectrum. These base stations have to be flexible, scalable, smart, aware of their environment and the users' requirements in order to guarantee high quality of service in variate working conditions without creating additional interference. Future communication networks will have to deal with the same set of problems, exacerbated by even higher datarate requirements and by a massive explosion of the number of served devices [6].

Novel concepts such as machine to machine communication (M2M) force a network to be aware of nearby transmissions happening within the its coverage area. Such communications may use the transmission technology of the umbrella network and have to be countered in order to minimise impact on the cellular users. As mobile devices increase in number, particular attention has to be paid to the overhead generated by the management of all these connections. The control information necessary to manage the network has to be carefully calibrated to allow many concurrent transmissions without saturating the network completely.

The radio resource management (RRM) problem, in modern and future cellular networks, consists then in finding a way to best share the available resources in order to maximise performance and to minimise the control signalling overhead. In a network composed by many cells, each serving a large number of users, it is, thus, important that each base station must be able to determine its best transmission settings in order to maximise the overall network capacity. In order to achieve this, knowledge needs to be shared between the network entities in order to minimise interference. This knowledge exchange has to be relevant and limited, so not to saturate the network with signalling information. Solutions to these problems have to also be achieved keeping in mind the practical constraints of a real-life cellular network.

1.2 Scope of this thesis

The main objective of this doctoral work is to find a good, practical solution for the radio resource management problem of a future heterogeneous network serving a massive number of mobile users. This dissertation finds solutions for the two following questions:

- Can a practical and implementable solution be found to allow an heterogeneous network to maximise overall performance by minimising overall interference?
- Can the total amount of control information necessary to allocate resources to the user be reduced without sacrificing payload performance?

Based on these two main goals, more specific issues are addressed in this work:

- How does the introduction of heterogeneous networks influence the effectiveness of interference management solutions?

- What happens if the different base stations have different capabilities and cannot communicate with one another?
- Can a base station achieve interference minimization locally when inter base station communication is unavailable?
- How much information does a user need to provide so that the network can assign resources most efficiently?
- Can the control information be reduced, in time and frequency, without loss?

The methods and results presented in this work are obtained with the usage of a system level LTE simulator purposefully modified to fit the LTE-A requirements. Specifically, the simulator chosen was designed by TUW and is thus named the VIENNA simulator. The choice of a simulation bound approach has been dictated by the limited access to actual LTE and LTE-A technologies at the beginning of this doctoral work. The simulation framework has been chosen because of its design in accordance with the LTE standard specifications and because it has already been used in a wide array of research on LTE network performance and has proven itself to be very good in modelling complex network behaviour [7–10], thus allowing for repeatability. The simulation environment also makes use of the WINNER propagation model, which has been validated in the field for various propagation scenarios in the LTE frequency range [11]. Furthermore, parts of the analysis performed in this work, such as the energy and power consumption of base stations, are obtained using the sophisticated energy model developed by imec for the EARTH project [12], designed to provide a very good representation of the power usage of an actual LTE-A base station.

It is important to notice that, even though the various aspects of the LTE-A downlink network studied in this dissertation are all simulated with the same software, the simulation parameters do vary from section to section, this is mostly due to the more computational intense nature of some simulations and to the nature of some of the problems studied, in which a more or less complex simulated environment may be necessary to determine the impact of the proposed methods. In any case, detailed tables containing the simulation parameters are included in each chapter.

1.3 Contributions

The contributions presented in this dissertation tackle three aspects of the RRM in a heterogeneous LTE-A network. The first part of the dissertation (Chapter

2) introduces the LTE and LTE-A network properties and focuses on the RRM within a cell. The second part analyses the inter-cell interference problem and finds a dynamic, distributed solution (Chapter 3), while the third part proposes methods to decrease the amount of signalling information necessary to operate the network (Chapters 4 and 5).

Specifically, the contributions are here listed and divided per chapter and related areas.

A In Chapter 2, the intra-cell resource allocation methods are presented and discussed, both in term of downlink performance and energy efficiency and the first minor contributions of this work are:

1 the performance analysis of commonly used scheduling methods, discussed in Section 2.3.1 and presented in [13].

2 the analysis of transport block limitations in LTE downlink and the proposal of a transport-block aware scheduler, discussed in Section 2.3.1 and presented in [14].

B Chapter 3 provides a solution to the RRM problem in a heterogeneous LTE-A network by utilising a low-complexity, distributed interference coordination solution. The effects of various base station properties and communication capabilities are first addressed. The proposed solution reaches excellent performance at low complexity. The conceived method makes use of combinatorial optimization techniques (i.e. the Hungarian algorithm [15]) to ultimately determine which frequency resources each cell has to restrict in order to maximise overall network performance. The proposed solution is fully distributed as it does not require a centralised network controller and takes advantage of communication capabilities between base stations, when this is possible, or makes use of local spectrum sensing techniques when it is not. Specifically the contributions in this area can be listed as:

1 A distributed, low-complexity interference management solution presented in [16].

2 The extension of the interference management method to heterogeneous networks, published as a first major journal contribution in [17].

3 A digital front-end for spectrum sensing presented as a journal publication in [18].

C Chapter 4 presents the effects of control information on the overall users' performance in the frequency domain. A solution to reduce the amount of

control information in the frequency domain, is presented. Such solution makes use of unsupervised machine learning techniques, in this case Q-Learning [19], to find an optimal amount of signalling information dynamically. The amount of control signal is adjusted based on a user's channel quality and requirements. The specific contributions of this chapter are:

1 the effects of feedback information reduction on performance presented in [20].

2 The static and multi-user solutions to the feedback allocation problem, presented as a journal publication in [21].

3 The effects of limited feedback on the interference management solution of Chapter 3, presented in [17].

D In Chapter 5, the amount of control overhead in the time domain is also addressed. The effects of reducing the users' channel information in time are analysed. In order to limit throughput loss due to the control information limitation a channel quality prediction based on Gaussian Process Regression (GPR) is presented. The same GPR framework is also used to determine an optimal channel prediction time-window in order to limit packet loss. A Dual Control with Active Learning [22] solution is used to determine such prediction window. The contributions of this chapter are outlined in the following list:

1 the Gaussian process regression method to estimate channel quality behaviour, presented in [23].

2 the Dual Control model to determine the optimal channel quality prediction window based on packet losses, published as a journal publication in [24].

Figure 1.1 shows how the different chapters (the blue rectangles) are related to one another and which chapter contains which contributions (the orange rectangles).

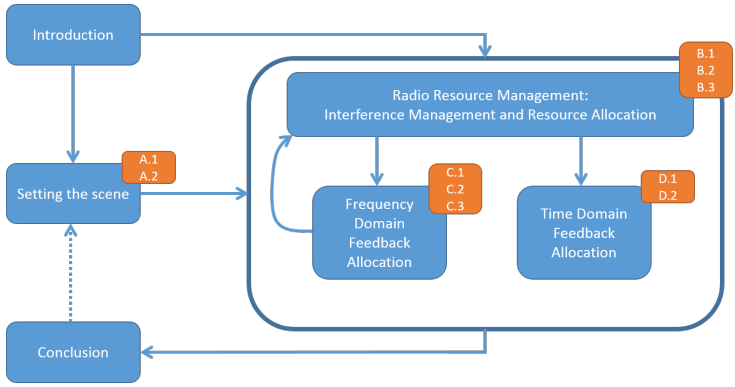

Figure 1.1: Contribution map

1.4 Structure of the following chapters

Chapter 2 presents an overview of the structure of an LTE-A network. The capabilities of the various base station types are discussed. The system model structure, from how a user reports channel quality to how a base station allocates resources is included. This chapter includes both an overview of the SoA and some additional minor contributions on the properties of resource allocation mechanisms in LTE-A.

Chapter 3 presents a low-complexity evolved distributed inter-cell interference coordination solution for an LTE-A heterogeneous downlink network.

Chapter 4 presents an analysis of the effects of frequency quantization on the users' channel quality control information. A reinforcement learning solution is presented in order to determine dynamically the optimal amount of channel information necessary for a user to be allocated efficiently. The effects of the frequency quantization techniques on the interference coordination technique introduced in Chapter 3 are finally presented.

Chapter 5 presents a solution of the quantization of channel control information in time. Firstly, the increasing time sampling intervals for channel information on the resource allocation performance is analysed. A GPR channel quality prediction technique is presented and a Dual Control solution to determine the appropriate duration of such prediction is given.

Chapter 6 concludes this doctoral dissertation. The summary of the current problems and results presented are discussed. Finally, the still open R&D challenges and the future necessary steps in order to achieve optimal RRM

solutions are examined.

1.5 Publications

Journal Papers (First Author Only)

1 Chiumento, A. and Hollevoet, L. and Pollin, S. and Naessens, F. and Dejonghe, A. and Van der Perre, L. "DIFFS: A Low Power, Multi-Mode, Multi-Standard Flexible Digital Front-End for Sensing in Future Cognitive Radios", Journal of Signal Processing Systems, Springer US, Vol. 76 (2), pp. 109-120, 2014.

2 Chiumento, A.; Desset, C.; Pollin, S.; Van der Perre, L.; Lauwereins, R., "Scalable HetNet Interference Management and the impact of limited Channel State Information", EURASIP Journal on Wireless Communications and Networking vol. 2015, no. 1, p. 74, 2015.

3 Chiumento, A.; Pollin, S.; Desset, C.; Van der Perre, L.; Lauwereins, R., "Impact of CSI Feedback Strategies on LTE Downlink and Reinforcement Learning Solutions for Optimal Allocation", accepted for publication in IEEE Transactions on Vehicular Technology, 2015.

4 Chiumento, A.; Bennis, M; Desset, C.; Van der Perre, L.; Pollin, S., "Adaptive CSI and Feedback Estimation in LTE and beyond: A Gaussian process regression approach", EURASIP Journal on Wireless Communications and Networking vol. 2015, no. 1, p. 168, 2015.

Conference Papers (First Author Only)

1 Chiumento, A.; Pollin, S.; Desset, C.; Van der Perre, L.; Lauwereins, R., "Analysis of power efficiency of schedulers in LTE," Communications and Vehicular Technology in the Benelux (SCVT), 2012 IEEE 19th Symposium on , vol., no., pp.1,4, 16-16 Nov. 2012

2 Chiumento, A.; Pollin, S.; Desset, C.; Van der Perre, L.; Lauwereins, R., "Scalable LTE interference mitigation solution for HetNet deployment," Wireless Communications and Networking Conference Workshops (WCNCW), 2014 IEEE , vol., no., pp.46,51, 6-9 April 2014

3 Chiumento, A.; Desset, C.; Polling, S.; Van der Perre, L.; Lauwereins, R., "The value of feedback for LTE resource allocation," Wireless Communications and Networking Conference (WCNC), 2014 IEEE , vol., no., pp.2073,2078, 6-9 April 2014

4 Chiumento, A.; Pollin, S.; Desset, C.; Van der Perre, L.; Lauwereins, R., "Exploiting transport-block constraints in LTE improves downlink performance," Wireless Communications and Networking Conference (WCNC), 2014 IEEE , vol., no., pp.1398,1402, 6-9 April 2014

5 Chiumento, A.; Blanch, C; Desset, C.; Pollin, S.; Van der Perre, L.; Lauwereins, R., "Multi-Objective Genetic Algorithm Downlink Resource Allocation in LTE: exploiting the Cell-edge vs. Cell-center trade-off," Communications and Vehicular Technology in the Benelux (SCVT), 2014 IEEE 21th Symposium on , vol., no., pp.X,X, 11-11 Nov. 2014

6 Chiumento, A.; Bennis, M.; Desset, C.; Bourdox, A.; Van der Perre, L.; Pollin, S., "Gaussian Process Regression for CSI and Feedback Estimation in LTE" presented in IEEE ICC 2015 - 4th IEEE International Workshop on Smart Communication Protocols and Algorithms (SCPA 2015)

Workshop abstracts and Co-Authored Papers

1 Baddour, R.; Chiumento, A.; Desset, C.; Torrea-Duran, R.; Pollin, S.; Van der Perre, L.; Lauwereins, R., "Energy-throughput simulation approach for heterogeneous LTE scenarios," Wireless Communication Systems (ISWCS), 2011 8th International Symposium on , vol., no., pp.327,331, 6-9 Nov. 2011

2 Chunshu Li; Min Li; Verhelst, M.; Bourdoux, A.; Borremans, J.; Pollin, S.; Chiumento, A.; Van der Perre, L.; Lauwereins, R., "A Generic Framework for Optimizing Digital Intensive Harmonic Rejection Receivers," Signal Processing Systems (SiPS), 2012 IEEE Workshop on , vol., no., pp.167,172, 17-19 Oct. 2012

3 Avez, P.; Van Wesemael, P.; Bourdoux, A.; Chiumento, A.; Pollin, S.; Moeyaert, V., "Tuning the Longley-Rice propagation model for improved TV white space detection," Communications and Vehicular Technology in the Benelux (SCVT), 2012 IEEE 19th Symposium on , vol., no., pp.1,6, 16-16 Nov. 2012

4 Chiumento, A., Desset, C., Pollin, S., Van der Perre, L., Lauwereins, R. (2013). "Transport block scheduling in LTE: advantages in structural limitations." 34th Symposium on Information Theory in the Benelux - WIC. Leuven Belgium, 30/05/2013 (pp. 108-115).

5 Chiumento, A., Pollin, S., Van der Perre, L., Lauwereins, R. (2013). "Towards a more granular LTE Resource ALLocation for CeLL Edge Users." 33rd Symposium on Information Theory in the Benelux - WIC. Boekelo, The Netherlands, 34-25/05/2012.

Chapter 2

Setting the Scene

The first part of the chapter describes the structure of the LTE-A network considered in this work. The RRM problem in a cellular network is then framed and split into three sections. First, the intra-cell resource allocation mechanisms normally used in LTE-A are discussed and their impact on network performance is analysed. Secondly, the interference management problem is stated and the most used solutions in literature are presented. Lastly, the signalling overhead problem is presented.

2.1 LTE Architecture

The general structure of the LTE network can be divided into three main categories as shown in Figure 2.1.

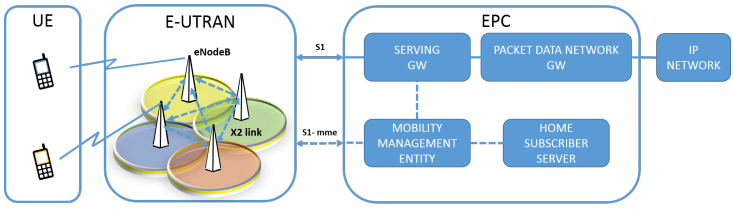

Figure 2.1: LTE network architecture

The Evolved Packet Core (EPC) is responsible for the overall control of the network and all the functions that do not related to radio access. The EPC builds the IP packet connection circuit between the mobile user and the internet and takes care of the network's mobility management. The Evolved - Universal Terrestrial Universal Radio Access Network (E-UTRAN), on the other hand, is responsible for all the radio access operations between the users and the base stations and between base stations. Figure 2.2 shows the functionalities of these blocks. The E-UTRAN takes care of the resource allocation within each cell and the inter-cell RRM; it defines the users' channel quality measurement protocols and manages the overall connections between terminals and base stations. Finally, the mobile terminal or User Equipment (UE) represents the last element of the network. The UEs are responsible to collect local information, such as their channel quality, report whether they receive the correct packets and other variables which influence the resource allocation. Since the main focus of this work falls on downlink RRM the two blocks considered here are the UE and the E-UTRAN.

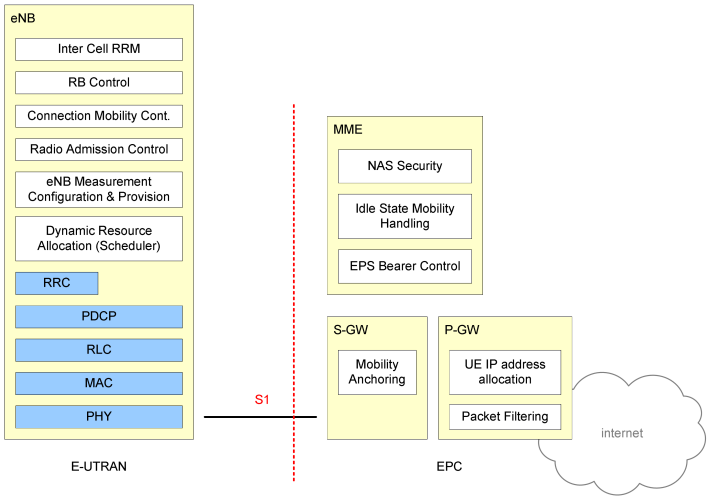

Figure 2.2: LTE EPC and E-UTRAN functionalities [1]

2.2 The E-UTRAN

The E-UTRAN is composed by the base stations responsible to send and receive transmissions to the UEs. These base stations are referred to as e-NodeBs or

eNBs. Each eNB is able to communicate with the EPC through an S1 link and can be connected with other eNBs through the X2 interface. The e-NodeB is responsible for the RRM, which includes tasks such as: the radio bearer control, the uplink and downlink resource allocation and dynamic scheduling and the mobility control [25]. There are different categories of eNBs within the LTE and LTE-A frameworks; each category of base station has different characteristics; these will be presented in section 2.2.2.

2.2.1 The Physical Layer

The LTE physical layer, or PHY, is tasked with the transportation of signals between the base stations and the mobile users, with high spectral efficiency. The two key enablers to achieve such results are the Orthogonal Frequency Division Multiplexing (OFDM) and the multiple-antenna technology (MIMO). OFDM consists in dividing the available spectrum into equally spaced, mutually orthogonal, narrow band sub-carriers. This brings the advantages, among others, of an absent inter symbol interference as each sub-carrier is orthogonal to the other ones, and simple receiver structures as each sub-carrier witnesses flat fading [26].

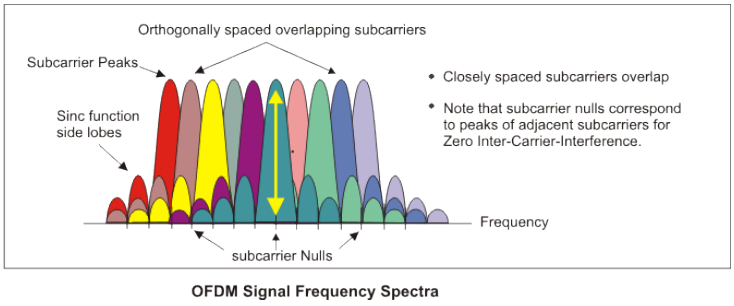

Figure 2.3: OFDM sub-carriers [2]

The LTE PHY layer makes use of OFDM in two different flavours for uplink and downlink. Orthogonal Frequency Division Multiple Access (OFDMA) is the key radio access technology for the downlink while Single Carrier Frequency Division Multiple Access (SC-FDMA) is used for the uplink.

Downlink OFDMA

OFDMA makes full use of the subdivision of the frequency bandwidth in sub-carriers given by the OFDM. These sub-carriers are then grouped into sub-channels. Furthermore, the time domain is also divided into consecutive slots, called OFDM symbols. OFDMA has then a time-frequency nature as it allows a base station to allocate specific groups of sub-channels - OFDM symbols pairs to different UEs. Figure 2.4 ventures to illustrate how OFDMA is used to split the time and frequency resources into a resource grid. Each

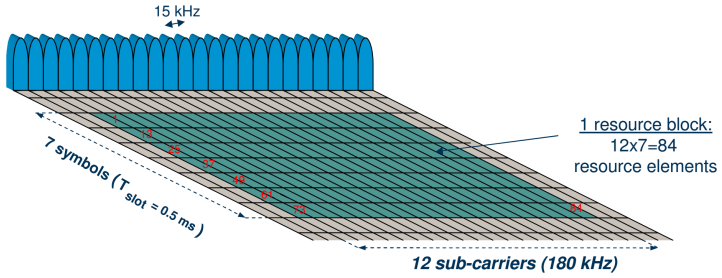

Figure 2.4: LTE downlink time-frequency resource grid

element of this grid is composed by one sub-carrier lasting for an OFDM symbol and is defined as a resource element (RE). A rectangular block of these resource elements composed by 12 adjacent sub-carriers and 7 OFDM symbols [1] is called a resource block (RB) and represents the smallest unit an e-NodeB is able to allocate to an UE. The amount of RBs depends on the bandwidth of the LTE downlink network. Table 2.1 presents the LTE physical parameters defining the number of RBs. LTE frames have duration of 10 ms and each is split into 1 ms sub-frames [27].

[1] A cyclic prefix is placed between each OFDM symbol to reduce inter-symbol interference. If a short cyclic prefix is used, then there are 7 OFDM symbols per RB, otherwise, a long cyclic prefix is employed lowering the amount of symbols to 6.

System Bandwidth MHz	1.25	2.5	5	10	15	20
Number of subcarriers	75	150	300	600	900	1200
Subcarrier spacing	15 kHz					
Subcarriers per RB	12					
FFT size	128	256	512	1024	1536	2048
Number of RBs	6	12	25	50	75	100

Table 2.1: LTE downlink parameters

LTE Frame Types

LTE allows for two modes of communication: Frequency Division Duplexing (FDD) and Time Division Duplexing (TDD). In FDD uplink and downlink transmissions happen on separate frequencies and can be carried out simultaneously. FDD is also the most used transmission method used in LTE [28].
TDD, on the other hand, uses only one carrier frequency and uplink and downlink are multiplexed in time. This brings the advantage of being able to exchange uplink for downlink bandwidths whether necessary, to limit the spectrum usage and have simpler receivers.

Adaptive Modulation and Coding

LTE supports different modulation and error coding schemes and allows the e-NodeB to select the most appropriate for each transmission to a user. This Advanced Modulation and Coding technique (AMC) increases the reliability of transmissions by adapting the transmission to the variable channel conditions witnessed by the user on each RB. For example, a robust Modulation and Coding Scheme (MCS) can be used by the e-NodeB when an UE reports poor channel conditions on a RB. Table 2.2 shows the possible modulation and coding schemes used in LTE. In order for the e-NodeB to choose a most suitable MCS, the channel quality at the receiver must be known.

MCS	SINR	CQI	modulation	code rate (x 1024)	spectral efficiency
MCS1	-6.93	1	QPSK	78	0.1523
MCS2	-5.14	2	QPSK	120	0.2344
MCS3	-3.18	3	QPSK	193	0.3770
MCS4	-1.25	4	QPSK	308	0.6016
MCS5	0.76	5	QPSK	449	0.8770
MCS6	2.69	6	QPSK	602	1.1758
MCS7	4.69	7	16QAM	378	1.4766
MCS8	6.52	8	16QAM	490	1.9141
MCS9	8.57	9	16QAM	616	2.4063
MCS10	10.36	10	64QAM	466	2.7305
MCS11	12.28	11	64QAM	567	3.3223
MCS12	14.17	12	64QAM	666	3.9023
MCS13	15.88	13	64QAM	772	4.5234
MCS14	17.81	14	64QAM	873	5.1152
MCS15	19.82	15	64QAM	948	5.5547

Table 2.2: SINR and CQI mapping to the MCSs

Channel Quality Indicators

Each UE has to measure the quality of the channel between itself and the serving base station. The universal figure of merit for such a measure is the Signal to Interference and Noise Ratio (SINR). The SINR for each RB k is given as:

$$\gamma_k = \frac{P^m_{x_i,k} G^m_{x_i,k}}{\sigma^2 + \sum_{n \neq m} P^m_{x_i,k} G^m_{x_i,k}} \tag{2.1}$$

where P^m and G^m are the transmit power and transmission gains of base station m serving user x_i on RB k while P^n and G^n are the transmit power and transmission gains of the interfering base stations n and σ^2 is the additive Gaussian noise.

The SINR measured by the mobile user is mapped onto a respective Channel Quality Indicator (CQI) value [29]. Each CQI represents the highest possible Modulation and Coding Scheme the terminal can process with a block error rate lower than 10%. This MCS defines then the instantaneous throughput the user would achieve per RB. The SINR to CQI mapping is shown in Table 2.2.

Each user then has to report this Channel State Information (CSI) containing the CQI values. Once the e-NodeB has the CQI for all the users over the whole

bandwidth, the MAC scheduler is able to allocate resources (RBs in this case) in order to maximise the cell's capacity or other figures of merit.

Channel Quality Information Reporting

The CQI values have to be reported to the e-NodeB frequently. This process is normally referred to as the CSI feedback (FB). The CQI information, although necessary for AMC, is not transmitted for every RB and every sub-frame as this would create an unsustainable overhead of control signals [30]. The FB information is then quantized in frequency, where each UE reports information only on portions of the bandwidth or for groups or RBs, and in time, where UEs report CQI values at specific time intervals larger than the LTE sub-frame.

- **Frequency domain feedback**
  The three FB reporting techniques allowed in the LTE standard are presented in [31].
  - Wideband: each user transmits a single 4-bit CQI value for all the RBs in the bandwidth.
  - Higher Layer configured or sub-band level: the bandwidth is divided into q sub-bands of k consecutive RBs and each user feeds back to the base station a 4-bit wideband CQI and a 2-bit differential CQI for each sub-band. The value of k is bandwidth dependent and is given in table 2.3, where N_{RB}^{DL} is the total number of downlink RBs in the bandwidth (table 7.2.1-2 in [31]).

System bandwidth N_{RB}^{DL}	Sub-band size (k)
6 - 7	NA
8 - 10	4
11 - 26	4
27 - 63	6
64 - 110	8

Table 2.3: Sub-band size (k) vs. System bandwidth for sub-band level feedback

  - User-selected, or $Best-M$: each user selects M preferred sub-bands of equal size k and transmits to the base station one 4-bit wideband CQI and a single 2-bit differential CQI value that reflects the channel quality over the selected M sub-bands. Additionally, the user reports

the position of the selected sub-bands using P_{FB} bits, where P_{FB}, as given in [31], is:

$$P_{FB} = \left\lceil log_2 \binom{N_{RB}^{DL}}{M} \right\rceil . \tag{2.2}$$

The value of M and the amount of RBs in each sub-band are given in table 2.4 (table 7.2.1-5 in [31]):

System bandwidth N_{RB}^{DL}	Sub-band Size (k)	M
6 - 7	NA	NA
8 - 10	2	1
11 - 26	2	3
27 - 63	3	5
64 - 110	4	6

Table 2.4: Sub-band size (k) and Number of Sub-bands (M) vs. System bandwidth for user-selected feedback

Amongst the three standard compliant feedback schemes only the sub-band level technique allows the base station to investigate the channel quality of the complete bandwidth with equal amount of detail between sub-bands.

- **Time domain feedback**
  The periodicity of CQI reporting is determined by the base station and the CQI signalling is divided into periodic and aperiodic reporting [32]. In case of aperiodic CQI signalling, the eNB specifically instructs each user on which frequency granularity to use and when the reporting has to occur. With aperiodic reporting, the eNB can make use of any of the CQI standard compliant feedback methods discussed above. Periodic CQI reporting, on the other hand, is more limited and only Wideband and User-selected feedback methods can be used. In this case, the CQI messages are transmitted to the base station with constant periodicity, e.g. in case of periodic wideband feedback in an FDD system, each user can report its CQI values every 2, 5, 10, 16, 20, 32, 40, 64, 80, 160 ms.

2.2.2 Extension of LTE to LTE-A

The introduction of LTE release 10, also known as LTE-Advanced, has brought some technological modifications in order to improve the overall capacity [33]. With the exception of carrier aggregation (CA), which is outside the scope of this dissertation, the PHY layer remains largely unchanged. Heterogeneous base stations have been introduced to the E-UTRAN to improve the overall spectral efficiency [34,35]. LTE-A includes small cells to the existing e-NodeB network to increase the network capacity and to remove indoor and outdoor coverage holes. These small cells have to operate in co-channel deployment, sharing the spectrum with the pre-existing e-NodeBs [36]. The implementation of such a multi-tiered network presents complex challenges in terms of coordination between the entities, in order to avoid interference and to maximise the downlink performance. The following sections describe the properties of the different base station types discussed in this work and present the set of advantages and challenges they impose.

Diverse Cell Categories

Three different kinds of base stations are considered in this work, they are summarized in Table 2.5.

Base Station	Transmit power	Cell radius	Communication interface
Macrocell	20W	500m - 30km	X2
Picocell	50mW - 1W	50 - 200m	X2
Femtocell	$\leq 100mW$	$\leq 20m$	None

Table 2.5: Heterogeneous cells present in LTE-A considered in this work

The PHY layer seen by each base station remains identical; they differ mainly in transmit power and how they communicate with the core network. The Macrocells are the pre-existing e-NodeBs present in the LTE network. They are positioned at fixed locations and posses the largest cell radius and highest transmit power. As seen in Figure 2.1 e-NodeBs can communicate with one another using the X2 backhaul interface. The X2 interface is a high data-rate, low latency peer-to-peer communication link that allows a base station to perform handovers and for the rapid coordination of radio resources [37]. Picocells are smaller, lower power base stations positioned, usually, in hotspots to

increase the overall coverage. These small cells, also make use of the X2 interface and can coordinate with one another [38]. Picocells are normally positioned within, or close by, the coverage area of one or more macro base stations. The final base station type, the femtocells, are the smallest cell available and are designed to use low transmission power to serve few, closely positioned users, in an indoor environment. These cells are owned by private customers and connect to the EPC via a dedicated gateway using private broadband links for backhaul; they do not posses the X2 interface and thus cannot be used for radio resource management like macro- and picocells. Furthermore, in this work the femtocells will operate in a closed subscriber group fashion, which doesn't allow macro and pico users to connect to a femto base station unless they are already part of that femtocell admissible users [39]. This is chosen as such conditions represent the worst case scenario regarding interference generated to macro and pico users. Figure 2.5 depicts the three base stations and their connections.

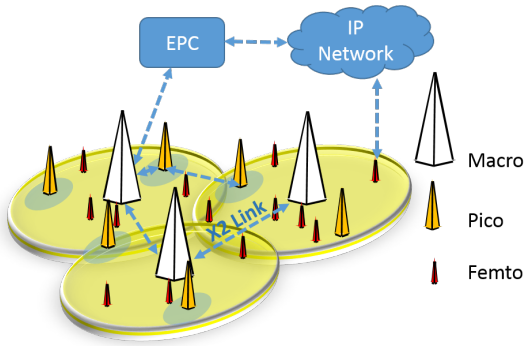

Figure 2.5: Heterogeneous network in LTE-A

Heterogeneous networks: a new layer of complexity

A multi-tiered network, where small cells work in a co-channel deployment together with underlying macrocells, presents both great advantages and challenges when compared with a single layer solution [39]. Small cells are intended to remove coverage holes and to compensate for naturally poor channel conditions, such as in indoor environments. The addition of user managed access points, i.e. femtocells, can also provide an increase in coverage without the cost of owning, positioning and managing a network operated base station. The main ordeal is the increment of inter-cell interference (ICI). As all base stations in LTE and LTE-A are designed to take advantage of a full spectrum

configuration, the amount of interference witnessed by a cell from its neighbours is a great limitation to the overall network performance [40]. Furthermore, as femtocells are not capable of communicating with a fast, dedicated link to neighbouring base stations, these cannot be taken into account for the RRM and alternative solutions have to be implemented [35, 41].

2.3 The RRM problem in the LTE-A framework

This section introduces the RRM problem in LTE-A networks and discusses the most common solutions present in literature. Radio resource management of a cellular network involves creating and maintaining a good radio connection between a base station and its mobile users (taking into account those users requirements), handling communication between cells so that the overall system's performance is maximised, being generally aware of the spectral conditions and being able to compensate for the network's loads variations. Figure 2.6 presents a view of some of the sub-problems of the RRM.

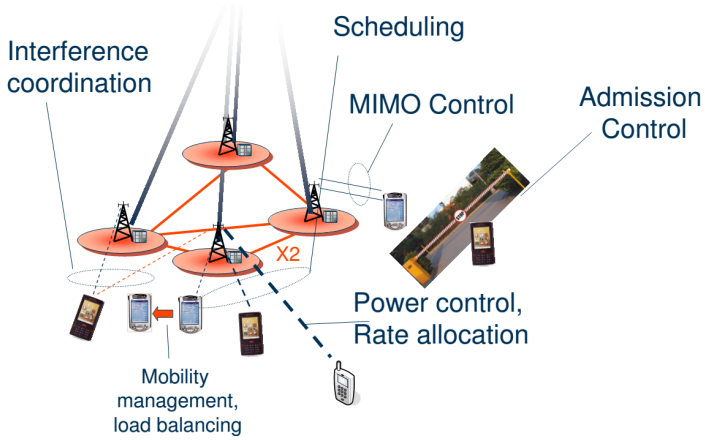

Figure 2.6: RRM: the big picture [3]

Using an OSI multi-layer convention, the RRM makes use of algorithms operating in all the layers, as shown in Figure 2.7. This work focuses on the RRM functions present in the PHY and MAC layer of the LTE radio protocol.

These algorithms, such as MAC scheduling, link adaptation and FB management are dynamic in nature, require constant monitoring and actions to be carried out frequently, usually every millisecond [27].

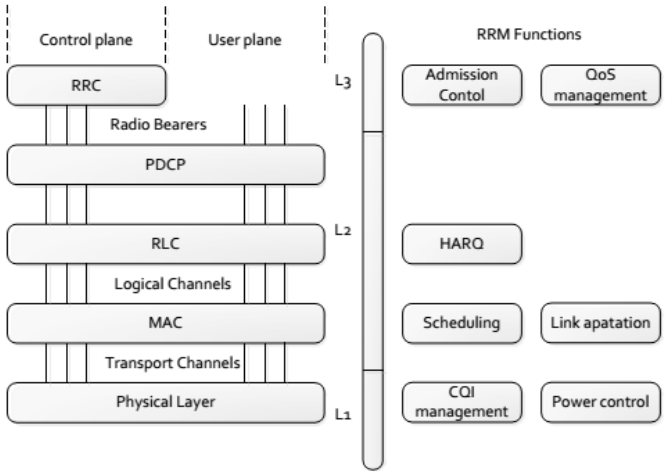

Figure 2.7: The RMM functions split by OSI layer

Generally speaking, the downlink RRM can be explained mathematically by a combinatorial optimization problem where the overall network performance is maximised with respect to some constraints.

The following section presents the MAC schedulers used in LTE and LTE-A. Their characteristics are explained and their differences analysed. Section 2.3.2 introduces the inter-cell interference problem in LTE-A and therein the most common solutions present in literature are discussed.

2.3.1 Downlink resource allocation in LTE-A cells

Once the base station registers the presence of a user, the resource allocation performed within an LTE-A cell is composed of multiple steps:

- Each UE transmits the channel quality information per RB and its requirements to the base station.
- The base station, then, converts the CQIs into the datarate each UE would witness using AMC, specifically Table 2.2.
- A scheduling algorithm allocates specific RBs to particular UEs so to maximise a particular figure of merit, which could be the cell capacity, the fairness or other QoS requirements.

There are many flavours of algorithms used to schedule downlink resources. Generally, they tend to maximise the cell's sum-rate while maintaining some fairness constraints. The next section describes the most common multi-user schedulers used in LTE-A and in the following section, the inherent energy-fairness-capacity trade-off present in these algorithms is explained.

Scheduling algorithms

In this section some of the used resource allocation mechanisms are presented.

- **Round Robin (RR)**
  The round robin scheduler assigns a RB per user and then rotates the users in its queue until all RBs are allocated. This way each user gets an equal amount of resources (excluding the remainder if the ratio between RBs and UEs is not integer). This scheduler makes no use of the UEs CQI feedback and thus it has no control on the quality of the resources assigned, making this algorithm the least preforming regarding the achievable user throughput [42].

- **Max-Min (MM)**
  The Max-Min scheduler takes into consideration all the resources available to the users and makes use of convex optimization strategies to determine a solution where no user can have an increase in datarate at the expense of another. This scheduler maximises thus the minimal rate each user can achieve [43].

- **Proportional Fair (PF)**
  This scheduler is designed to aim for high throughput while maintaining fairness amongst users. PF schedules users when they are at their peak rates relative to their own average rates, at a given time instant t, PF schedules user $x_i = \arg\max \frac{r_{i,k}(t)}{R_i(t)}$, where $r_{i,k}(t)$ is the instantaneous data rate of user x_i on RB K at time t and $R_i(t)$ is the average throughput computed, with moving window T as, $R_i(t) = \frac{1}{T}\sum_{j=t-T}^{t} r_i(j)$. [44].

- **Resource Fair (RF)**
  The main characteristic of this scheduler is to assign an equal amount of RBs to each served user. The scheduler, then, through convex optimization, determines which set of RBs grants maximum user rate [45].

- **Iterative Hungarian Scheduler (IHS)**
  This scheduler uses the Hungarian assignment method [15] in its iterative form. The Hungarian assignment method is optimal when the number

of users equals the number of RBs. In case this identity is not valid, the scheduler has to reiterate and assign one RB per user per iteration until all the RBs are exhausted. The IHS has been deemed a good sub-optimal solution that trades off some performance for reduced complexity [46].

- **Best-CQI (BC)**
  This scheduler, also called max-rate, is a greedy algorithm which allocates, on each RB, the user that presents highest channel quality. The cell throughput is maximised but the scheduler does not attempt to assign resources equally and thus the fairness between users is minimised [42].

Fairness-Capacity-Energy trade-off

The effects of scheduler choice on a base station's performance are modelled in literature. As an initial **contribution**, in this dissertation, the energy consumption, on the other hand usually ignored, is modelled and studied. A new set of simulations have been carried out to present the behaviour of a modern LTE-A base station when different resource allocation mechanisms are used and the results are included in the papers [13]. To show the difference between the schedulers, three figures of merit have been chosen: the average user rate, the fairness and the energy-per-bit. The average sum-rate is computed directly form the LTE-A downlink system level simulator. The fairness of each scheduler is expressed using Jains's fairness index [47]: $\mathrm{F} = \frac{(\sum_{m=1}^{M} R_m)^2}{M \cdot \sum_{m=1}^{M} R_m^2}$, where M is the total number of users and R_m is the datarate of user m.

The energy consumption of the base station using the different schedulers has been modelled with a reliable power consumption model. Such model takes into account the power spent in RF circuits, base band processing, power amplifiers and overheads such as cooling and dc/dc energy transformation [12].

Throughout this thesis, all the results presented are obtained via the open source VIENNA LTE downlink system level simulator [45]. This simulator has been chosen for its openness, wide distribution and support in the research community and for its compliance with the 3GPP LTE standard. The simulator has then been opportunely modified to fit the LTE-A characteristics necessary for this work, such as the implementation of small cells and feedback control mechanisms.

Simulations have been performed for varying numbers of served users in an LTE e-NodeB cell in a full buffer configuration. When operating in full buffer, the average sector throughput and fairness, presented in figure 2.8 (a) and (b) do not variate much with the number of served users, this is expected and in

accordance with [48]. The main exception is the Best CQI scheduler, which is designed to take advantage of user diversity and therefore performs better as the number of users increases. The small fluctuations present in these results are due to the diverse channel gains experienced by the different sets of users. Figure 2.8 (c) presents the power drawn by the average e-NodeB when different

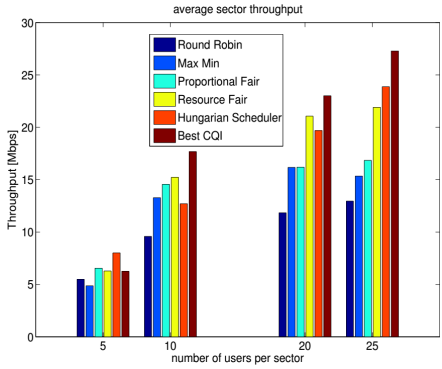

((a)) Throughput

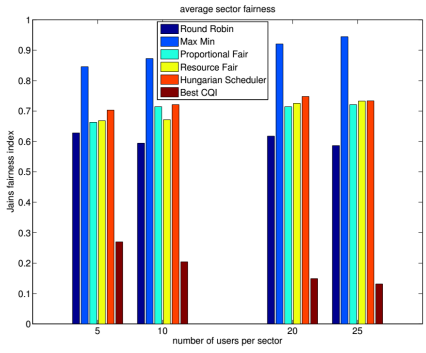

((b)) Fairness

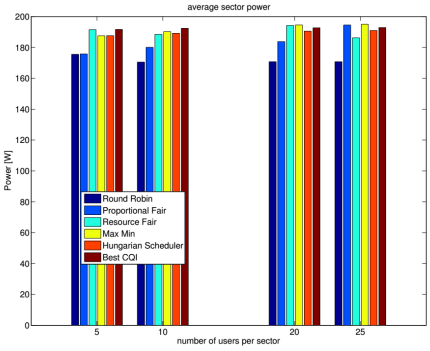

((c)) Power

Figure 2.8: Average e-NodeB throughput, fairness and power consumption in a full load scenario

schedulers are in use. The differences between resource allocation mechanisms are minimal because of the full buffer configuration. Since all the resources are used, the base station transmits on the whole bandwidth and the variations between schedules can be ascribed to different baseband processing. For a more meaningful comparison the energy-per-bit has been chosen to present the different energy efficiency of each scheduler; see figure 2.9.

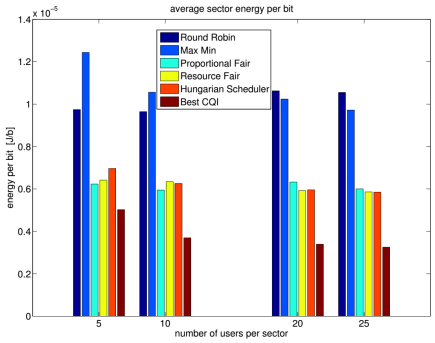

Figure 2.9: Average e-NodeB Energy per bit

To fully comprehend the trade offs between the different schedulers, when a full buffer configuration is used, it is useful to analyse the relation between the throughput each scheduler can achieve and the fairness it grants to the users. Figure 2.10 shows the behaviour of the schedulers, in terms of fairness as a function of the normalized throughput (using the round robin as basal scheduler). From figure 2.10 it is possible to extrapolate that the Best CQI

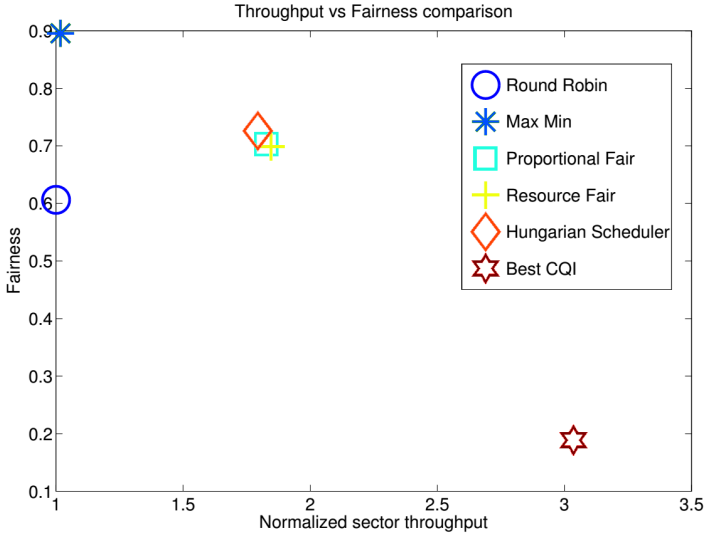

Figure 2.10: Throughput over Fairness

scheduler performs, by far, better than the other ones in terms of throughput

but severely lacks in fairness. The Max-Min is exactly the dual, achieving almost perfect fairness but at the cost of reduced data rate. The other algorithms, with an exception for the Round Robin scheduler, which is a poor outlier, perform similarly and present both increased throughput and fairness compared to the Round Robin. Since the energy-per-bit is inversely proportional to the throughput, the latter does indeed suffice as a figure of merit to gauge qualitatively the power efficiency of scheduling algorithms in full buffer.

Transport Block Awareness in Resource Allocation

Another interesting, although normally overlooked, characteristic of the LTE and LTE-A downlink PHY layer is that although in principle, AMC can be used on every RB independently, only one MCS may be used for each transmission to an UE at a given time. This means that independently of how many RBs a user is assigned only one modulation and coding scheme can be used for transmission to that user [49]. This effect can cause a reduction in overall performance if a user is allocated a group of RBs with inhomogeneous CQIs [14]. The group of allocated RBs forms a transport block (TB) and, in fact, an effective CQI quality is assigned to each TB so that the corresponding MCS can guarantee correct transmission. In LTE and LTE-A, the base station chooses the transport block's MCS by performing an Effective Exponential Signal-to-noise-ratio Mapping (EESM) [49, 50]. As a second novel **contribution**, the effects of using only one CQI value for the whole TB on the downlink performance are discussed, furthermore, a TB-aware scheduler is presented to take advantage of this structural limitation in LTE and LTE-A. The effective transport block SINR γ_{eff}, obtained with EESM, is computed with:

$$\gamma_{eff} = -\lambda \cdot \log\left(\frac{1}{length_{TB}} \sum_{k^* \in TB} exp^{\frac{k^*}{\lambda}}\right) \tag{2.3}$$

where λ is a parameter empirically calibrated by the base station as a function of the MCS and k^* represents the selection of RBs composing the TB. The throughput of each user, and the power spent by the base station, per transmission interval, then, are not the aggregate ones of the combined RBs, but they are non-linear functions of the SINRs of the assigned RBs. The lowest quality CQIs will then dominate the overall TB BLER significantly, and will drive the base station decision towards a lower AMC, reducing so the user's overall throughput. By adjusting the size of the transport block, removing or adding RBs, it is then possible to take advantage of the non-linear mapping described above and design a scheduler that can maximise the cell's rate, minimise its power or be tuned to fit the network's loads.

Algorithm 1 TB aware scheduler

Phase One: perform internal scheduling with the algorithms of Section 2.3.1
Phase Two:TB aware assignment
% loop for each scheduled user
for $u \in$ pool of users **do**
  RBs_u = RBs assigned to user u from phase one;
  $CQIs_u$ = CQI values relative to RBs_u;
  reorder $CQIs_u$ **and** RBs_u **from worst to best**
  for $k \in RBs_u$ **do**
    % determine the effective CQI for the assigned TB, from (2.3)
    $CQI_{u,TB_u} = EESM(CQIs_u(i : end))$;
    % compute the effective rate for the iteration
    $CQI_{u,TB_u} \rightarrow R^i_{u,TB_u}$;
    % remove the 1st RB from the TB and repeat until the TB is empty
  end for
  % find max data rate value
  find i **such that** $R^i = \max R$**;**
  % remove all the RBs that lower the rate
  $RBs_u(1 : i) = empty$;
end for
=0

The TB aware scheduler can be constructed by adding a second computation on top of the previously shown LTE MAC schedulers. Algorithm 1 shows a scheduler where, after the traditional resource allocation is performed, checks whether all the RBs in the assigned TBs contribute positively to the UE's datarate. If not the RBs are removed, thus possibly increasing throughput and decreasing overall power consumption as portions of the bandwidth are freed. Figure 2.11 presents the improvements by applying the TB aware scheduling onto LTE resource allocation mechanisms. The figure shows the throughput of an e-NodeB over the consumption power normalized for a full load base station. The figure shows the average e-NodeB's throughput over the average power gain for the different resource allocation mechanisms. In order to guarantee a fair representation, the power results obtained by each scheduler are expressed as fractions with respect to the maximum power consumed by a base station in full load with highest MCS. The empty markers represent the schedulers in their RB only configuration and the full markers the TB aware version of the same schedulers. Every scheduler presents an improvement when TB aware allocation is considered, showing that taking into consideration the intrinsic limitations of the network can play a great role in determining the final user's

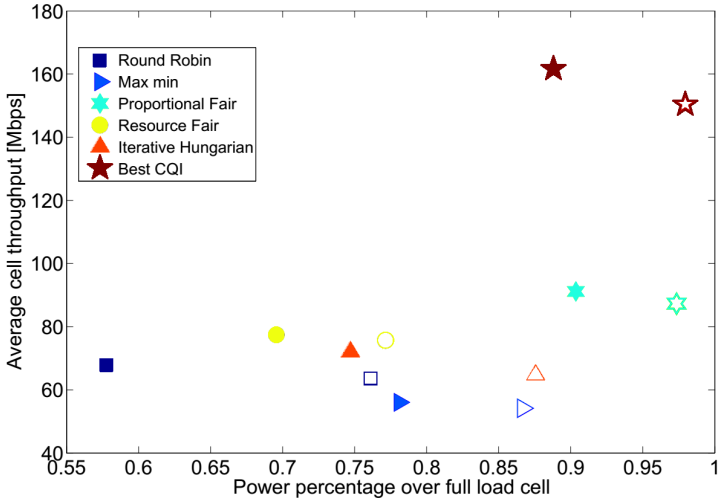

Figure 2.11: Throughput over Power comparison for different state-of-the-art schedulers with and without TB awareness.

performance. Table 2.6 shows the improvements in throughput and power for each scheduler.

Scheduler	Throughput increase	Power Reduction
Round Robin	6.61%	23.21%
Max Min	3.47%	9.56%
Proportional Fair	4.46%	7.2%
Resource Fair	2.29%	9.46%
Iterative Hungarian	8.02%	12.31%
Best CQI	7.54%	9.35%

Table 2.6: Improvement in datarate and power consumption for the different implemented schedulers.

The round robin scheduler shows the largest gains. This comes from the fact that it randomly assigns RBs to users, leading to more diversity in CQI values for the RBs of a given user. Hence, suppressing low-CQI RBs enables a significant gain of the TB effective CQI while not wasting power on poor RBs. The improvement seen over its performances caused by the TB aware scheduling is directly dependent on the amount of poorly assigned RBs present in the

first phase of the resource allocation. All the other schedulers present decisive improvement as well. The Iterative Hungarian scheduler assigns RBs to users such that each user receives a mixture of high quality and low quality resources. The improvement in datarate given by the TB awareness is indicative then of how influential the EESM mechanism is on the user's throughput. The TB aware scheduler will always improve over a state-of-the-art one, the improvement would be avoided only if each allocated user would witness perfect channel quality on each RB. The TB aware addition allows then the resource allocation to be carried more efficiently, achieving superior datarate while using less resources.

2.3.2 Resource Allocation Between Cells

Together with the per-cell resource allocation, the other aspect of the radio resource management problem is to maximise the overall network performance by making sure all the cells are able to operate efficiently. In past homogeneous cellular networks, this was obtained with careful network planning. In more modern networks this is not possible any more as every cell uses the full spectrum, furthermore with the introduction of small cells the position and capabilities of some base stations might be unknown [40].

Full reuse networks such as LTE and LTE-A are thus severely limited by interference [51] and the introduction of small cells exacerbates the problem as these are normally placed within larger cell's coverage area. The absence of real-time communication between femtocells and the rest of the network also adds a new layer of complexity to the RRM problem. The two main technical challenges, regarding inter-cell RRM, this work is addressing are then:

- How to manage the spectral resources of each cell dynamically so that the inter-cell interference (ICI) is minimised and the network's load balanced.
- How to assure that cross-tier interference is mitigated without the implementation of a communication link between cells of different tiers.

The following sections will give an introduction on the practices normally used to reduce the ICI and how such solutions can be extended to an heterogeneous network.

A Historical Perspective on Inter-Cell Interference Management

Interference management in a full reuse network is, generally, not an easy task. Historically, methods have been divided into these major families: interference randomization, cancellation, avoidance and multi-antenna techniques [8].

In *interference randomization* the transmission is spread over a large portion of the bandwidth in order to average the effect of interference on the desired signal and achieve diversity gain [52]. The interference is not actually removed but spread over the spectrum.

In *interference cancellation*, a receiver is able to reject the unwanted signal by first decoding it and subtracting it from the desired one [35]. This could allow a network to operate effectively even with high levels of interference. Although feasible in LTE, cancellation techniques require a complex receiver, able to perform adequate signal processing, normally not found in UE devices, thus forcing such methods to be used only in uplink [53]. These limitations may be overcome in the future as more powerful baseband processors may be implemented cheaply within mobile equipments [18].

Multi-antenna techniques can be used to increase SINR at the receiver by beamforming the desired signal. Multi user MIMO can also be used between base stations to coordinate transmission to a specific UE thus annulling interference; the main challenge to such technique is imposed by the relatively high latency time present in the X2 link (20 ms) which is much higher than the internal scheduling time (1ms) [8, 53].

Finally, *interference avoidance* consists in creating conditions in the network in which interference is prevented by reducing the amount of collisions due to concurrent transmissions over the same frequency resources. This can be obtained in the frequency domain, by dividing the available spectrum among cells, in the time domain, by allowing base station to transmit to their users at different intervals or in the power domain by shaping the transmit power of each base station to limit the generated interference [40]. Combinations of the above interference avoidance methods can be integrated into inter-cell interference coordination (ICIC) techniques in which cells communicate with one another and reduce their resources in order to maximise the overall network performance.

ICIC schemes cover a wide range of techniques, from low complexity static methods in which the spectrum division between cells is decided a priori, to more complex dynamic and distributed techniques, where a cell is able to adapt the amount of spectrum used (and transmit power) to specific network's conditions.

Static interference avoidance schemes

The simplest interference avoidance schemes are the frequency reuse mechanisms. Each cell is able to access only a limited portion of the available spectrum in order to remove interference completely or to reduce it [54]. Different power levels can also be used in various coverage areas within a cell to minimise the interference [55–57]. Reuse 1 represents the case in which every cell makes use

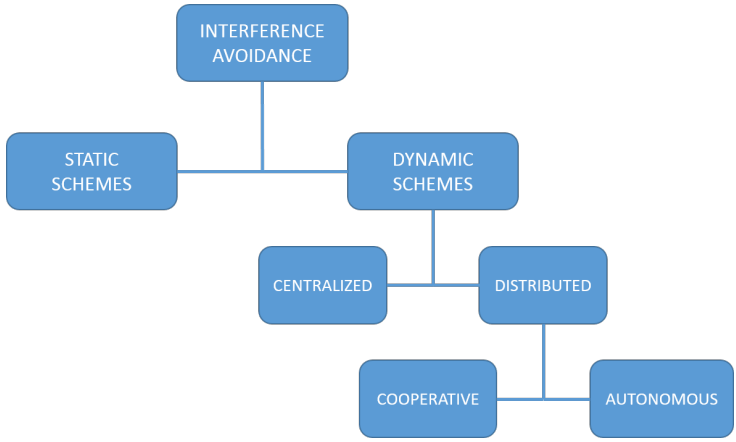

Figure 2.12: Interference avoidance

of the complete spectrum, as shown in Figure 2.13 (a). In this case there is no ICIC and the interference is not limited. Reuse 3 techniques split the available spectrum into thirds, Figure 2.13 (b); the interference is completely removed but the spectral efficiency of the network drops considerably as the users normally positioned close to the base station, which are not interference limited, can only access a severely limited portion of the spectrum; the aggregate throughput of a Reuse 3 scheme is about 75 percent of the aggregate throughput of an equivalent system using Reuse 1 [53].

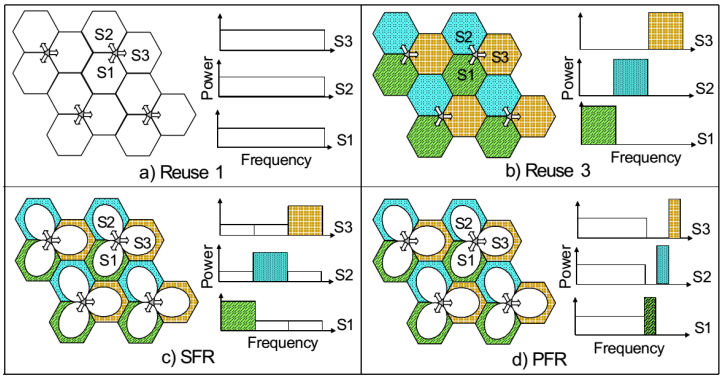

Figure 2.13: Frequency Reuse Schemes [4]

More advanced techniques such as Soft Frequency Reuse (SFR) divide the

spectrum into three parts and assign two to users positioned close to the base station while the last third is assigned to users positioned at the edge of the cell. Neighbouring cells assign non-overlapping sections of the spectrum to the cell edge users. Furthermore, transmissions on the resources dedicated to center-cell UEs use reduced power, as shown in Figure 2.13 (c) [58]. Partial Frequency Reuse (PFR), functions similarly to SFR, only the spectrum dedicated to cell-edge users is further split into three parts and only one third is assigned in each cell. This removes overlap in spectrum as shown in Figure 2.13 (d)

Static techniques were designed to be applied on networks with known and stable cell planning. They are, in fact, unsuitable in networks in which loads change dynamically and especially where small cells might be placed within the coverage area of larger base stations [40, 59, 60]. Furthermore, optimal settings for static ICIC methods are dependent on network geometry and irregular cell layout can penalize cells which receive more interference and are unable to modify their bandwidth allocation [61, 62].

Dynamic interference avoidance schemes
ICIC can be enhanced by taking into account the actual interference received by the users. By using actual UE measurements it is possible to optimise spatial utility, as not every user witnesses interference, and network load, as some cells might need to serve more UEs than others [63].

Dynamic ICIC solutions can then shape the frequency-time-power functions in order to maximise the overall network performance. As shown in Figure 2.12, dynamic ICIC can be divided into centralised, cooperative distributed and autonomous distributed categories.

In **centralized schemes**, a single control unit is responsible to manage the ICIC of the whole network. This Radio Network Controller (RNC) can be used to control the actual RB allocation of every user in every cell [64, 65], or to leave the internal resource allocation to each e-NodeB and just shape each cell's frequency/power resources to maximise performance [46, 66–68]. In the first case, each e-NodeB has to forward instantaneous CQI packets to the RNC and receive the allocation information. Because of the extremely high bandwidth costs of the increased signalling in the backhaul such centralized schemes are not often proposed [69].

The second family of centralized controllers, on the other hand, uses the RNC just to solve the ICI without considering the RB-UE allocation. Graph theory based approaches have been proposed in [66–68], in these methods an interference graph is generated with the information collected by the UEs. Graph colouring is then used to adapt spectrum allocation in the cells. A centralised ICIC

method based on resource negotiation was presented in [46]. In this work each UE is able to measure the power received by the two highest interferers and this information is sent back to their serving e-NodeB. Based on this information, each e-NodeB creates a list with the most interfered RBs and utility measures which quantify the effect of such interference, such as SINR difference with and without interference. This information is then relayed to a RNC via the X2 link and the controller applies convex optimization algorithms to solve the ICI problem and thus determines the set of RBs each cell can transmit on in order to maximise total downlink throughput.The system keeps transmit power constant over the whole spectrum. In [70] the authors introduce a multi-level centralized controller to reduce the computational complexity inherent in a network wide optimization. The proposed solution consists of two layers of control, first the throughput maximization between few cells (in the article, the authors refer to 3) is modelled as a mixed integer-linear problem. The result of such problem gives the resource allocation of the cells considered with minimised interference. A second layer of control builds an interference map between the groups of already allocated cells and limits the resources each group of cells can access. Both control layers are implemented and make use of convex optimization techniques to obtain a solution. The computational complexity of a network wide ICIC and RRM carried out by a single controller and the extremely high amount of signalling necessary make centralised solutions poor candidates for this class of problems [8].

When a central controller is discarded in favour of a distributed solution, coordination between cells becomes considerably more important, specially if effects such as fast channel fading and high mobility users have to be taken into account given the non-negligible latency of the X2 interface [71].

Cooperative distributed ICIC solutions allow to reduce the computational complexity of a centralized problem by increasing the signalling between cells. Most of these solutions are based on a form of adaptive frequency and power reuse where base stations limit the RBs accessible for communication and modulate their transmission power in order to reduce interference to specific users. These schemes divide the multi-cell optimization problem into simpler single-cell optimization ones solved by each e-NodeB; then information is exchanged with interfering neighbours to reduce ICIC [4, 72–77].

In [4] the authors propose an ICIC scheme similar to [46] in which the e-NodeBs exchange CQI and utility information with only the closest neighbours and perform an optimization process based on this limited exchange. This approach reduces the performance of the solution, when compared to [46]. In [72] a dynamic, distributed resource allocation algorithm is presented, where users are allocated only on high gain RBs. Subsequently, neighbouring cells communicate their edge users' resource allocation to each other in order to

minimize interference. Power control is then applied onto the assigned RBs. The method provides increased cell edge performance without, however, analysing the degradation at the cell's center. Typically, techniques that improve cell edge performance have large penalty on cell center, so it should be studied.

The solution proposed in [73] consists of a dynamic version of SFR. The method selects cell-edge bands based on interference measurements and network's load information coming from exchange between cells. A limitation of such scheme is that each e-NodeB selects a limited number of RBs for its edge bands, which reduces the impact of such technique in case of variable amounts of cell-edge users. [74,75] propose solutions similar to [73] in which the base stations are not limited in the amount of RBs allocable in each band but only contiguous RBs may be assigned in each band. In [75] the base stations use variable frequency reuse when the network is experience low load. As the load increases the amount of available bandwidth also increases and priority scheduling limits the power on the RBs more likely to cause interference.

In [76] the authors explore the effect of combining power control, fractional frequency reuse and fractional load (switching off completely bands of the available spectrum). The results show that while power control and FFR present the best results, fractional load is technologically simpler. Furthermore, solutions in which power control has been added to fractional load have been shown to outperform the traditional fractional load methods. The authors of [77] propose a solution based on channel muting. Each base station mutes parts of their resources if this increases the sum-rate of a group of neighbouring cells. In order to limit the backhaul's latency problems they assume each e-NodeB is equipped with fast optic connections able to transfer data between cells at no cost.

Even though cooperative distributed ICIC techniques can achieve performance very close to the more complex centralised methods, they have to rely on communication exchange to converge to an efficient solution. This is not always practical, as such links might either be too slow [78] or might not even be present, such a in a femtocell network.

To compensate for these shortcomings, a lot of attention has been paid to **autonomous distributed** interference avoidance methods [79–86]. In these solutions, each cell minimises interference without interaction with its neighbours but relying solely on local information or by minimising communication. The solution proposed in [79] and [80] use power allocation algorithms to set autonomously the transmit powers to highly interfered users using limited inter-e-NodeB communication. The ICIC is presented in a form of a multi-armed bandit problem in [81]. Each cell deduces the spectrum occupancy of its neighbours by applying a set of rules which steers the base station into finding,

for each UE, the RBs with lowest interference, over a time period, while also considering the neighbours resource utilization pattern. The algorithm converges to a solution in which each cell avoids certain RBs if they are frequently used by the neighbours and uses only the ones which present consistent low interference.

Efforts on game theoretic autonomous ICIC approaches have been performed in [82,83,85]. In these works the ICIC is modelled as a non cooperative game with the objective to reach a Nash equilibrium in which the interference is minimised. In [82], the network operates in full reuse and the throughput is maximised by finding the optimum transmit power for each user using game theory based schemes. The authors of [83] divide the ICIC into two subgames in which each player is composed by a UE-e-NodeB pair. In the first subgame, the RBs are allocated while avoiding interference, while the second game has the objective to further reduce interference by modifying the power allocation on the pre-assigned resources. The approach proposed in [85] is based on a congestion game. Each e-NodeB starts with a random set of RBs and modifies it by removing or adding, if possible, RBs and re-allocating RBs to different users iteratively, until the system converges to a Nash equilibrium and interference is minimised. In [86], on the other hand, two algorithms aimed to minimize the dissatisfaction of the users in terms of datarate and to minimize the cell's transmit power are proposed. The solutions are reached by using harmonic search algorithms where the RB allocation and power selection are improved iteratively, searching possible future RB and power allocations based on previous assignments.

ICIC for HetNet LTE-A

When a multi-tier structure is considered, the solutions to the ICIC problem found in literature tend to combine some of the previously described ICIC categories [35,40,87,88]. Considering an LTE-A deployment with co-channel femto, pico and macro network, cooperative distributed solutions are often proposed for femtocell deployment even though no communication is designed between layers [89, 90]. These solutions though effective are of difficult application. Autonomous methods such as [91–93] present self-organizing solutions for co-tier femtocell deployment. These solutions, generally, ignore the ICI of the higher macro and pico layer.

Particularly interesting is the concept of the **cognitive femtocell**, where the femto base station is able to overhear either uplink communication from nearby macro or pico users, or is able to decode the downlink of macro/pico cells in order to minimise interference [94–99].

This thesis presents a simple, elegant solution to the ICI problem in heterogeneous LTE-A networks. The solution presented in chapter 3 combines cooperative

distributed and autonomous distributed algorithms to solve interference at macro/pico level and femto level orthogonally. The proposed method makes use of frequency domain techniques to split resources dynamically, based on the network's load and UE requirements. Power domain techniques are implemented in the small cells and femtocells possess cognitive and self-organizing capabilities. In chapter 4 the effects of signalling overhead are analysed and the impact of CQI FB reduction on the proposed ICIC solution is quantified.

2.4 Signalling control information overhead

The final part of the RRM problem analysed in this dissertation consists in the reduction of the signalling overhead naturally present with the internal resource allocation and the ICIC techniques. For the AMC scheme to work efficiently, reliable and frequent CQI feedback is requested from the UEs. This information can occupy a large amount of a user's uplink bandwidth. In fact, full feedback in LTE is completely infeasible in a multi-user context as, just the CQI information would saturate the cell's uplink resources with just 80 served users [20]. The effects of imperfect and partial channel information on the resource allocation in OFDMA systems have been studied extensively [100–103].

Different feedback reduction techniques have been proposed for OFDMA systems, in [104] the authors discuss and compare a number of frequency feedback reduction methods; these can be divided into two categories: **threshold-based** and **subband grouping** [104]. The first method allows a user to feed back CSI, for an RB, only if the channel quality exceeds a pre-determined threshold. This method reduces indeed the amount of feedback information sent by the users but at the cost of reduced datarate [105]. In order to determine how many bits are necessary for a multi-user downlink network to maintain high capacity, the authors in [106,107] show that 1-bit CSI feedback can achieve near maximum capacity if the number of users is sufficiently high.

The second method, allows the users to transmit CSI only on groups of RBs instead of single ones. This is the technique normally implemented in LTE as seen in section 2.2.1. A lot of attention has been paid especially to the $Best-M$ reporting scheme. The $Best-M$ policy has been proven to be efficient when paired with opportunistic resource allocation [108] and to reach performance close to the more demanding "sub-band level feedback" when the number of served users is sufficiently high [109,110]. Although these methods can achieve good performance, it has been shown that greater improvement can be obtained by tailoring the amount of feedback based on each user's channel conditions and requirements [111,112]. Other works show that (close to) optimal scheduling can

be achieved with imperfect CSI [113–115]. These works, nevertheless, provide an information theoretical bound that does not take into account the limitations of a practical cellular downlink network.

On top of AMC requirements coming from the internal resource allocation, the amount of CSI present does influence also the efficiency of ICIC techniques where the e-NodeBs or a central controller, need to receive detailed information on the channel conditions of all the users to coordinate properly. Limited CSI feedback impacts ICIC considerably [116–119] and has to be addressed.

Finally, another aspect to consider is that CSI information has to be relevant still relevant when received by the base station. It is possible to reduce the signalling overhead by applying **time domain quantization** but the delayed channel quality information will impact the downlink performance [120]. Even though delayed feedback is better than none at all [121]; it is important to develop strategies to predict the channel quality of each UE properly. In [122] the authors implement and compare various SINR prediction algorithms and conclude that high gains can be expected with covariance based predictors for low mobility users. In [123], the authors present a prediction method used to compensate for CSI delay. The estimation is performed at the mobile user side and the predictor takes into account the Doppler shift of each user for more accurate estimation. Both works make use of the users' Doppler shift to determine the time duration of the channel quality estimation; this procedure, although well established, might lead to erroneous predictions, even though a negative correlation is generally present between prediction quality and Doppler shift, the SINR is dependent also on interference and the overall channel conditions. A high mobility user might witness a better, less variable channel than a low mobility user. Furthermore, users have to predict the SINR themselves, depleting battery life. In [124] the authors propose a dynamic CQI allocation method predicted at the base station. The CQI allocation time of each user is adapted based on the instantaneous packet loss of each user. In [125] the same authors expand their results by including CQI prediction at the base station. They use a linear predictor and compensate for errors by reducing or increasing the prediction windows based on the users' packet loss. In [126] the authors present a non predictive signalling reduction scheme where only users with low SINR are allowed to feed back expensive instantaneous CQI information while high SINR users only transmit wideband information. Even though the method decreases the signalling information, it is carried out for a limited and fixed time window (2 ms) and is studied in a single cell scenario, ignoring the underlying network dynamics due to interference, traffic load, etc.

In this dissertation, the impact of CSI feedback quantization on the network's RRM is considered. Both resource allocation and inter-cell coordination are considered. Novel and practical solutions in the frequency and time domain

are discussed to combat the loss of performance due to limited CSI feedback in chapters 4 and 5.

Chapter 3

Interference Coordination in Heterogeneous LTE-A Downlink Networks

In this chapter, the general inter-cell interference minimization problem in heterogeneous networks is described. The problem is first framed and a heuristic, distributed solution suitable for a heterogeneous LTE-A network is further presented.

The method here proposed takes into consideration the capabilities of the various base station types and is able to minimize the interference while keeping a very high quality of service to the UEs. Large consideration is given to the fact that no communication is possible between tiers and that a practical solution has to adapt to this necessity. For this reason, the ICIC method splits the interference reduction into two parallel algorithms targeting the co-tier and cross-tier interference respectively. Further, power control is possible for pico and femto base stations allowing for flexibility in the resources power allocation. The proposed method makes use of the concept of the cognitive femtocell, where information exchange is avoided but the base station is able to sense relevant information from nearby cells and interfered users.

3.1 The Multi-Cell Rate Maximization Problem

The usual network optimization procedures have the objective to maximise the overall system throughput. In a generic multi-cell OFDMA network with C cells, each cell c serving X_c users and where the bandwidth is split into K parts, this is accomplished by a sum-rate problem such as:

$$\max \sum_{c}^{C} \sum_{x_c}^{X_c} \sum_{k}^{K} r_{x_c,k}, \tag{3.1}$$

where $r_{u_c,k}$ is the rate user u_c experiences on frequency resource k. The overall rate is then the sum of the throughput of every user over all the frequency resources assigned to those users. The throughput is, generally, function of the channel quality and proportional to the SINR a user witnesses on that specific frequency resource. In the LTE system model in Section 2.1, it was discussed that the LTE-A downlink makes use of slotted frequency resources, where the smallest unit assignable to a single user was defined as resource block RB. Furthermore, the throughput attainable is not a continuous function of the SINR but is function of the discrete CQI values and their mapping onto discrete modulations and coding rates. The CQIs are implicit channel quality measures that take into account the SINR a terminal is witnessing and the actual properties of that terminal [127]. This means that a more advanced UE may have the same SINR as a less advanced one but might feed back a higher CQI value if able to perform better signal processing. The network's sum rate, then, depends on two factors:

1. Which RBs are going to be allocated to which UE
2. The SINR each user has on each RB

The first factor is function of the internal resource allocation discussed in Section 2.3.1. Each scheduling algorithm maximises different figures of merit, thus in this work, each base station is able to use a preferred method on top of the interference coordination method proposed.

The SINR that each UE sees on each RB is function of the power received by the UE from its serving base station, the noise present in the channel and, finally, the interference caused by the neighbouring cells. The equation for the SINR is re-proposed here:

$$\gamma_{x_i,k} = \frac{P^i_{x_i,k} \cdot G^i_{x_i,k}}{\sigma^2 + \sum_{\substack{j=1 \\ j \neq i}} P^j_{x_i,k} \cdot G^j_{x_i,k}}, \tag{3.2}$$

where the interference witnessed is itself function of the resource allocation and transmit power used by the neighbouring base stations. The rate optimization problem is then combinatorial in nature and very difficult to solve optimally [128]. If, instead of a generic OFDMA network, one considers the specifics of an LTE-A system, the problem can be deconstructed and sub-optimal but practical solutions might be achieved by considering the inherent limitations of a real-life network.

The following section presents the system model discussed in this work and adapts the generic sum-rate problem for the LTE-A downlink network. Section 3.3.1 presents the proposed solution for the macro- and pico- cells while the solution for femtocells is discussed in Section 3.3.2. The results are presented in Section 3.4 and, finally, conclusions are drawn in Section 3.5.

3.2 System Model of LTE-A Downlink Network

Figure 3.1 presents the interference scenario studied in the considered downlink LTE-A network.

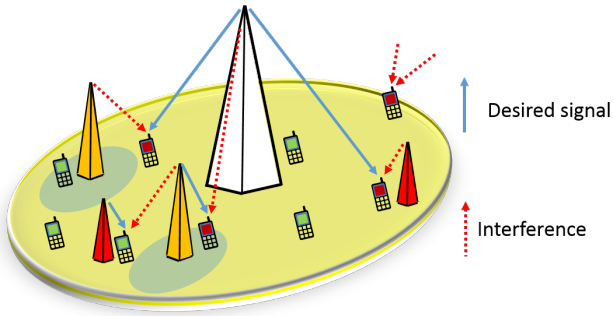

Figure 3.1: LTE-A interference scenario

From the figure it is possible to recognize that not every user in a cell is affected by interference. Users positioned in areas where the desired signal is strong are in fact bandwidth limited and their performance does not improve by limiting interference but either with better resource allocation or by increasing the frequency spectrum. The performance of these users is sometimes ignored in ICIC methods as these target the interfered UEs but do not take into account

the performance loss that reducing interference may cause on the users with excellent channel conditions [72]. Furthermore, even in a homogeneous network, where each cell is designed to have a well defined coverage region, as depicted in figure 3.2 *(a)*, it is impossible to predict the area in which a user is certain to experience good channel conditions. While it is reasonable to assume that the closest neighbours contribute to the largest part of the interference, it is also important to notice that when phenomena like shadowing and channel fading are considered, the geometry of the network varies drastically. Figure 3.2 *(b)* shows how the cells coverage areas may be affected. Hence, the concept of neighbour needs to be redefined, not as spatially close but as a base station that influences substantially the SINR.

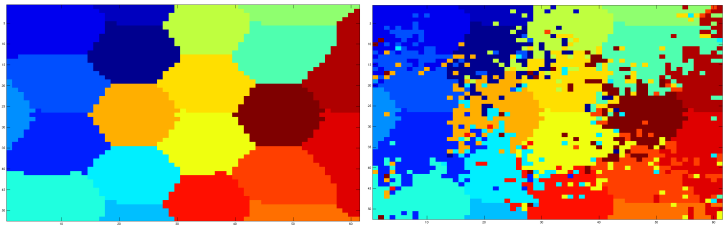

((a)) Sectors coverage areas

((b)) Sectors coverage areas with 10 dB shadowing and fading

Figure 3.2: Coverage Areas

The sum-rate is good indicator of the overall network capacity but doesn't allow for a fair network-wide resource allocation as only the users with excellent rate would be assigned. The maximisation is, thus, generally bounded by a set of constraints selected to assure a correct network behaviour. In fact, the maximisation procedure is either a modified version of the sum-rate, where some fairness parameter is included with the rate, or the fairness is used as a constraint to the optimisation process. The methods presented in this work are based on the one presented by Rahaman in [46].

Let us consider a heterogeneous LTE-A downlink OFDMA network composed of C macro base stations. Each macro base station is composed by S orthogonal sectors; each sector is responsible to serve a portion of the overall cell area. There are, thus, a total of $M = C \cdot S$ macrocell sectors in the network. There are also P picocells and F femtocells. These small cells contain only 1 sector each. Each macrocell's sector serves X_m terminals while each pico and femto base station serves X_p and X_f users respectively. K physical RBs can be allocated per sector. Given that the datarate $r_{x_i,k}$ possible for each UE x_i on RB k can

be directly determined from its SINR $\gamma_{x_i,k}$, the maximisation process for the considered network becomes:

$$\max \sum_{i}^{M+P+F} \sum_{x_i}^{X_i} \sum_{k}^{K} r_{x_i,k} \cdot d_{x_i} \cdot a_{x_i,k} \tag{3.3}$$

where

$$a_{x_i,k} = \begin{cases} 1 & \text{when user } x_i \text{ is assigned on RB } k \\ 0 & \text{otherwise} \end{cases} \tag{3.4}$$

$$\sum_{x_i}^{X_i} a_{x_i,k} \leq 1, \forall k \in K, \tag{3.5}$$

$$\sum_{k_i}^{K_i} P_{k_i} \leq P_{max} \quad \text{for each base station } i \tag{3.6}$$

where d_{x_i} is called a demand factor, it is introduced to add some fairness to the allocation; $d_{x_i} = \frac{\mu_{x_i}}{\bar{R}}$ where $\bar{R}$ is the average rate received by the user over a past time window and μ_{x_i} is the requested rate. The users that have received the lowest rate in the previous transport blocks are then advantaged in the resource allocation process. Constraint (3.5) makes sure that one RB k might not be assigned to multiple users in a cell. Constraint (3.6), on the other hand, makes sure that the sum of the power transmitted by a base station on all the RBs remains below the maximum allowed power; the power in (3.6) is then the same as in (3.2).

A computational solution for this problem is difficult to find [129]. The Hungarian Algorithm (HA) was firstly proposed by Kuhn [15] as a simple solution to binary integer problems under specific conditions, and its iterative version [46] has been studied as a good sub-optimal solution for the assignment problem in homogeneous networks. The proposed algorithm to solve (3.3 - 3.6) is presented in Section 3.3.

Before introducing the scalable solution presented here, it is important to note the difference between the various base station categories which motivate specific design choices in the proposed method and the assumptions made on the UEs. Macrocells and picocells are able to communicate with the EPC via the X2 interface. This allows for coordination between the base stations and exchange of the CSI collected by the users. The main difference between a macrocell and a picocell, except for the transmit power, is that the smaller base stations are able to perform power optimization, generally unavailable to bigger base stations [127]. Thus, the solution implemented for macrocells optimises the RBs each base station has to restrict in order to maximise performance while

the solution for picocells allows a base station to waterfill transmit power on the resources that would have been otherwise restricted. Femtocells, on the other hand, do not allow communication for coordination, with neither other femtocells nor macro/pico base stations. For these reasons the maximisation process (3.3) cannot take into account the rate coming from the femto users as there is no way for a distributed controller to know it. Nevertheless, a femtocell has still the duty to minimize interference to macro or pico users as these form an underlying network managed by the operator [39]. For this reason the femtocell considered in this work possesses *"cognitive capabilities"*, is able to sense the environment, overhear communication between macro or pico UEs and their serving base stations and to determine whether it is interfering and how much.

The vast majority of ICIC techniques makes the assumption that the users are able to determine their channel conditions for the whole bandwidth with a high resolution. Furthermore, each user is supposed to be able to differentiate between the interfering base stations. In a practical system, however, there is a limit in CSI estimation accuracy as well as feedback bandwidth availability. The users are only able to report CSI information on a limited subset of the overall bandwidth. They might not be able to identify the highest interferer, and this interferer's power, on the complete bandwidth, as assumed by traditional ICIC schemes. The work proposed in this chapter makes use of the common perfect CSI knowledge at the receiver to showcase the strengths and weaknesses of the ICIC; in Chapter 4 a framework to study the impact of this CSI signalling information is presented and the ICIC method proposed here is modified accordingly and results will show that the proposed solution is able to guarantee high performance even when the CSI information is incomplete.

The proposed method on how macro- and pico-cells can coordinate information in order to reduce interference and maximise the sum-rate is presented in Section 3.3.1. Further expansion on the nature of the cognitive femtocell and the proposed solution to reduce interference from femto base stations to macro and pico UEs are presented in Section 3.3.2.

3.3 Proposed Scalable Interference Management Approach

The scope of this section is to present a distributed interference management scheme which solves problem (3.3 - 3.6), is not computationally intense and can be applied to practical HetNets. The proposed scheme is divided into two parallel parts. The first part deals with interference coming from neighbouring

macro or pico base stations while the second part deals with the interference generated by femto base stations.

3.3.1 Macro and Pico interference management

The ICI mitigation technique is composed of two phases. Firstly, in the "restriction definition" phase, each sector determines locally which other sectors are producing harmful interference on specific resource blocks and generates a list of resource blocks that the interfering sectors would have to restrict or limit transmit power in order to improve on that sector's throughput. This is done concurrently with the sector's internal resource scheduling. Secondly, the sectors exchange information with the interfering sectors and in the "restriction negotiation" phase each sector computes which resource blocks it has to restrict in order to maximize the overall network throughput. The IHA algorithm will be used here to determine which restrictions make sense from a system point of view. Below, the details of the algorithms are explained and summarised in Algorithm 2.

Before the actual introduction of the algorithm, a clarification of the notations used in this work is necessary. Every scalar used in this work is being expressed using a lower case italic letter, i.e. x; an array is presented by a lower case bold italic letter, such as $\mathbf{l}$ and a matrix is written using a bold capital letter: $\boldsymbol{Y}_{a*b}$ where a and b represent the rows and columns of the matrix. Each entry of such matrix is expressed with the same letter used to name the matrix, but in lower case.

Restriction definition

A sector receives the CSI packets containing the CQIs from all the attached users and the interference power received by each user on each resource block from all the neighbouring base stations. The CSI packets also contain the rate requested by each user and the set of RBs assigned to each user by the base station scheduler. The base station i then, computes the SINR that each user x_i experiences on all the resource blocks: $\boldsymbol{\gamma}^1_{x_i}$ and the SINR $\boldsymbol{\gamma}^2_{x_i}$ the user would experience if the highest interfering sector on each resource block is forced to zero. Only the highest interferer is considered because of two main reasons, first, the effects of interferers above the second on the SINR become negligible [46] and, second, it is very impractical for a receiver to decode signal coming from a an interferer if there is already a stronger one present [17].

These SINR values are then mapped into their relative data rates, $\boldsymbol{r}^1_{x_i}$ and $\boldsymbol{r}^2_{x_i}$, for each user x_i using the MCS schemes from table 2.2. The rate vectors of each user are then converted into utility vectors $\boldsymbol{u_{x_i}}^1$ and $\boldsymbol{u_{x_i}}^2$ defined as:

$$u^1_{x_i,k} = r^1_{x_i,k} \cdot d_{x_i} \quad \text{and} \quad u^2_{x_i,k} = r^2_{x_i,k} \cdot d_{x_i}; \tag{3.7}$$

where d_{x_i} is the demand of user x_i. All the utility vectors $\boldsymbol{u}^1_{x_i}$ and $\boldsymbol{u}^2_{x_i}$ are then collected in two utility matrices $\boldsymbol{U}^1$ and $\boldsymbol{U}^2$ of dimensions $X_i \cdot K$, where X_i is the number of users served in the cell (either X_m or X_p). The restriction choice of a specific resource block k is performed by comparing the utility $u^1_{x_i,k}$ user x_i experiences on RB k with the higher utility $u^2_{x_i,k}$ and a threshold value $th_{x_i,k}$:

$$\text{If } u^2_{x_i,k} \geq u^1_{x_i,k} + th_{x_i}, \tag{3.8}$$

then user x_i would see an improved data rate on RB k if the highest interfering sector would be restricted; th_{x_i} can be dynamically adjusted, in this work it is equal to the minimal rate requested (see table 3.1). If a user is well placed (i.e. in the cell center), or does not witness interference, the improved utility $\boldsymbol{u^2_{x_i}}$ would not be considerably higher than the measured one $\boldsymbol{u^1_{x_i}}$.

This criterion, then, targets users which see an improvement when the interference is reduced, generally speaking these are referred to as "starved users".

Not all the resource blocks that fulfil the above criterion will actually be blocked or used at limited power by the neighbours but only the ones that maximise the utility of the sector when all the attached users are scheduled on all the available resource blocks: each sector generates a restriction list $\mathbf{R}$ by applying the Iterative Hungarian Algorithm onto the utility matrix $\boldsymbol{U}^1$. At each iteration h the IHA determines which set of RBs $\hat{k}_h$ can be assigned to the attached users X, as defined in the system model section, so that the utility of the scheduled users for that transport block is maximized. This optimisation considers interference, pathloss and shadowing.

If there is improvement by restricting the assigned resource blocks, i.e. if user x_i is assigned RB $\hat{k_{h,x_i}}$ at iteration h and $u^2_{x_i,\hat{k_{h,i}}} \geq u^1_{x_i,\hat{k_{h,x_i}}} + th_{x_i}$ then the corresponding entry of the restriction list $\mathbf{R}$ is updated with the highest interferer for that RB $\hat{k_{h,x_i}}$, with the corresponding ideal utility $u^2_{x_i,\hat{k_{h,x_i}}}$ for the same RB and the user x_i scheduled on that RB and with the difference between the ideal and measured SINR $\gamma^2_{x_i,k} - \gamma^1_{x_i,k}$. This information becomes relevant in the case of picocells as they are able to perform power control. The columns of $\boldsymbol{U^1}$, corresponding to the assigned set of resource blocks $\hat{k}_h$, are deleted and the process is repeated until all the resource blocks have been assigned. The

Hungarian Algorithm has been proven to be optimal in an assignment problem where the number of resource blocks is equal to the number of users [15]. In case this identity is not valid the IHA provides a good suboptimal solution that trades off performance for lowered computational complexity when compared with traditional convex optimisation techniques.

Restriction negotiation

We define as a cluster the group of cells interfering with each other. A cluster can then have variable size depending on the propagation conditions as shown in Figure 3.2 and how the users are distributed within each cell. If there are many users in the cell edge, these will witness higher interference coming from the surrounding cells. Each sector exchanges with all the other sectors in a cluster its restriction list $\mathbf{R}$. The entries of the restriction lists contain information on which RB k each sector would like the interfering sectors to block, the ideal utility $u^2_{x_i,k}$ user x_i, scheduled on RB k, in sector s would achieve and difference between the ideal and measured SINR $\gamma^2_{x_i,k} - \gamma^1_{x_i,k}$. From now on we refer to utility $u^2_{x_i,k}$ as the utility the sector would achieve on RB k: $u^2_{s,k}$. Then each sector generates a cluster utility matrix $\mathbf{Z}$ in this manner: Each row of $\mathbf{Z}$ represents each sector in the cluster. If RB k is marked for restriction in the restriction list of sector s then $z_{s,k}$ is equal to the utility $u^2_{x,k}$. If multiple sectors request the same RB then the utilities $u^2_{s,k}$ are organized in descending order. For each conflicting sector a new column, corresponding to the RB k is generated to account for multiple RB assignments. Each entry of these columns is zero except for the utility of the sector. If two or more of these utilities are equal they remain on the same column. The cluster utility is then at most $S \cdot S \cdot K$ large in the absolute worst case scenario where all sectors interfere with all other sectors on all the resource blocks. Each sector possesses its cluster utility matrix $\mathbf{Z}$ and proceeds in assigning resource blocks to each sector using the IHA described previously. The base station can use the same process in the "restriction definition" as well as in the "restriction negotiation" thus the complexity of the overall algorithm is just function of the size of $\mathbf{Z}$. Once all the resource blocks are assigned to the sectors, these represent the resources each sector needs to maximise the global cluster rate and are stored in the final assignment matrix $\mathbf{A}$. Subsequently, the highest interferers present in the restriction list, corresponding to each entry in $\mathbf{A}$, have to be restricted.

Each macrocell sector, then, determines from its $\mathbf{A}$ and the restriction list which resource blocks it has to restrict and avoids transmission on those resources thus maximizing the capacity in its cluster. A picocell, on the other hand, makes use of the difference between the ideal SINR and the measured one $\gamma^{dif}_{s,k} = \gamma^2_{s,k} - \gamma^1_{s,k}$ exchanged by the interfered sector s. If RB k is then scheduled to be restricted,

the transmit power of the picocell, on that RB, is reduced by the same difference in SINRs:

$$P_k = \max(P_{max} - \gamma_{s,k}^{dif}, 0), \tag{3.9}$$

where P_{max} is the maximum transmit power per RB in dB. In this way, if the SINR difference is lower than the maximum transmit power on the RB, the pico base station can re-use that RB for additional transmission otherwise it is restricted in the same way as for the macro base station.

Algorithm 2 Algorithm for macro and picocell interference coordination

Phase One: Restriction definition
% Base station's sector receives CSI information from the served users and maps it into received and ideal utility as defined in (3.7)
for $x \in X$ **do**
  for $k \in K$ **do**
    $\gamma^1_{x,k} \longrightarrow r^1_{x,k} \longrightarrow u^1_{x,k}$
    $\gamma^2_{x,k} \longrightarrow r^2_{x,k} \longrightarrow u^2_{x,k}$
  end for
end for
% The sector applies IHA on U^1 and compares entries with to U^2 to find Restriction List R
$K_h = K$
while $U^1 \neq \emptyset$ **do**
  $HA = hungarian(U^1)$
  for $r \in$ *rows of* HA **do**
    if the entry k_h of HA is allocated **and** $u^2_{r,k_h} \geq u^1_{r,k_h} + threshold_r$ **then**
      $t_{k_h} = [\ 1;\ u^2_{r,k_h}$; max interferer for RB k_h; $\gamma^2_{x,k} - \gamma^1_{x,k}\ ]$
    end if
    Delete colums of $\boldsymbol{U}^{1,2}$ corresponding to allocated RBs
    Delete entries of K_h corresponding to allocated RBs
  end for
end while
% Sector shares matrix R with all the interfering neighbours
Phase Two: Restriction negotiation
% Build cluster utility matrix Z
% Maximise Z to find restricted RBs
$K_s = K$
while $Z \neq \emptyset$ **do**
  $HA = hungarian(Z)$
  for $r \in$ *rows of* HA **do**
    if the entry k_s of HA is allocated **then**
      $A_{r,k_s} = 1$
    end if
  end for
  Delete columns of $\boldsymbol{Z}$ corresponding to allocated RBs
  Delete entries of K_s corresponding to allocated RBs
end while
% Now the sector knows which RBs is supposed to use from A and determines which ones it has to restrict restrict
for $s \in$ Interfering Neighbours **do**
  for $k \in K$ **do**
    if $a_{s,k} = 1$ and the max interferer of sector s on RB k is current sector **then**
      if current sector is macrocell **then**
        $P_k = 0$;
      else if current sector is picocell **then**
        $\gamma^{dif}_{s,k} = \gamma^2_{s,k} - \gamma^1_{s,k}$
        $P_k = \max(P_{max} - \gamma^{dif}_{s,k}, 0)$
      end if
    end if
  end for
end for
=0

3.3.2 Femto interference management

An independent algorithm at the femtocell side is proposed to limit the interference introduced by these unplanned and uncontrolled small cells. Since no fast backhaul communication between the tiers is assumed each femto access point has to be able to determine whether it creates interference to macro (or pico) cell users. In this work femto base stations possess sensing capabilities and are able to overhear uplink communication between close by macro and pico users to their serving base stations.

Enabling the cognitive femtocell: the digital front end

The assumption that a femtocell is able to sense its environment and react accordingly is gaining a lot of interest in the wireless community [94–99]. Generally, the literature refers to generic capabilities of the device without considering technological limitations. In this work, on the other hand, the assumptions made in the ICIC method are easily achievable technologically by employing the digital front-end DIFFS presented in [18] and included as another **contribution** to this dissertation. The Digital Front-end For Sensing and Synchronization (DIFFS) is a low-power, multi-mode, multi-standard flexible digital front-end (DFE) able to perform simultaneous sensing and reception, allowing the radio to acquire real-time channel information and take an informed decision.

A DFE is an essential building block of a reconfigurable radio, as shown in Figure 3.3. The reconfigurable radio can adapt and be reprogrammed easily to fit a vast number of applications. This flexibility is granted by its three building blocks: the analog front-end (AFE) is with the reception of the RF signals and their conversion to the digital domain, it can have either a fixed design or it might be flexible and reconfigurable such as [18]. The DFE receives data from the AFE and performs sensing and synchronization. If desirable information is found, the DFE sends it to the baseband processing unit (BPU). The DFE is then tasked with determining whether the signals received can be used by the radio; this tasks makes it ideal in analysing interfered signals.

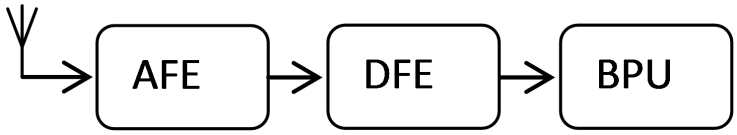

Figure 3.3: Reconfigurable Radio Block Diagram

The structure of the proposed DFE is shown in Figure 3.4. The various building

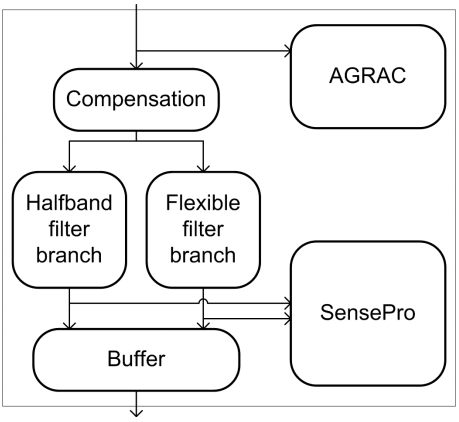

Figure 3.4: DIFFS Structure

blocks composing the DIFFS are responsible for the correct behaviour of the structure and are hereafter briefly explained.

The communication between the AFE and the DFE is controlled by the Automatic Gain and Resource Activity Controller (AGRAC). As the name suggests, the AGRAC is responsible for certain front-end settings that require a short control loop, such as the front-end gain and the remaining DC offset (DCO) compensation. The AGRAC is also responsible for controlling the mode of operation of the DFE; it can enable or disable the other blocks of the DFE as needed: in normal receive mode, the AGRAC activates the SensePro to carry out signal synchronization and if found it activates also the baseband processor. In sensing mode, the AGRAC can activate the SensePro to perform signal processing if no power is sensed, if a signal is otherwise detected, the sensing is stopped or receive mode is initiated.

Once the incoming samples have gone through the analog non-idealities compensation block they reach the filtering stage. This stage consists of two filter branches that can operate on the data in parallel. One filter branch is a power-optimized set of halfband filters/downsamplers that allow low-pass filtering and downsampling by factors 2 and 4. The second branch is composed of fully programmable filters capable of down-conversion, band selection, and non-integer rate conversion. In order to guarantee narrowband performance with strict out-of-band attenuation flexible CIC filter in conjunction with programmable FIR filters have been selected. All filter blocks are implemented in full precision, and a quantization selection block after each stage allows the algorithm designer to select the most relevant bits from the output of the filter.

The reason is that the quantization for strong signal reception is different from the quantization for faint signal detection as used in sensing. The parallel filter branch design allows trading off power and performance at software-level by merely selecting a specific filter branch, and allows operation on one or multiple radio channels in parallel depending on the objectives of the cognitive radio or femtocell. More specifically, it allows sensing/reception in different bands in parallel.

After passing through the filters, the data is acquired by the SensePro. The purpose of this block is to execute both the advanced spectrum sensing algorithms and the coarse time synchronization. The SensePro is a programmable logic processor used for all the flexible numerical operations required by the different sensing algorithms, such as min/max, averaging and thresholding, for loop control. It is also able to perform 128-point Fourier transform, vector rotation and correlation operations. Together with the parallel filter branches, the SensePro allows the DFE to sense the channel and receive signals simultaneously. For example, figure 3.5 shows an LTE spectrum containing two bands. If the radio is programmed in receive mode and already possesses the necessary parameters to receive the LTE signal in the lower frequency band the AGRAC instructs the SensePro to perform signal synchronization. The received signal is then sent through the halfband filter branch and sent to the baseband processor without any further interaction with the AGRAC or the SensePro. During normal reception, the SensePro can be loaded with new firmware that enables LTE sensing, and the reconfigurable filter branch is programmed and activated to transfer the content of the upper frequency band to the SensePro. This way, the cognitive femtocell can scan the upper band while receiving the lower band.

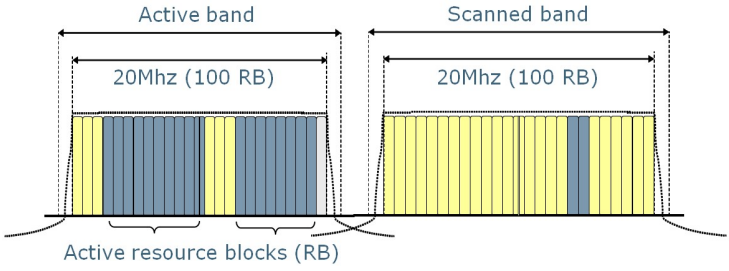

Figure 3.5: Parallel reception and sensing for LTE

The output buffer is a key element in the architecture when the DFE is used for data reception. When synchronization is required, both the SensePro and the buffer are enabled simultaneously by the AGRAC. The SensePro then

searches for sync while the received and filtered samples are being stored in the buffer. When synchronization is detected, the SensePro passes the absolute synchronization index to the buffer to update the read pointer. Subsequently, the AGRAC interrupts the platform controller to notify that data is available for reading. When the radio platform starts reading out samples from the buffer, only the samples starting from the synchronization point on are transferred to the baseband engine.

This design allows the DFE to be used for a various array of applications, from simply sensing if a channel is occupied to detecting specific signals and decoding whether they are LTE or not. A key example for the application proposed in this dissertation is the feature detection of LTE control signals. The DIFFS can be implemented onto a femto base station to overhear and decode the signal a neighbouring base station or UE is transmitting and regulate its parameters accordingly. The DFE has been used successfully already to perform multiband energy detection and synchronization-aided sensing [18]. The second case is particularly interesting for the investigated scenario as it allows the DFE to detect the specific LTE channels carrying the information of which RBs are going to be occupied in the following scheduling intervals. In [18] the DIFFS was used to detect the Physical Downlink Shared Channel of an LTE over the whole downlink bandwidth. Without the knowledge of the exact position of the PDSCH, the Reference Signal (RS) and the Primary Downlink Control Channel (PDCCH) will generate a constant False Alarm making the Energy Detection based sensing of available resource blocks not useful. The Primary Synchronization Channel (P-SCH) time reference will allow the sensing engine to build a resource map containing both time and frequency information of the amount of resources available in the band.

To showcase the effectiveness of the DIFFS on detecting neighbouring LTE cells, a downlink LTE signal using 20 MHz bandwidth has been detected. Two types of sub-frames are transmitted: a sub-frame containing control information and a non-control information sub-frame. A small degradation is observed in the Probability of Detection (PD) for the control sub-frame due to the lower number of observation windows. The Probability of False Alarm (PFA) remains well below the targeted 10% for both types of sub-frames. The results are shown in figure 3.6.

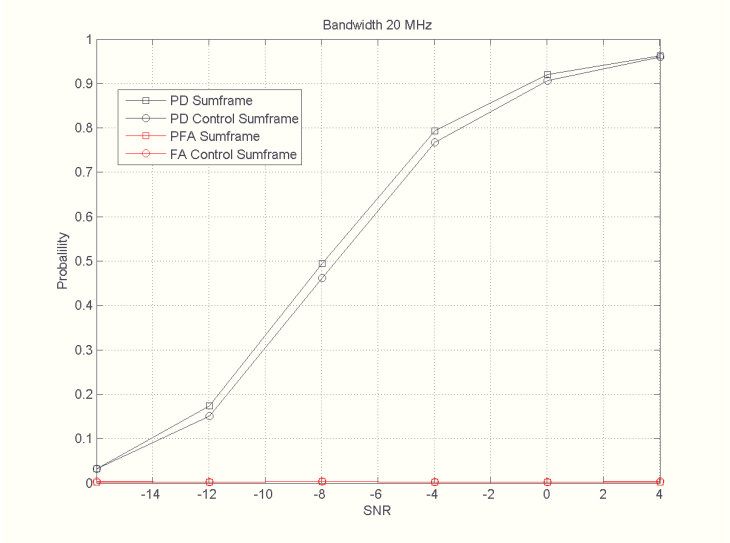

Figure 3.6: Probability of detection of LTE signals

Femtocell interference management solution

The femto access point then determines the channel gain between itself and the macro or pico neighbouring base stations; it also determines the channel gains between itself and the macro (or pico) users near by. The femtocell is then able to use water-filling to reduce the transmit power on the RBs assigned to the macro (or pico) user. Algorithm 3 presents the interference management solution implemented on the femto base station.

Algorithm 3 Algorithm for femtocell interference avoidance

% Each femto base station determines the channel between itself and a nearby UE by sensing the environment
% The femtocell decodes the channels and determines whether the UE is going to be scheduled
for $k \in K$ **do**
  if RB k is assigned to sensed UE **then**
    % The femtocell determines the SINR the UE would have if femto transmission power is lowered
    $\gamma_{s,k}^{dif} = \gamma_{s,k}^{2} - \gamma_{s,k}^{1}$
    $P_k = \max(P_{max} - \gamma_{s,k}^{dif}, 0)$
  end if
end for
=0

3.3.3 Notes on the Iterative Hungarian Algorithm

The Hungarian algorithm was found to be an optimal solution method for the assignment problem for square matrices in strongly polynomial time. This method remains optimal as long as the number of workers is identical to the number of resources to be assigned. If this is not the same, as in the problem considered, the optimal solution cannot be found so readily. One either strives for optimality using algorithms for complete searches in combinatorial optimisation, such as the branch-and-bound [130], or applies a sub-optimal solution, such as the IHA. In [131], the authors have compared these two methods and have noted that the IHA is able to reach a solution close to the optimal one found by the branch-and-bound (up to 96.5% of the optimal solution) at a significantly reduced computational complexity (the IHA converges in 3.8% of the time required by the optimal method). In [132], the authors compare the IHA with an optimal myopic search for dynamic spectrum access. They show that the former reaches solutions very close to the optimal method but the computational complexity reduced by 25 times. The IHA is then able to reach a good sub-optimal solution at the fraction of an exhaustive search.

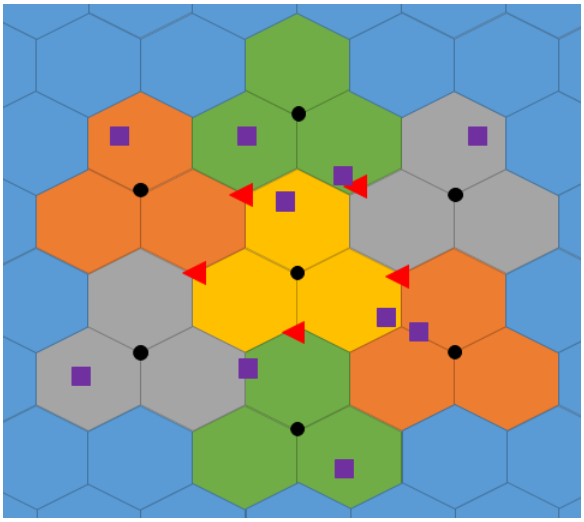

Figure 3.7: Network simulated with hexagonal macrocells (•) and pico (△) and femtocells (□) disseminated within their coverage area

3.4 ICIC Results

In this section the simulation scenarios and performance results are presented and discussed. A downlink heterogeneous LTE network has been simulated with 7 macrocells and 5 picocells placed around the central macrocell. A fixed number of 10 randomly placed femtocells is used. The number of cells and the other simulation parameters were chosen so that at least a ring of macrocells would be simulated around a central cell subject to interference from its neighbours and small cells, while, at the same time, keep the overall computational load manageable. Users are randomly scattered over the area and feature constant mobility for the whole duration of the simulations. Figure 3.7 presents the network under test, where the hexagons represent the sectors of the macrocells, the triangle represent the picocells and the squares represent the femtocells.

The network operates in full buffer and full CSI accuracy is assumed. The throughput, the signal power received by each user and the behaviour of each cell are recorded and analysed. A mixed indoor-outdoor environment has been considered for the pathloss, with the parameters presented in [45]. For all the simulations the internal cell resource allocation is performed with the Iterative Hungarian Scheduler [13]. The simulation parameters are contained in table 3.1.

Parameters	Symbols	Values
Number of macrocells	M	7
Sectors per macrocell	S	3
Inter macrocell distance		500 m
Macrocell radius		150 m
Macro users per sector	X_m	20
Macro transmit Power		46 dBm
Number of picocells	P	5
Picocell radius		20 m
Pico users per sector	X_p	4
Pico transmit Power		20 dBm
Number of femtocells	F	10
Femtocell radius		10 m
Femto users per sector	X_f	2
Femto transmit Power		10 dBm
System bandwidth		20 MHz
Available Resource Blocks		100
Carrier frequency		2.1 Ghz
Propagation model		WINNER II model [11]
Internal base station scheduler		Hungarian scheduler
Antenna configuration		SISO
Traffic model		Full buffer
Minimal throughput requested	th	1 Mbps

Table 3.1: System parameters for LTA-A ICIC simulations

3.4.1 Results for homogeneous networks

The average throughput of the macrocell users in a homogeneous LTE downlink network is analysed; the users are organized in percentiles, these represent the portions of the users in the bottom % of their categories: the 5^{th} percentile users are the bottom 5% of the overall users, usually referred to as "cell edge users". The 100^{th} percentile, on the other hand, represents the average cell rate. In these simulations the proposed method is compared to the standard resource allocation (where no interference coordination is applied and only the internal allocation is performed) and the frequency reuse 3 where each cell uses one third of the available bandwidth, not overlapping with the neighbours, thus avoiding interference. The gains of the proposed method and the frequency reuse 3 technique over the non-coordinated solution are presented in Figure 3.8, where ICIC is the proposed method.

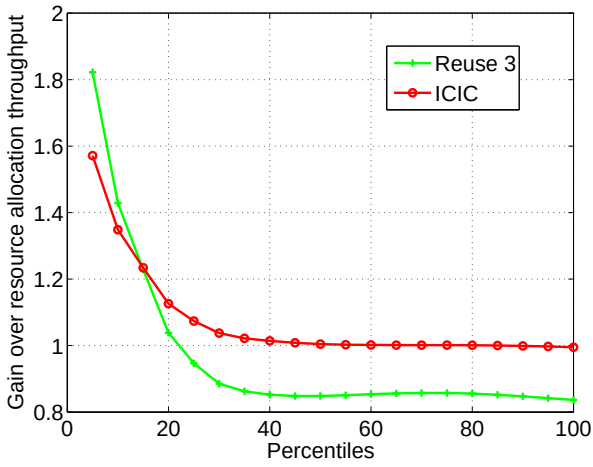

Figure 3.8: Average gain of ICIC and Reuse 3 methods over no coordination in a homogeneous network

Figure 3.8 shows that, since the proposed ICIC method is designed to target mainly the users which suffer from interference and are poorly served (lowest 5-10%), it achieves high gain for low percentiles and no loss for high ones. On the contrary the "Reuse 3" method targets the whole bandwidth achieving high gain for the poorest served users but very high losses for all the other ones. The proposed method reaches, then, 86% of the gain of the other solution without any of its drawbacks.

3.4.2 Results for heterogeneous networks

Once the solution is extended to a heterogeneous network, with the parameters contained in Table 3.1, the impact of the proposed method on macrocell users decreases as the macro users now witness additional interference coming from the pico- and femto-cells and there are more cells which have to coordinate for the same amount of resources and the method can only address the highest interferer. Figure 3.9 presents the gains of the proposed solution for macro, pico and femto users (without any power control on pico or femto cells but only restricting the interfering RBs completely).

It is noticeable that both macro and pico cell edge user performances increase considerably, with a slight (4%) loss for the highest performing macrocell users; this is due to the fact that picocells still interfere for those users but they

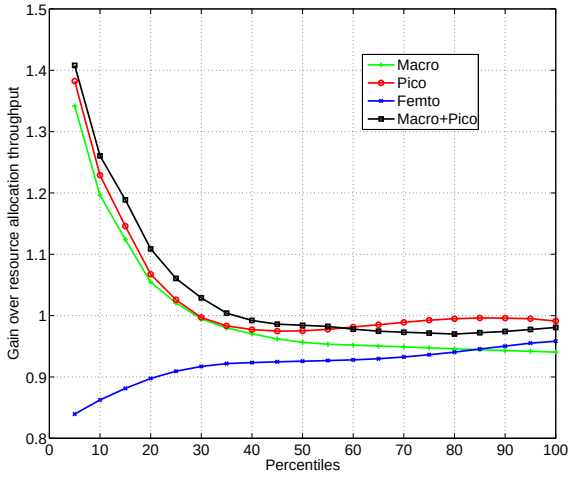

Figure 3.9: Gains of proposed method for macro, pico and femto users over resource allocation without any power control

do not get selected by the proposed method because of their good channel quality conditions (as the proposed solution only targets starved users). The combined gain for macro and pico users is shown in the black curve. On the other hand, femtocell users witness a lower performance due to the absence of communication between the tiers.

If power water-filling is allowed for pico and femto base stations in order to minimize losses, while still reducing overall interference the gains improve as shown in Figure 3.10. At the price of a very slight loss for macrocells users (2%) due to the minimal increase in interference due to the non complete restriction in transmission power we see an increase in performance in both pico and femto users (10% and 4% respectively). The effect on the combine macrocell and picocell users shows that the picocell users tend to have higher throughput than the macrocell ones and thus the gains at lower percentiles are higher when compared to the previous implementation in Figure 3.9 but less than for just the picocell users. On the other hand, the complete gain shows also an improvement for the high percentiles, reducing the loss to 3%. The results show that the proposed method works well and allows for a consistent increase in performance for the macro and pico users which outperforms traditional static solutions.

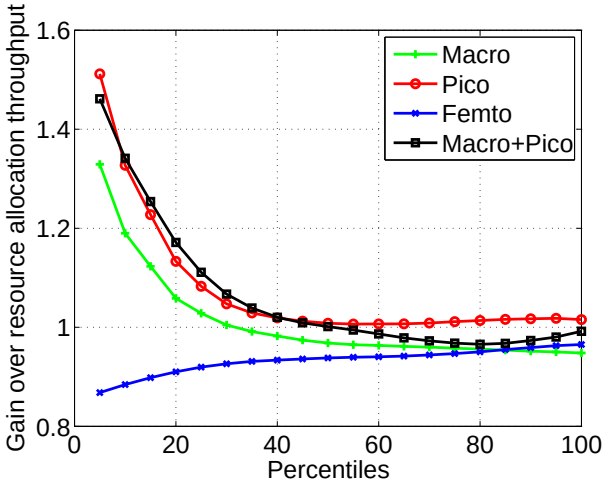

Figure 3.10: Gains of proposed method for macro, pico and femto users over resource allocation with power control

3.5 Conclusions

In this chapter a cooperative distributed heuristic algorithm for interference management in heterogeneous LTE networks was presented. The proposed scheme efficiently allocates resources and reduces interference as it adapts to the network conditions. The method proposed here is scalable and adapts well to the dynamic behaviour of HetNets. Comparisons to well known reference methods show that the proposed method delivers a consistent gain for the starved user's data rate in both homogeneous and heterogeneous networks. The scheme requires only communication between macro and pico base stations while the femtocells operate autonomously. It generates a gain of 45% for the combined macro and pico edge users at a very small cost for the cell center lower than 4%. It optimises greatly picocell performance, with improvements of more than 50% at a small cost for femtocell users (15%).

In the next chapters a new framework to study the effects of CSI quantization on the resource allocation and ICIC are presented.

Chapter 4

Reducing the Signalling Overhead in the Frequency Domain

In this chapter, the influence of signalling information on the downlink and uplink throughput is quantified and solutions which allow to lower the amount of CSI information in the frequency domain, while maintaining high performance, are presented. First, the standard compliant LTE-A signalling mechanisms are analysed and the need for a novel, flexible feedback scheme is discussed; such scheme is presented and a model to determine the impact of signalling on the system's performance is introduced. In order to provide the base stations with the means to assign a flexible and on-demand amount of feedback, reinforcement learning solutions are presented in order to find optimal operating points. Furthermore, the proposed signalling reduction method is applied to the ICIC solution presented in the previous chapter and results show that performance can be increased overall in the network by transmitting the control information with higher accuracy where it is most useful rather than using averaging methods.

4.1 CSI feedback in LTE and its limitations

As introduced in Section 2.2.1, the LTE standard allows for three different CSI reporting techniques in the frequency domain:

- Wideband: each user transmits a single 4-bit CQI value for all the RBs in the bandwidth.
- Higher Layer configured or subband level: the bandwidth is divided into subbands of consecutive RBs and each user feeds back to the base station one 4-bit wideband CQI and a 2-bit differential CQI for each subband.
- User-selected, or $Best-M$: each user selects M preferred subbands of equal size and will transmit to the base station one 4-bit wideband CQI, a single 2-bit differential CQI value that reflects the channel quality only over all the selected M subbands and the positions of these subbands in the bandwidth. The number M of selected subbands is bandwidth dependent and fixed.

The three standard compliant feedback schemes do limit the amount of overhead information transmitted by the users but they do not allow the base station to request a variable amount of feedback to the user. This could be particularity interesting to, first, study the impact that control information has on the data rate and, secondly, enhance multi-user diversity by allowing different quantities of CQI feedback to users based on their channel conditions. On top of the standard compliant feedback schemes, two extra FB allocation mechanisms have been implemented in order to understand the effects that feedback scarcity has on the downlink capacity.

- Full feedback scheme: each user transmits a 4-bit wideband CQI value and a 2-bit differential CQI for each RB. This scheme gives an indication of the maximum capacity the network can achieve when full feedback resolution is available.
- Variable $Best-M$: This scheme is a flexible implementation of the user-selected one above. The number of subbands M is adapted as a function of the number of users and the system's conditions. Also, there will be a 2-bit differential CQI value fed back for each subband instead of a single one valid across all subbands.

These two different reporting schemes can provide a large amount of feedback information, in case of the former, and can deliver this information where more necessary in case of the latter.

In the following section, a model to determine the impact of feedback information on a cell's performance is introduced.

4.2 Feedback Model

In this section, the amount of resources required by the feedback is quantified and a mathematical model is provided. This model will be combined with simulation results providing spectral efficiency obtained by scheduling with reduced feedback, in order to optimise the amount of signalling for the maximal network net capacity. Table 4.1 includes the bit cost of the different feedback allocation methods presented in the previous section for a number of served users N_U and for N_{RB}^{DL} downlink RBs .

Feedback Scheme	Bit cost
Wideband	$2 \cdot (4 \cdot N_U)$
Subband level	$2 \cdot (4 + 2 \cdot q) \cdot N_U$
User-selected	$2 \cdot (4 + 2 + \lceil log_2 \binom{N_{RB}^{DL}}{M} \rceil) \cdot N_U$
Full feedback	$2 \cdot (4 + 2 \cdot N_{RB}^{DL}) \cdot N_U$
Variable Best-M	$2 \cdot (4 + 2 \cdot M + \lceil log_2 \binom{N_{RB}^{DL}}{M} \rceil) \cdot N_U$

Table 4.1: Bit cost of the various feedback schemes

The equations expressed in table 4.1 refer to a single stream of data. If the system makes use of Multiple Input Multiple Output (MIMO), the amount of feedback necessary is multiplied by the number of streams. This does not affect the relation to the network's capacity since it is also scaled by the same factor, if UL MIMO is also used for transmitting the feedback information.

Figure 4.1 shows the amount of feedback required for the different schemes as a function of the number of users with a 20MHz (100 RBs) UL bandwidth using QPSK modulation. The Figure shows that the full feedback scheme is practically not achievable but also the standard compliant methods can utilise more than 20% of the overall uplink bandwidth for 100 users.

In order to quantify the portion of resources required by the feedback, it is beneficial to redefine the number of feedback bits into modulation symbols since the uplink and downlink channels can carry only a specific number of symbols per RB.

The uplink bandwidth of the LTE system, even though it makes use of SC-FDMA instead of OFDMA, also uses RBs and contains an identical number of modulation symbols per physical resource block as the downlink. Each RB can carry 84 modulation symbols and has a duration of 0.5 ms. The symbol rate is then $S = S_{ul} = S_{dl} = 168 \cdot 10^3 \cdot N_{RB}^{DL}$, in the downlink and in the uplink [32].

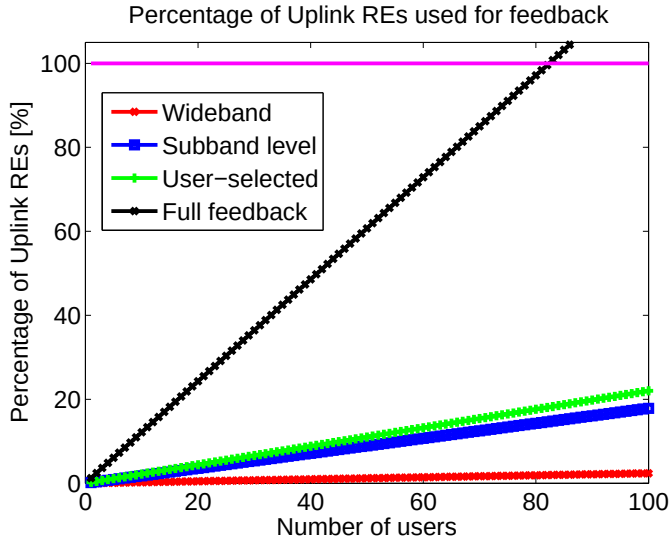

Figure 4.1: Portion of Uplink used by FB

The relation between Baud rate S and the bit rate T is given by:

$$S = \frac{T}{\gamma}, \tag{4.1}$$

where γ is a coefficient which determines how many bits are carried in a symbol; it depends on the modulation and the code rate used. The modulations supported by uplink LTE are QPSK, 16QAM and, only for a highest category of mobile users, 64QAM [32]. Which means that each uncoded modulation symbol can carry either 2, 4 or 6 bits for QPSK, 16QAM and 64QAM respectively.

The amount of feedback can then be expressed in modulation symbols, and is here called S_{fb}.

The total amount of data transmitted, per second, is defined as:

$$T_{tot} = T_{dl} + T_{ul} = T_{dl} + T_{ul,data} + T_{ul,fb}, \tag{4.2}$$

where T_{dl} and T_{ul} represent the amount of bits being transmitted in the downlink and the uplink at each frame. $T_{ul,data}$ is the amount of payload-only throughput in the uplink and $T_{ul,fb}$ is the feedback throughput obtained by multiplying the bit values expressed in table 4.1 by 10^3 as each frame is 1 ms long.

Using Equation (4.1) it is possible to define (4.2) as:

$$T_p = \gamma_{dl} \cdot S_{dl} + \gamma_{ul} \cdot S_{ul} - \gamma_{fb} \cdot S_{ul,fb}, \tag{4.3}$$

where $T_p = T_{dl} + T_{ul,data}$ is the throughput of the payload data in both uplink and downlink. γ_{ul} and γ_{fb} are considered, generally, different as the system might request a more robust modulation for signalling information over payload data. Since $S = S_{ul} = S_{dl}$, Eq. (4.3) can be written as:

$$T_p = (\gamma_{dl} + \gamma_{ul}) \cdot S - \gamma_{fb} \cdot S_{ul,fb}. \tag{4.4}$$

One of the main problems in determining the uplink channel parameters, is that uplink and downlink are generally not symmetrical. In case of TDD LTE uplink and downlink bandwidth could be exchanged if more traffic is demanded on one of the two, making the trade-off very relevant. If FDD LTE is used, on the other hand, the downlink and uplink frequency bands are separate. Nevertheless, the amount of feedback information is still reducing the amount of uplink bandwidth available. In order to model the impact, on the uplink performance, of feedback signalling in a downlink simulator we impose $\gamma_{dl} = 4\gamma_{ul}$, as the LTE downlink spectral efficiency can be up to 4 times higher than the LTE uplink spectral efficiency [32]. Equation (4.4) becomes then

$$T_p = \frac{5}{4}\gamma_{dl} \cdot S - \gamma_{fb} \cdot S_{ul,fb}. \tag{4.5}$$

Finally, γ_{dl} is obtained directly from (4.1):

$$T_p = \frac{5}{4}T_{dl} - \gamma_{fb} \cdot S_{ul,fb}. \tag{4.6}$$

Using equation (4.6) it is possible to determine whether adding feedback to the system actually improves its performance. More feedback would, on the one hand, reduce the amount of symbols available for the payload (higher $S_{ul,fb}$) but, on the other hand, increase the downlink throughput T_{dl}. In order to quantify the effect of each user on the total useful throughput T_p, is possible to redefine it as the sum of the contribution of each user u:

$$T_p = \sum_{u=1}^{N_U} T_p^u = \sum_{u=1}^{N_U} \left(\frac{5}{4} T_{dl}^u - \gamma_{fb}^u \cdot S_{ul,fb}^u \right). \tag{4.7}$$

For the remainder of this paper a value of $\gamma_{fb} = 2$ has been chosen; this is indicative of a 16QAM modulation with a coding rate of 1/2.

4.3 Feedback Impact

4.3.1 Schedulers

In order to determine the impact of the resource allocation mechanisms on the feedback amount, three different schedulers have been implemented: the Best-CQI (BCQI), Proportional Fair (PF) and Max-Min (MM). The first is a maximum throughput scheduler in which only the users with best channel quality are served and the last one is the ultimately fair algorithm which allocates the same amount of RBs to all users in order to maximise their worse rate. The PF, on the other hand, is somewhere in between and allocates resources in order to maximise downlink throughput while maintaining a certain amount of fairness.

4.3.2 Simulation Parameters

The system has been simulated using the open source VIENNA system level simulator [45]. An urban multicell environment is considered to include the effects of multipath propagation and interference. Adaptive modulation and coding are used by the base station to allocate resources to the users. To model the impact of feedback on a cell's resource allocation, no cooperation between cells is initially considered. ICIC techniques are then introduced to investigate how feedback scarcity can influence the whole network's performance. The simulation parameters are included in table 4.2.

Parameters	Values
Number of Macrocells	7
Sectors per Macrocell	3
Inter-cell distance	500 m
Macro antenna gain	15 dB
Macro Transmit Power	46 dBm
Macro users per sector	2 to 100
Frequency	2.1 GHz
System Bandwidth	20 MHz
Number of RBs	100
Access technology	OFDMA FDD
Number of antennae	1(Tx and Rx)
Channel model	Winner Channel Model II [11]
Block fading mean	0 dB
Block fading deviation	10 dB
Fast fading	10 dB
Thermal noise density	-174 dBm/Hz
Users speed	1 m/s

Table 4.2: System parameters for the LTE-A feedback reduction in frequency

4.3.3 Impact of resource allocation on FB selection

The influence of the different FB allocation strategies for the three schedulers is presented in figures 4.2 - 4.4. These figures show the throughput T_p gain of the different strategies over the subband-level allocation for a varying number of served users. The x-axis shows the feedback method used for the simulations, where $BM1$ indicates the *Variable Best-M* with $M = 1$ and $BM2$ the *Variable Best-M* with $M = 2$ and so on. UES and SBL are instead representative of the *user-selected* and *subband-level* feedback mechanisms.

When the BCQI scheduler is employed, the eNodeB maximises the downlink capacity; the best FB allocation strategy allows the users with best channel quality to obtain the highest throughput. As the number of cell users increases, the impact of FB information becomes increasingly relevant and with 100 concurrent users, the highest number of concurrent transmissions in an LTE cell, choosing the *Variable Best-M* with $M = 1$ FB allocation brings about a 6% gain in total throughput. This limited effect can be ascribed to the BCQI scheduler exploiting multi-user diversity and selecting few users which might contribute to most of the downlink throughput.

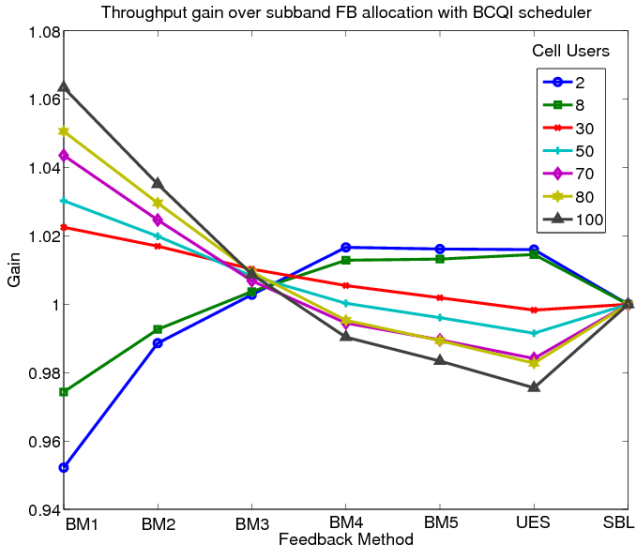

Figure 4.2: Throughput gain for BCQI Scheduler for various FB allocation strategies

The results for the PF scheduler are presented in Figure 4.3. In this case a much larger gain of 20% with 100 users can be achieved. This gain can be attributed to the inherent trade-off between throughput and fairness of the PF scheduler. As the number of users increases, each individual user gets allocated less RBs, thus less knowledge of the complete bandwidth is necessary.
Furthermore, if a limited amount of RBs are assigned, the *Variable Best-M* FB allocation allows the base station to have a better information of the users' channel quality only in the portion of bandwidth most likely to be assigned.: i.e. if only 3 RBs are going to be assigned a *Variable Best-M* with $M = 1$ strategy averages the CQIs over 4 RBs instead than over 8, like with the *subband level* strategy.

Finally, Figure 4.4 presents the results for the MM scheduler. This scheduler tries to maximise the fairness by improving each user's worst-RB throughput. Even though this algorithm is the opposite of the BCQI, the impact of FB allocation on the throughput is similar. This is due to the fact that, even though more reliable information is available in the M best subbands fed back by the users, the scheduler is designed to maximise the worst rate and thereby to increase the likelihood that the users are scheduled on a portion of the bandwidth that only reports the wideband CQI. Thus there is not a real improvement in the downlink rate but the gain comes from not having a loss

while reducing FB overhead.

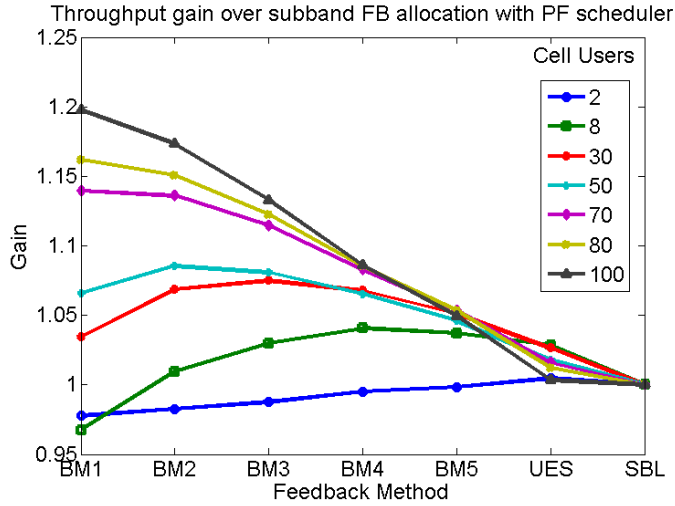

Figure 4.3: Throughput gain for PF Scheduler for various FB allocation strategies

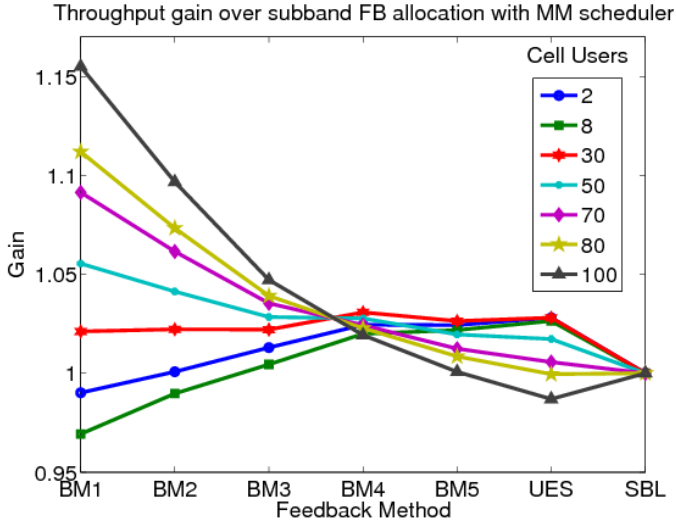

Figure 4.4: Throughput gain for MM Scheduler for various FB allocation strategies

The *Variable Best-M* feedback strategy allows a then base station to vary the

amount of feedback necessary to maximise payload throughput according to the number of served users and to the fairness of the resource allocation method.

If the base station were to allocate the FB dynamically to each user differently, the multi-user diversity could be better exploited. Figure 4.5 presents a comparison between a homogeneous and a dynamic multi-user FB allocation. The curves in the continuous line represent the best gains for the different number of users of Figures 4.2 - 4.4. The curves with dotted line represent the improvement obtainable by performing a dynamic multi-user resource allocation. In order to obtain the results for a dynamic multi-user FB allocation, the simulations have been run at full feedback and the resource allocation decisions of the base stations have been recorded. Afterwards, the simulations have been re-run and only the appropriate amount of FB, computed with the previously obtained results, has been allocated.

As the BCQI is the scheduler that better makes use of multi-user diversity, it is also the one that benefits the most from a dynamic FB allocation. Since the MM scheduler maximises fairness, the amount of RBs allocated to each user tends to be equal; this way the benefit of a dynamic FB resource allocation is lost. The PF scheduler makes use, albeit to a lesser extent than the BCQI, of multi-user diversity, and thus sees an improvement with dynamic FB allocation. The gains of the dynamic FB allocation over the static one, in percentage, are

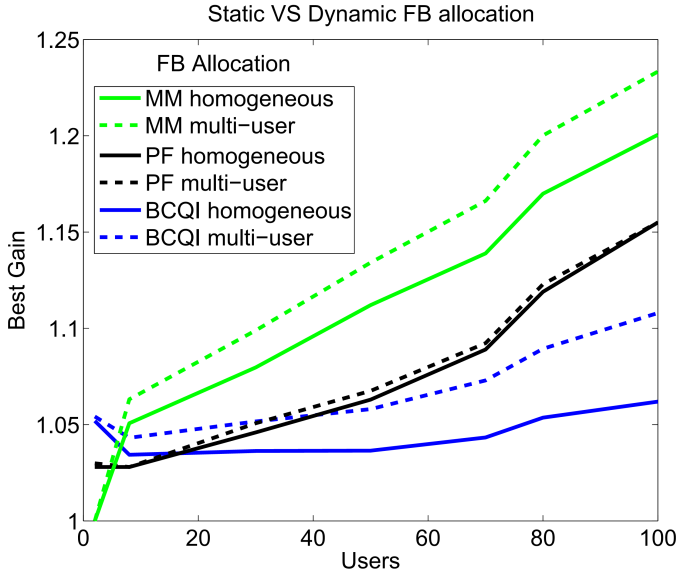

Figure 4.5: Gain of dynamic FB VS static FB allocation

presented in table 4.3. The results for the Max Min scheduler are omitted as the performance improvement was within 0.5% for all users configuration.

Users/Schedulers	Best CQI	Proportional Fair
2	0.25	0
8	1	1.2
30	1.6	2
50	2.2	2.2
70	3	2.7
80	3.8	3
100	5	3.3

Table 4.3: Percentage gain of dynamic FB allocation over static one for BCQI and PF schedulers

4.4 Reinforcement Learning Solutions

A dynamic controller, capable of positioning the eNodeB in an optimal operating point with respect to the FB allocation, is a desirable device. In the previous section, the proposed variable best-M FB strategy has been proven effective but the system is not able to adjust the number of subbands necessary dynamically with an unknown resource allocation strategy.

Such system has to learn from the cell's current and previous behaviours and makes an informed and intelligent decision on the amount of FB to be allocated to the users. Learning methods have been used successfully in wireless networks and reinforcement learning (RL) is a family of techniques which seems to work particularly well in the context of self-organization and resource allocation problems in LTE [133–136].

Differently than the ICIC problem from the previous chapter, the problem considered here is not just an optimization problem but it concerns a system with unknown properties. The IHA has shown to provide a good solution to the resource allocation problem but the weight of each assignment had to be known before hand. The effects of feedback allocation on a user, on the other hand, depend on that user's channel quality and on which, unknown, resource allocation method used by the base station. A learning approach, thus, has been selected to reduce the assumptions on the nature of the environment and allow an agent to reach a solution with limited previous knowledge.

A great advantage of RL over other learning techniques is its model-free nature. It does not require an extensive representation of the environment and it learns incrementally, without a teacher, until enough information is obtained by the agent.

4.4.1 Reinforcement Learning Structure

Reinforcement learning allows an agent to learn from its environment by acting upon it and observing the effects of such actions. The general structure of RL is depicted in Figure 4.6.

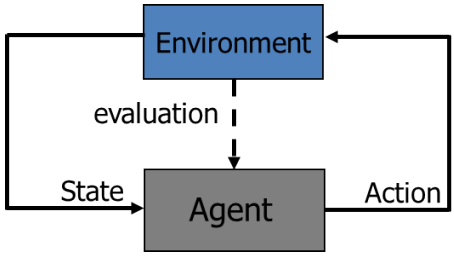

Figure 4.6: RL structure

In order for RL to be applied, the system has to be described as a Markov Decision Process (MDP). An MDP is a discrete time stochastic control process useful for systems where the outcome of a decision is partly in control of the agent and partly random. Such process is defined by a 5-tuple :

- A discrete number N_S of states $\mathbf{S}$: at each time t the agent monitors the environment via a set of states $\mathbf{S}(t) = s^1(t), s^2(t), s^3(t)...s^{N_S}(t)$.
- A discrete set of actions $\mathbf{A}$: once the condition of the environment is known, the agent performs a different action according to the values of the input states.
- A reward function $\mathbf{R}$: after the actions have been taken, the environment has changed and the states have now shifted from $\mathbf{S}(t)$ to $\mathbf{S}(t+1)$. Associated with this state changes is then a reward $r(t+1)$ indicative of the benefit of such change.
- A state transition function $P^i_{\mathbf{S}(t),\mathbf{S}(t+1)}(a)$ which maps the probability that environment's state will shift from $\mathbf{S}(t)$ to $\mathbf{S}(t+1)$ given that action $a(t)$ is taken at step t.

- A discount factor γ which determines the influence of future rewards over the current ones.

The purpose of RL is to find the optimal policy π_s^* that maximises the reward for each state s. In the case of *infinite horizon model*, where the lifetime of the agent is unknown a priori, the *value function* that determines which π_s^* is the optimal policy is defined as:

$$V^*_{\mathbf{S}(t)} = \max_{\pi} \mathbb{E}\left(\sum_{t=1}^{\infty} \gamma(t) \cdot r(t)\right), \tag{4.8}$$

where $\mathbb{E}$ is the expected value operation and π is the complete decision policy and $\gamma(t) \in [0, 1]$ is a discount factor which limits the influences of future rewards. $V^*_{\mathbf{S}(t)}$ is then the maximum infinite sum of the discounted rewards that the agent would obtain if it started from state $\mathbf{S}(t)$ and followed policy $\pi^*_{\mathbf{S}(t)}$. Using Bellman's analysis [137] it is possible to determine that such policy exists and that the solution to the value function is unique and given by:

$$V^*_{\mathbf{S}(t)} = \max_{a(t)} \left(r(t+1) + \gamma(t) \sum_{\mathbf{S}(t+1)} P_{\mathbf{S}(t),\mathbf{S}(t+1)}(a(t)) \cdot V^*_{\mathbf{S}(t+1)}\right), \tag{4.9}$$

The value given to the current state $\mathbf{S}(t)$ is then equal to the reward for taking action $a(t)$ summed with the discounted value of the next state when the best action is taken. The optimal policy is then the argument that maximises (4.9):

$$\pi^*_{\mathbf{S}(t)} = \arg\max_{a(t)} \left(r(t+1) + \gamma(t) \sum_{\mathbf{S}(t+1)} P_{\mathbf{S}(t),\mathbf{S}(t+1)}(a(t)) \cdot V^*_{\mathbf{S}(t+1)}\right). \tag{4.10}$$

For each policy, the value of taking action $a(t)$ in state $\mathbf{S}(t)$ following policy π_s can be determined. The *action-value function* $q_{\pi^*}(\mathbf{S}(t), a(t))$ obtained with the optimal policy $\pi^*_{\mathbf{S}(t)}$, is then defined as:

$$q^{\pi^*}(\mathbf{S}(t), a(t)) = \left(r(t+1) + \gamma(t) \sum_{\mathbf{S}(t+1)} P_{\mathbf{S}(t),\mathbf{S}(t+1)}(a(t)) \cdot V^*_{\mathbf{S}(t+1)}\right). \tag{4.11}$$

Generally, it is rarely possible to generate optimal policies. It is very computationally and memory intense to find the state-transition probabilities in the MDP 5-tuple. A different flavour of reinforcement learning, Q-learning, avoids this problem by exploring the search space without requiring the state-transition probabilities.

4.4.2 Q-Learning Structure

Q-learning (QL) is one method of the reinforcement learning family designed to find an optimal action-selection policy by acting upon the environment and determining the impact the action has caused on the following state. By taking and action in a given state, the QL agent learns an action-value function, from which an optimal policy is constructed. Specifically, the QL agent finds a function $Q(s(t), a(t))$ which converges to an optimal value $q^{\pi^*}(s(t), a(t))$ independently of which policy is followed [138].

The system consists of an agent and its environment. Each agent can be in any state $s \in \boldsymbol{S}$, can perform any action $a \in \boldsymbol{A}$ to pass from the current state to the next one. Once the action is performed and the new state acquired, a reward r is obtained. The objective of the agent is to maximise the total expected reward. The optimal action, for each state, is the one that presents the highest long term reward. The *learned action-value function* $Q(s(t), a(t))$, also called *Q-value*, is defined as:

$$Q(s(t), a(t)) \leftarrow Q(s(t), a(t)) + \beta \left[r(t+1) + \gamma(t) \max_a Q(s(t+1), a) - Q(s(t), a(t)) \right] \tag{4.12}$$

where the *learning factor* $\beta \in [0, 1]$ weights the influence of previous experiences. The smaller the learning factor, the higher is the effect of previous Q-values. A high value of γ weights greatly the influence that the best action taken for the state $s(t+1)$ has in taking the current action $a(t)$. The system builds, thus, a Q-Table of size $\mathbf{S} \cdot \mathbf{A}$ and updates the Q-values at each time interval t. All that is required for the convergence of the function is that all state-action pairs are visited [19]; this requirement forces the design of an *exploration-exploitation* policy so that the Q-Table can be completed. In the most common strategy, named $\epsilon - greedy$, the agent chooses an action $a(t+1)$ such as:

$$a(t+1) = \begin{cases} \arg\max_a Q(s(t+1), a), & \text{with probability } (1-\epsilon) \\ random, & \text{with probability } \epsilon \end{cases} \tag{4.13}$$

This method allows for continuous exploration with a non-zero ϵ. The value has to be carefully selected so that the systems has enough randomness to visit every action-state pair but is able to exploit the Q-Table so to converge to the optimum. Alternatively, an other frequently used solution assigns high exploration at the beginning of the learning process and gradually diminishes the value, increasing exploitation. A common example of such strategy is given by

$$Pr(a(t+1)) = \frac{e^{\frac{Q(s(t+1), a(t+1))}{\tau}}}{\sum_a e^{\frac{Q(s(t+1), a)}{\tau}}}, \tag{4.14}$$

where τ is a temperature function which decays with time [137]. At the beginning the actions are all equally probable and, as time progresses and the Q-Table is built, the actions with highest Q-values will be selected more often. In this work, the problem of determining the correct FB allocation in an LTE network is approached. Since the base station has to decide on the next allocation based on the information fed back by the users, without loss of generality, instead of the transition between times t and $t+1$, the transition $t-1$ to t is evaluated and the action analysed is $a(t-1)$ instead of $a(t)$.

4.4.3 Q-Learning homogeneous FB allocation

For this implementation the learning agent is placed in the eNodeB and has to select a single FB allocation strategy based on the number of served users.

In order to determine the reward for each action, the value of T_p, determined in Eq. (4.6), is chosen. $T_p$depends on the users' channel quality and on the resource and FB allocation strategies. This means that different channel qualities can give very different results even though the FB allocation strategy remains unchanged. For these reasons the payload throughput is not used as an input state but as the reward function. The state, actions and rewards of the algorithm are here defined.

States

The state of the base station at time t is defined as

$$\mathbf{S}(t) = \{CQI_{avg}(t), N_{UE}(t)\}\,. \tag{4.15}$$

Where $CQI_{avg}(t)$ is the average CQI reported by all the users; this is used in order for the base station to account for channel fluctuations normally occurring in a wireless scenarios and for other effects such as user mobility and interference. A finite number S_{CQI} of quantized CQI states is available for $CQI_{avg}(t) \in \{1...S_{CQI}\}$. Each user's reported CQI is partially function of the feedback allocation method chosen, as seen in previous sections, the feedback allocation method will have a user report on portions of the bandwidth with more or less accuracy. N_{UE} is the number of users served by the eNodeB.

Actions

The set of actions A the agent can take are the different FB methods described in section 4.2; There are then 7 possible actions as shown in table 4.4.

action a	FB allocation
1	Var. Best M with $M = 1$
2	Var. Best M with $M = 2$
3	Var. Best M with $M = 3$
4	Var. Best M with $M = 4$
5	Var. Best M with $M = 5$
6	User-select
7	Subband-select

Table 4.4: Possible actions and their relative FB allocation strategies

Reward

The throughput $T_p(t)$ determines if the action taken in the previous interval $a(t-1)$ has been beneficial or not. An **impact matrix** $\boldsymbol{I}$ which puts in relation the system's state, the actions and the throughput $T_p(t)$, is used. This matrix has size $S_{CQI} \cdot A \cdot N_{UE}$ and each entry has value:

$$I(CQI_{avg}(t), a(t-1), N_{UE}(t)) = \begin{cases} T_p(t), & \text{if } \; T_p(t) > I(CQI_{avg}(t), a(t-1), N_{UE}(t)) \\ I(CQI_{avg}(t), a(t-1), N_{UE}(t)), & \text{otherwise} \end{cases} \tag{4.16}$$

The condition that the current value has to be greater than the previous one, in order for the matrix to be updated, is taken from [139], where the authors have shown a greater convergence when this condition is enforced in reinforcement learning.

The reward $r(t)$ is then assigned based on the entries in $\boldsymbol{I}$:

$$r(t) = \frac{I(CQI_{avg}(t), a(t-1), N_{UE}(t))}{\max I(CQI_{avg}(t), :, N_{UE}(t))}, \tag{4.17}$$

Learning

The Q-Table **QT** has then the same dimensions as the impact matrix **I** and is updated at every time step t following equation (4.12). Once **QT** has been updated a new action is selected at instant t based on equation (4.14) for $t+1$. The algorithmic representation of this implementation is shown in Algorithm 4.

Algorithm 4 QL implementation for homogeneous FB allocation

Initialization:
$t = 0$
$\boldsymbol{Q - Table} \leftarrow \emptyset$
$\boldsymbol{I} \leftarrow \emptyset$
choose random action $a(0)$
for t **do**
    (1) Receive feedback from the users;
    Evaluate input state:

$$S(t) = \{CQI_{avg}(t), N_{UE}(t)\}$$

    (2) eNodeB performs resource allocation with one of the schedulers described in Section 2.3.1 .
    (3) Measure the payload throughput $T_p(t)$.
    (4) Update impact matrix $\boldsymbol{I}$ as in (4.16):

$$I(CQI_{avg}(t), a(t-1), N_{UE}(t)) = \begin{cases} T_p(t), & \text{if } T_p(t) > I(CQI_{avg}(t), a(t-1), N_{UE}(t)) \\ I(CQI_{avg}(t), a(t-1), N_{UE}(t)), & \text{otherwise} \end{cases}$$

    (5) Compute reward $r(t)$ based on (4.17)

$$r(t) = \frac{I(CQI_{avg}(t), a(t-1), N_{UE}(t))}{\max I(CQI_{avg}(t), :, N_{UE}(t))};$$

    (6) Update the Q-Table $\boldsymbol{QT}$ as described in (4.12):

$$Q(S(t-1), a(t-1)) \leftarrow Q(S(t-1), a(t-1)) + \beta \left[r(t) + \gamma \max_a Q(S(t), :) - Q(S(t-1), a(t-1)) \right],$$

    (7) Choose action $a(t)$ which determines which FB strategy will be used in the next iteration (4.14):

$$Pr(a(t)) = \frac{e^{\frac{Q(S(t),a(t))}{\tau}}}{\sum_a e^{\frac{Q(S(t),a)}{\tau}}},$$

end for=0

4.4.4 Q-Learning multi-user FB allocation

In case of a dynamic multi-user FB allocation, different users will be able to use different FB methods based on how much they contribute to the system's throughput and how their channel qualities are distributed within the cell. This implementation is built directly from the homogeneous one, the structure remains almost unchanged, the major difference is given by the input states which have now to consider, on top of the absolute channel qualities, the data rates of each user and their distribution with respect to each other.

The design of the QL system is explained in the following subsection.

States

The purpose of the agent is to assign a specific FB allocation method to a user given its channel quality. A new, relative channel quality value CQI^u_{rel}, is then introduced to compare the users to each other:

$$CQI^u_{rel} = CQI^u(t) - CQI_{avg}(t), \forall \text{user u} \tag{4.18}$$

The users are then divided into $N_Q = 5$ categories using the thresholds in table 4.5. The number of channel quality categories has been fixed to 5 as this was found to bring a good compromise between being able to differentiate the channel quality witnessed by the users with enough accuracy (i.e. by being able do capture the overall quality spread) without having to make a category for all possible CQI values.

Channel Quality	Very Low (VL)	Low (L)	Average (M)	High (H)	Very High (VH)
CQI^u_{rel}	-5	-2	0	+2	+5

Table 4.5: Channel quality categories and CQI thresholds

The state of the base station at time t is then defined as

$$S(t) = \{CQI_{avg}(t), Q_{channel}(t)\}\,. \tag{4.19}$$

Where $CQI_{avg}(t)$ is the average CQI of all the users and $Q_{channel}(t)$ indicates whether users of each category are present (e.g. if there are users with channel qualities "Average" and "Very High" then $Q_{channel}(t) = [0\ 0\ 1\ 0\ 1]$).

Actions

The set of available actions is the same as defined in section 4.4.3. The only difference with the previous implementation is that now N_Q actions are chosen at each time t instead of 1.

Rewards

Differently than in the single FB allocation algorithm, here the throughput contribution of each user category, $T_Q(t)$ is considered. The value is obtained from $T_p^u(t)$, defined as:

$$T_Q(t) = \frac{1}{N_{U_Q}} \sum_{u^*}^{N_{U_Q}} T_p^{u^*}(t), \forall Q = 1 \cdots N_Q \tag{4.20}$$

where N_{U_Q} is the number of users belonging to the category Q. $T_Q(t)$ represents the throughput contribution of the users in the different quality categories, normalized for one user. The range of these values can vary considerably since it is dependent on the absolute channel quality; it is further impossible to infer if users in a specific category are served consistently more than users in other categories. For example, a user with $CQI^u(t)$ equal to 10 might be in a "Very Good" channel quality group if the average cell CQI $CQI_{avg}(t)$ is 4, but the very same user would have "Low" channel quality if $CQI_{avg}(t)$ were 13. For this reason the contribution of the different channel quality categories to the rate is expressed in relative form:

$$RR_Q(t) = \frac{T_Q(t)}{\sum_{q=1}^{N_Q} T_Q(t)}; \tag{4.21}$$

At each time t, the agent can then build an **impact matrix** $\boldsymbol{I}$, of size $S_{CQI} \cdot N_Q \cdot A$, which relates the input states (average cell CQI and relative user channel quality) with the rate contribution of each category of users and the actions taken. Each entry of $\boldsymbol{I}$ has value:

$$I(t)(CQI_{avg}(t), Q, a_Q(t-1)) = \begin{cases} RR_{\hat{Q}}(t), & \text{if } Q_{Q_{channel}}(t) \neq 0 \\ 0, & \text{otherwise} \end{cases} \tag{4.22}$$

Similarly, the reward associated with each action (for every channel quality) $r_Q(t)$ is equal to the same entries of the impact matrix $\boldsymbol{I}$. This way, if users

in a specific category are contributing highly (poorly) to the throughput, that category will receive a high (low) reward or will receive no reward if not scheduled.

Algorithm 5 QL implementation for dynamic multi-user FB allocation

Initialization

$t = 0$

$\boldsymbol{QT} \leftarrow \emptyset$

$\boldsymbol{I} \leftarrow \emptyset$

choose random actions $a_Q(0)\ \forall Q = 1 : N_Q$

for t **do**

(1) Receive feedback from the users and divide them into different channel quality categories; evaluate input state

$$S(t) = \{CQI_{avg}(t), Q_{channel}(t)\}$$

(2) eNodeB performs resource allocation with one of the schedulers described in Section 2.3.1 .

(3) Measure the payload throughput for each category $T_Q(t)$ (4.20):

$$T_Q(t) = \frac{1}{N_{U_Q}} \sum_{u^*}^{N_{U_Q}} T_{u^*}(t), \forall Q = 1 \cdots N_Q$$

(4) Create categories in which to divide the different channel quality categories based on their throughput contribution (4.21):

$$RR_Q(t) = \frac{T_Q(t)}{\sum_{q=1}^{N_Q} T_Q(t)};$$

(5) Update impact matrix $\boldsymbol{I}$ for each category as in (4.22):

$$I(CQI_{avg}(t), Q, a_{Q,t-1})(t) = \begin{cases} RR(t)(T_Q(t)), & \text{if } Q_Q channel(t) \neq 0 \\ 0, & \text{otherwise} \end{cases}$$

(6) Compute each category's reward $\boldsymbol{R}(t)$:

$$r_Q(t) = \boldsymbol{I}(CQI_{avg}(t), Q, a_Q(t-1), \forall Q = 1 \cdots N_Q$$

(7) Update each category's Q-Table $\boldsymbol{QT}$ as described in (4.12):

$$Q(S(t-1), a(t-1)) \leftarrow Q(S(t-1), a(t-1)) + \beta \left[r(t) + \gamma \max_a Q(S(t), :) - Q(S(t-1), a(t-1)) \right],$$

(8) Choose action $a(t)$ which determines which FB strategy will be used in the next iteration for each category Q (4.14):

$$Pr(a(t)) = \frac{e^{\frac{Q(S(t),a(t))}{\tau}}}{\sum_a e^{\frac{Q(S(t),a)}{\tau}}},$$

end for=0

Learning

The Q-Table **QT** has then the same dimensions as the impact matrix **I** and is initialized to zero at $t = 0$, **QT** is updated at every time step t following equation (4.12). After the update the actions for the following time slot $a_Q(t+1)$ are chosen using equation (4.14). The algorithmic representation of this implementation is shown in Algorithm 5.

4.5 QL Results

	Static solution	Dynamic solution
State space	$30 \cdot 100$	$30 \cdot 5$
Action space	7	7
Learning Factor	0.8	0.8
Discount Factor	0.9	0.9
Exploration temperature	200	200

Table 4.6: Channel quality categories and CQI thresholds

In this section convergence results for the two proposed Q-Learning algorithms are presented. Simulation settings for the methods are contained in Table 4.6 In Figures 4.7 (a) - (d) the actions taken, at each time interval for a base station using a PF scheduler for subsets of 2, 30, 50 and 100 users respectively are shown. This sample of users has been chosen because they require different homogeneous FB allocation actions as shown in Figure 4.3;

The effective actions taken by the agent are presented in blue, they are selected randomly at the beginning of the simulations. After the initial exploratory phase, each base station converges to the optimal FB allocation determined experimentally in Section 4.3. This convergence is visible if the action function is smoothed with a moving average filter as the red curve in the figures shows. To further show the convergence and stability of the proposed method to the optimal solutions determined in Section 4.3.3, the root mean square (RMSE) of the actions taken, with respect to the optimal solutions, is presented in Figure 4.8. For all the studied user configurations, the proposed solution converges to the optimal static solution and maintains it stably.

In case of multi-user FB allocation strategies, only the results for the BCQI scheduler are presented. The agent has to select the best FB allocation based on

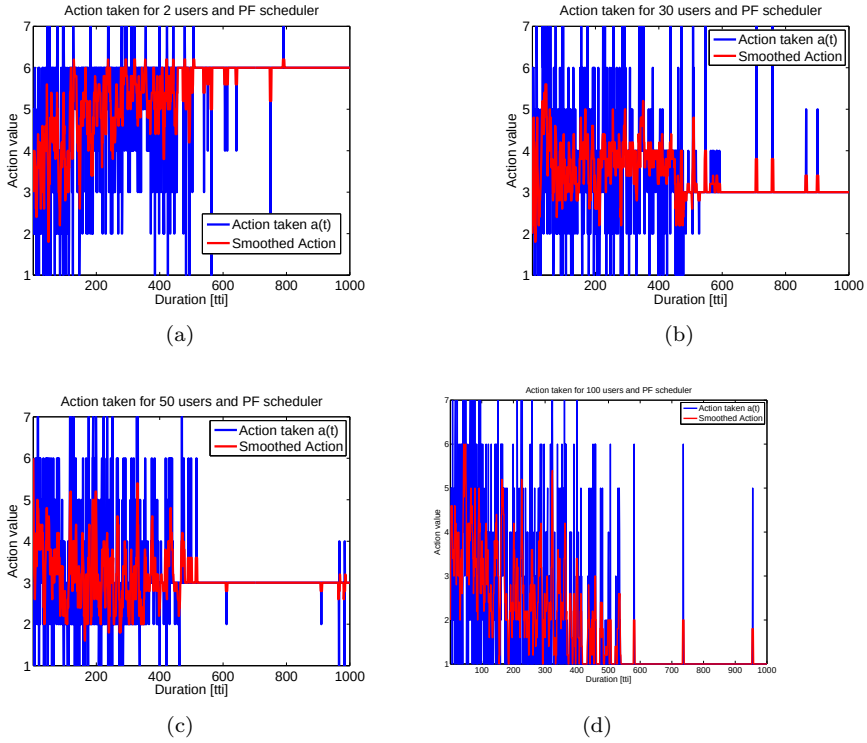

Figure 4.7: Action taken and smoothed action with PF scheduling for 2 (a), 30 (b), 50 (c) and 100 (d) users

the channel quality of the users. Figure 4.9 (a) - (c) shows the action taken, and thus the FB allocation chosen, for users with different channel qualities. Since the BCQI only allocates resources to the users with the best channel quality, the agent learns to allocate only minimal feedback to the users in categories "very low", "low" and "average", while the others get more depending on how good their channel is and how much they contribute to the cell's payload throughput. Users with "very high" channel quality obtain the most feedback. Like in the previous case, the RMSE has been used to verify the convergence and stability of the proposed dynamic solution. Figure 4.10 shows that the RMSE decreases with each QL iteration and that the final results are very close to the optimal actions. The small oscillations present in the RMSE after convergence is reached are due to the discrete nature of the action-state space. In fact, the proposed method might oscillate between two equally good actions or equally distant from the actual optimal solution.

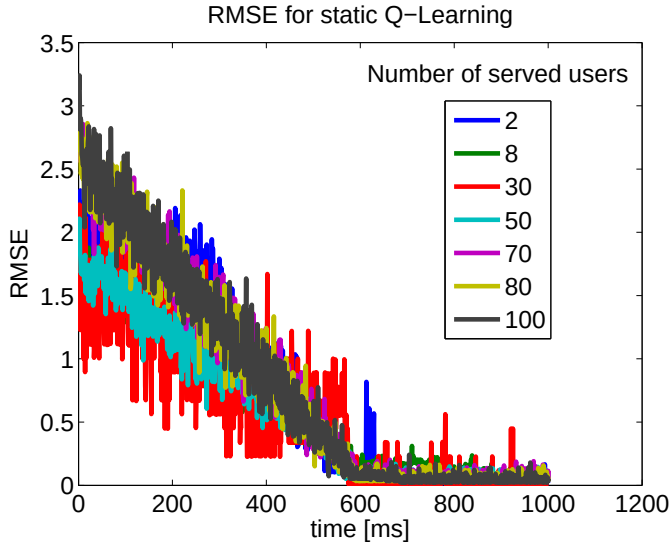

Figure 4.8: RMSE convergence for the proposed static QL solution

Finally, in Figure 4.11 the average results for the QL multi-user FB allocation in case of a BCQI scheduler are compared with the homogeneous allocation of Section 4.3 and the ideal dynamic FB allocation of Figure 4.5. The proposed dynamic multi-user method outperforms the homogeneous allocation and follows asymptotically the ideal solution. The dynamic nature of the multipath propagation environment with mobility users make perfect and reliable allocation very difficult and thus the ideal value is never reached, nonetheless, the proposed solution provides a close to optimal gain (80% of the ideal solution).

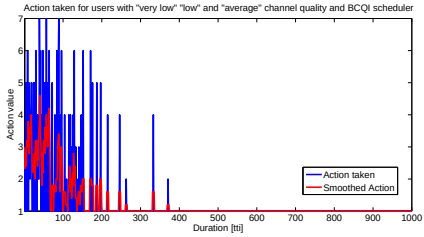

(a)

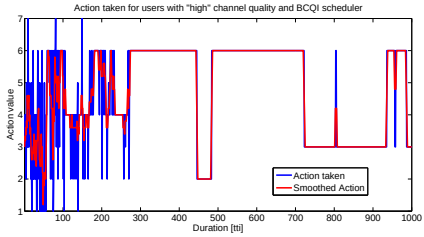

(b)

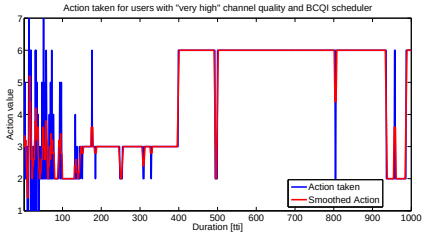

(c)

Figure 4.9: Action taken and smoothed action with a BSQI scheduler for users with for "very low", "low" and "average" channel quality (a), "high" channel quality (b) and "very high" channel quality (c)

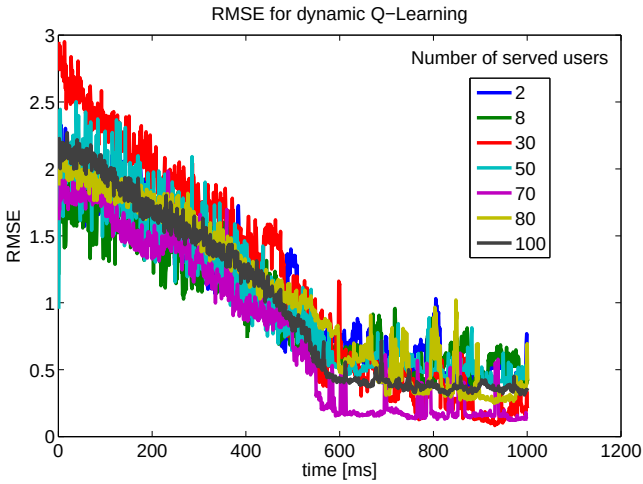

Figure 4.10: RMSE convergence for the proposed dynamic QL solution

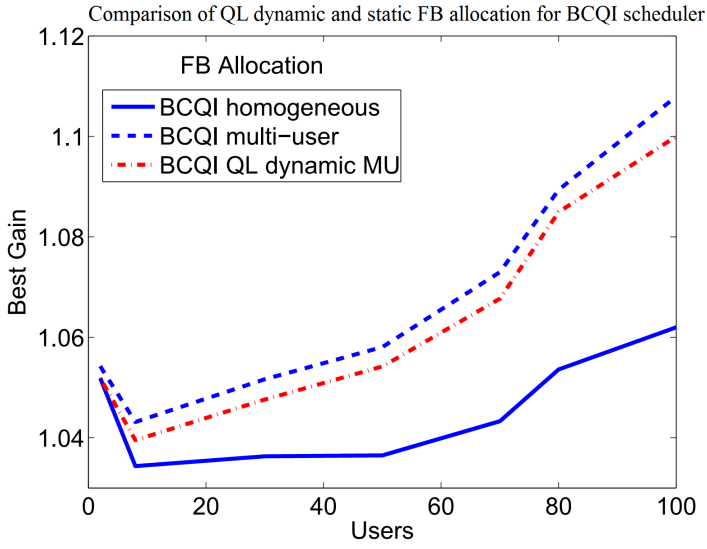

Figure 4.11: Comparison for QL dynamic FB allocation with static and ideal dynamic FB allocation

4.5.1 Notes on Complexity

In this section, the complexity of the proposed methods is compared to other operations normally carried out within an LTE base station. It is interesting to note that the proposed solutions make use of information already necessary for the AMC and dynamic frequency scheduling, such as the downlink throughput and the CQI values. This information comes, then, at no extra cost for the eNodeB. In this section, to show the implementation cost of the reinforcement learning methods the memory requirements and the computational complexity are analysed [140–142].

Memory Requirements

The amount of memory of the static and multi-user QL algorithms is directly correlated with the amount of states and actions. The data required is, in fact, contained within the Q-Table and the Impact Matrix, both of dimensions $\boldsymbol{S} \cdot \boldsymbol{A}$, where $\boldsymbol{S}$ represents the number of states and $\boldsymbol{A}$ represents the number of actions. The memory size is then linear in both the number of states and the number of actions: $O(\boldsymbol{SA})$. Specifically, for the static QL algorithm, the number of

states is $\boldsymbol{S} = \boldsymbol{S_{CQI}} \cdot \boldsymbol{N_{UE}}$, and the Q-Table has dimensions $\boldsymbol{S} \cdot \boldsymbol{A}$. Given the worst case scenario of $N_{UE} = 100$ and where each entry of the Q-Table is bound to 1 Byte, the total size of the Q-Table is then $(30 \cdot 100 \cdot 7)8 = 168kb$. Thus the total memory space requested by the Q-Table and Impact matrix is $336kb$. Considering instead the dynamic QL algorithm, the Q-Table size is not function of the number of served users but only of the channel quality categories. The number of states is is then $\boldsymbol{S} = \boldsymbol{S_{CQI}} \cdot \boldsymbol{Q_{channel}}$. If the same conditions as above are considered, The Q-Table size becomes $(30 \cdot 5 \cdot 7)8 = 8.4kb$. The total memory requirement is then $16.8kb$.

Computational Complexity

The computational complexity of QL algorithms is limited by the amount of operations necessary to update the Q-Table. Since at any given moment the agent can be in only one state, the complexity increases linearly with the amount of actions available to the agent [143]. For the problem at hand, the QL agent needs then to determine the current state, update the impact matrix, compute the reward, update the Q-table and finally choose the appropriate action. In a form similar to [142, 144], Tables 4.7 and 4.8 present the total number of operations required by each steps of the static and dynamic solutions respectively. The static method requires only 97 overall instructions per iteration. The dynamic method requires considerably more, 3797 instructions if the absolutely worst case scenario of all 5 categories are present while serving 100 users.

The complexity of the proposed methods is actually negligible if compared with other operations normally carried out in an eNodeB base band processor. In fact, at every transmission interval, the base station computes one iteration of the FB reduction methods proposed. At the same time, the base stations has to compute 1 FFT for each of the 14 OFDM symbols present in the frame. For each FFT $2 \cdot Nlog_2(N)$ MAC operations need to be carried out, where $N = 2048$ if the bandwidth is 20 MHz [32]. The total amount of operations is thus 630784. Given the computational requirements of such a necessary operation as the FFT, the impact of the proposed solutions on the processing power of an LTE base station is negligible.

Steps	Instructions
Identification of current and previous states	2 read 30 comparisons
Update of impact matrix	1 read 1 comparison 1 write
Compute reward	6 read 7 comparisons 1 division
Update Q-Table	10 read 6 comparisons 5 MAC 1 write
Choose next action	8 read 3 divisions 7 MAC 8 exponentiation
Total	97

Table 4.7: Computational requirements for the static QL method

Steps	Instructions
Identification of current and previous states	2 read $100 \cdot 30$ comparisons
Measure payload for each category	$5 \cdot 100$ MAC 5 divisions
Create categories	5 MAC 5 division
Update of impact matrix	5 read 5 comparisons 5 write
Compute reward Update Q-Table	5 read 50 read 50 comparisons 25 MAC 5 write
Choose next action	40 read 15 divisions 35 MAC 40 exponentiation
Total	3797

Table 4.8: Computational requirements for the dynamic QL method

4.6 Variable Feedback and ICIC

In order for any ICIC mechanism to work, the users need to communicate some identifying information on the interferers to their serving base station. This procedure can be quite costly, in terms of bandwidth as a global cell identifier in LTE is set to be 28 bits long [145]. It is reasonable to assume that much fewer bits might be necessary for the system to operate as each base station can build a look-up table where the identities of the interfering neighbours are stored and each user simply feeds back the relative entries in the table. This additional overhead is not considered in this analysis as it is beyond the scope of this work to develop a compression scheme for the cell identifying information.

Furthermore, the assumption that each user is capable of determining the identity of all the interfering base stations and to differentiate between the power received by them is a very common but weak one. In reality a mobile user would not be capable of sensing the power of a signal with power very much lower than the wanted signal; an alternative solution is for a user to determine the identity of a wideband interferer by collecting the synchronization information over time.

Resolution		Percentiles gain			FB amount	Uplink
Useful Signal	Interference	5^{th}	50^{th}	95^{th}	(bits)	percentage
Full	Full	8.65	2.21	1.77	408	4.9
Full	SL	6.1	1.78	1.44	264	2.8
Full	W	5.6	1.7	1.4	206	2.4
SL	SL	1	1	1	120	0.71
SL	W	0.8	0.99	0.99	62	0.38
BM	BM	0.94	1.03	1.01	148	0.85
BM	W	0.86	1.01	1	76	0.46
B5	W	2.1	1.2	1.12	84	0.5
B4	W	2	1.12	1.05	70	0.43
B3	W	1.9	1.1	1	58	0.35
B2	W	1.65	0.9	0.9	44	0.27
B1	W	1.46	0.9	0.89	26	0.18

Table 4.9: Effects of CSI quantization on desired and interference signals and relative amount of signalling bits and uplink portion used per user

Table 4.9 presents the throughput results for the 5th, 50th, and 95th percentiles

normalized over the standard compliant "subband level" feedback method. The different quantizations are applied to the useful signal in order to determine the user's channel quality and to the interference signals in order to determine the impact of the CSI quantization on the proposed ICIC method. In the table the acronyms $Full$, SL, BM and W refer to full resolution (per RB, no quantization), subband level, Best M and wideband (only one CQI value is transmitted associated with the highest interferer) respectively. The variable Best-M method is indicated instead with Bx where x represents the amount of subbands used in the method. The throughput gains (or losses) are normalized over the subband level method as it represent the default method chosen in the LTE standard. Since acquiring information on the interference is more difficult than on the wanted signal, the CSI on the former is assumed to have, generally, lower resolution than for the wanted signal. The last two columns in the table represent the cost of this signalling information on the uplink bandwidth in bits per single user and the amount of uplink bandwidth used by each user (with a 1/2 code rate and a 16QAM modulation for a 20MHz bandwidth).

The full resolution scenario is the one with the highest performance but in practice it cannot be used as it requires almost 4 times the amount of signalling information; this means that with only 20 users a uplink 20 MHz uplink bandwidth would be exhausted [20].

Interestingly, methods such as variable $Best - M$ can successfully increase performance for low performing users over the subband level state-of-the-art while decreasing the overall amount of signalling. This is due the fact that, with this method, users are able to allocate high resolution feedback to the subbands which present the highest quality and are thus most likely to be scheduled. A universal solution should take into account the practical limitations of the network and adapt the amount of signalling information necessary by each user accordingly to their relative performance.

4.7 Conclusion

In this chapter it is shown that the feedback overhead cannot be overlooked as the number of connected devices keeps increasing. The proposed model shows that a trade-off is indeed possible between downlink performance and uplink overhead. Such trade-off is determined by the downlink resource allocation strategy, the number of users served within a cell and their channel quality with respect to the average channel quality of the users. The results show that the gain can be considerable if the proposed feedback allocation techniques are implemented. The proposed Q-Learning techniques allow the base station

to achieve such gains in a dynamic environment and do not require external controllers and coordination. Furthermore, if the feedback allocation strategy is incorporated with ICIC techniques, there is clear improvement over SoA standard-compliant methods as more relevant information can be gathered rather than averaged values.

Chapter 5

Reducing the Signalling Overhead in the Time Domain

In the previous chapter, it has been shown that, by limiting frequency channel state information, a gain in performance is achieved as the freed uplink bandwidth is allocated for payload communication. In this chapter, the impact of reducing CSI feedback in the time domain is analysed. Timely CSI information is extremely important to allow a base station to correctly assign a modulation that reflects the actual user's channel characteristics. CSI packets, on the other hand, are not fed back continuously but there is a time interval between the discrete feedback points. This means that the CSI information received might not be relevant as the user's channel conditions may have varied in the mean while. It is, then, interesting to study how the channel quality behaves in the time domain and try to estimate this behaviour. By predicting a user's channel quality, it would then be possible to use the estimated values in between the feed back intervals with the dual gain of delivering higher performance or, by increasing the intervals, minimising the amount of required feedback. A Gaussian Process CSI prediction is here presented and the results show that the proposed solution is able to well estimate the user's evolving channel conditions. The same estimation process is then later used to adapt the prediction window in order to limit each user's packet loss due to the mis-estimation of the channel conditions.

5.1 CSI Time-domain feedback

Time-domain feedback in LTE, as introduced in Section 2.2.1 can be divided in periodic and aperiodic. Aperiodic CQI signalling entails that the base station can instruct each user on which part of the bandwidth to feed back and how often. With aperiodic reporting, the base station can make use of any of the CQI standard compliant feedback methods discussed in Section 2.2.1. On the other hand, periodic CQI reporting is limited to only Wideband and User-selected feedback methods. In this case, the CQI messages are transmitted to the base station with constant periodicity. For the remainder of this chapter, it is assumed that aperiodic feedback is used, as this allows the eNB controller to adapt the CQI transmission time more freely than with periodic reporting.

Amongst the three standard compliant frequency feedback models discussed in the previous chapter, only the subband level technique allows the base station to investigate the channel quality of the complete bandwidth with equal amount of detail between subbands. For this reason it has been chosen, in this chapter, as the preferred FB method.

In the following section, the bases for channel prediction in LTE and LTE-A are introduced. The Gaussian Process Regression (GPR) technique is discussed and its benefits for channel estimation are illustrated.

5.2 CQI Prediction

In this section, the CQI estimation method used in this dissertation, is described. The estimation process is carried out to compensate for the reduction in CQI reporting in time. Given the relationship between CQI and SINR described in Section 2.2.1, predicting the CQI is equivalent to predicting a noisy function of the relative effective SINR. Due to the Gaussian nature of the SINR distribution and the inherent flexibility of Gaussian Processes for regression, these have been selected.

5.2.1 Gaussian Process Regression

The objective of GPR is to estimate a function f in an online manner with low complexity. A Gaussian Process (GP) is defined as a probability distribution over some variables, where any finite subset of these variables forms a joint Gaussian distribution [146]. This means that, instead of making assumptions on the elements of a dataset a GP infers their distribution. Let us consider

a dataset $D = \{x_i, y_i\}$ with $i = 1, 2, ...N$, where each x_i and y_i represent the input and output pairs. The relation between the target value y and the input vector $\boldsymbol{x}$ is defined as

$$y = f(\boldsymbol{x}) + n, \tag{5.1}$$

where n is a zero-mean Gaussian noise with variance σ^2. A GP is defined as a collection of random variables, such that any finite set has a joint Gaussian distribution. Since a Gaussian distribution is completely defined by its mean and covariance matrix, a GP is completely defined by its mean function $m(\boldsymbol{x})$ and covariance function $k(\boldsymbol{x}, \tilde{\boldsymbol{x}})$, expressed as:

$$f(\boldsymbol{x}) \sim GP(m(\boldsymbol{x}), k(\boldsymbol{x}, \tilde{\boldsymbol{x}})), \tag{5.2}$$

where

$$\begin{array}{lcl} m(\boldsymbol{x}) & = & \mathbb{E}[f(\boldsymbol{x})] \\ k(\boldsymbol{x}, \tilde{\boldsymbol{x}}) & = & \mathbb{E}[(f(\boldsymbol{x}) - m(\boldsymbol{x}))(f(\tilde{\boldsymbol{x}}) - m(\tilde{\boldsymbol{x}}))]. \end{array} \tag{5.3}$$

The output can be defined by a GP, such that:

$$y \sim GP(m(\boldsymbol{x}), k(\boldsymbol{x}, \tilde{\boldsymbol{x}}) + \sigma^2 \boldsymbol{I}) \ , \tag{5.4}$$

By aggregating the outputs into a vector $\boldsymbol{Y}$ and renaming the input vector as $\boldsymbol{X}$, the GP estimates the value of $\hat{y}$ at a future point x_*, assuming a multi-variate distribution:

$$\begin{bmatrix} \boldsymbol{Y} \\ \hat{y} \end{bmatrix} \sim N\left(\begin{bmatrix} m \\ m_* \end{bmatrix}, \begin{bmatrix} K(\boldsymbol{X}, \boldsymbol{X}) + \sigma^2 \boldsymbol{I} & K(\boldsymbol{X}, x_*) \\ K(\boldsymbol{X}, x_*) & k(x_*, x_*) \end{bmatrix} \right) \tag{5.5}$$

$K(\boldsymbol{X}, \boldsymbol{X})$ is the matrix representation of the covariance functions of the input samples and $K(\boldsymbol{X}, x_*)$ is the covariance matrix of the overall input dataset and $k(x_*, x_*)$ is the autocorrelation of the future data point. The posterior probability $\hat{y}|\boldsymbol{Y}$ is given by [147]:

$$\hat{y}|\boldsymbol{Y} \sim N\Big(K(\boldsymbol{X}, x_*)[K(\boldsymbol{X}, \boldsymbol{X}) + \sigma_n^2 \boldsymbol{I}]^{-1} \boldsymbol{Y}, \ k(x_*, x_*) - K(\boldsymbol{X}, x_*)[K(\boldsymbol{X}, \boldsymbol{X}) + \sigma_n^2 \boldsymbol{I}]^{-1} K(\boldsymbol{X}, x_*)^T \Big), \tag{5.6}$$

The best estimate for $\hat{y}$ is given by the mean of such distribution
$m(\hat{\boldsymbol{Y}}) = K(\boldsymbol{X}, x_*)[K(\boldsymbol{X}, \boldsymbol{X}) + \sigma_n^2 \boldsymbol{I}]^{-1} \boldsymbol{Y}$ and the variance
$Var(\hat{\boldsymbol{Y}}) = k(x_*, x_*) - K(\boldsymbol{X}, x_*)[K(\boldsymbol{X}, \boldsymbol{X}) + \sigma_n^2 \boldsymbol{I}]^{-1} K(\boldsymbol{X}, x_*)^T$ represents the uncertainty of the current estimate. The GP is then fully defined by its covariance and mean functions and their parameters.

5.2.2 Covariance function selection

In order to obtain a good estimate of the future measure and its underlying distribution, a covariance function that best fits the nature of the system has to be selected. As the mean can easily be set to zero if some pre-processing is carried out, it is usually ignored [147]. Although the covariance function K is limited to positive semi-definite functions, many choices are present in literature able to fit to dynamic, time-varying systems [146]. The most important feature when choosing a covariance function is its smoothness, i.e. how much the value of the function sampled at a point x_* correlates with the same function at points close to x_*. A function that presents high smoothness might not be representative of a fast-varying system. It could be possible, in theory, to observe a large realization of an input dataset and generate a specific covariance function which models the witnessed behaviour very closely. This is normally not performed as a few families of covariance functions are present in literature which adapt quite well to a large selection of problems in which the data can be modelled as a multivariate Gaussian distribution [147]. For this reason, in the current task of modelling the channel quality for users with varying mobility a Matérn class covariance function has been selected [148]:

$$k(x, x_*) = h^2 \frac{2^{1-v}}{\Gamma(v)} \left(\sqrt{2v} \left| \frac{x - x_*}{w} \right| \right) \mathcal{K}_v \left(\sqrt{2v} \left| \frac{x - x_*}{w} \right| \right), \tag{5.7}$$

where $\mathcal{K}_v$ is the modified Bessel function. The Matérn covariance functions, such as the one selected in this work, include both the exponential autocorrelation (if the smoothness v is equal to $\frac{1}{2}$) and the Gaussian autocorrelation (with infinite smoothness). These conditions make the Matérn class of covariance functions very flexible as they are able to strike a balance between the two extremes [149]. The variables h, v and w are defined as hyperparameters of the covariance function. They determine the shape of the covariance function and have to be fine-tuned in order for the GP to converge to an appropriate solution. By increasing the smoothness hyperparameter v, the function becomes smoother in time and fast variations of datapoints are ignored. By increasing the width hyperparameter w, the covariance function considers a wider set of datapoints and by increasing the height hyperparameter h, larger variations in datapoints values are allowed. Once the covariance function is selected, the following step is to determine the values of the hyperparameters. This is performed by maximising the marginal likelihood of the Gaussian Process. Since GPR is a form of Bayesian regression, the marginal likelihood is equal to the integral over the product of the prior and the likelihood function. Since both are Gaussian,

the marginal likelihood is also Gaussian and is expressed in analytical form:

$$\begin{aligned} p(\boldsymbol{Y}|\boldsymbol{X},\theta,\sigma^2) &= \int p(\boldsymbol{Y}|f,\boldsymbol{X},\theta,\sigma^2)p(f|\boldsymbol{X},\theta)df \\ &= \int \mathcal{N}(f,\sigma^2,\boldsymbol{I})\mathcal{N}(0,\boldsymbol{K})df \\ &= \frac{1}{(2\pi)^{\frac{n}{2}}|\boldsymbol{K}+\sigma^2\boldsymbol{I}|^{\frac{1}{2}}}\exp(-\frac{1}{2}y^T(\boldsymbol{K}+\sigma^2\boldsymbol{I})^{-1}y) \end{aligned} \tag{5.8}$$

Where θ is the set of hyperparameters. Generally speaking, for simplicity, the log marginal likelihood is maximised [147]:

$$\log p(\boldsymbol{Y}|\boldsymbol{X},\theta) = -\frac{1}{2}\boldsymbol{Y}^T(K+\sigma_n^2\boldsymbol{I})^{-1}\boldsymbol{Y} - \frac{1}{2}\log|K+\sigma_n^2\boldsymbol{I}| - \frac{n}{2}\log 2\pi. \tag{5.9}$$

By using any multivariate optimization algorithm, the set of hyperparameters θ can be estimated analytically. After the optimization process has reached the analytical solution, the numerical values of the hyperparameters are simply obtained by using the measured input and output signals. This is a great advantage over other types of regression as it allows the system to evolve without pre-specifying the parameters and thus limiting the range of estimations [150].

5.2.3 GPR for CQI prediction

In this work, the eNB makes use of GPR to predict the CQIs values for every subband seen by each user. In order to make realistic predictions, the input vector $\boldsymbol{X}$ is used to train the GP. For each user, the base station receives the CQI information for the complete bandwidth, using the subband-level FB quantization scheme discussed in Section 2.2.1 and in the previous chapter, every $t_{samp} = 2ms$. The value of the sampling window t_{samp} is chosen as the minimum allowed by LTE standard to acquire a high number of samples in a short time [151]. For a fixed prediction window t_w, the GPR has he objective to estimate the CQI values of each user over all the frequency subbands, for the duration of such prediction window. After the observation time elapses, say at instant t_0, the eNB uses GPR to predict the future CQI values in each subband for the duration of the pre-imposed prediction window, as shown in Algorithm 6. The duration of the prediction window is going to be optimised in the following sections, for each user, based on the quality of the prediction.

Algorithm 6 CQI estimation with GPR

for each user u **do**
  for each subband $s \in q$ **do**
    Initialization: Input vector $\boldsymbol{cqi_{samp}}$, Output vector $\boldsymbol{cqi_{pred}}$, Covariance function $\mathbf{K}$, Noise level $\boldsymbol{\sigma}$, Prediction window $\boldsymbol{t_w}$
    while $\boldsymbol{t < t_0}$ **do**
      Build historical dataset $\boldsymbol{cqi_{hist}(t) = cqi_{samp}(t)}$.
    end while
    while $\boldsymbol{t \geq t_0}$ **do**
      if $\boldsymbol{t \leq t_w}$ **then**
        (1) The GP is trained with the vector $\boldsymbol{cqi_{hist}}$.
        (2) The hyperparameters are found by maximising the log-likelihood (5.9)
        (3) The predicted CQIs vector $\boldsymbol{cqi_{pred}}$ of length $\boldsymbol{t_w}$ is generated using GPR.
        (4)The base station uses $\boldsymbol{cqi_{pred}}$ to allocate the users for the next $\boldsymbol{t_w}$ intervals as seen in Chapter 3
      else
        Update the input dataset with the new sampled value $\boldsymbol{cqi_{hist}(t) = cqi_{samp}(t)}$
      end if
    end while
  end for
end for=0

5.3 Dynamic time-window Optimisation

In this section, a control mechanism to determine the appropriate duration of the CQI prediction window is presented. Such technique allows the eNB to maintain each user's performance within a specified loss margin. Firstly the dual control system based on active learning is introduced and, secondly, its implementation in an LTE base station for time windows optimisation is presented.

5.3.1 Dual Control with Active Learning

A dual control agent is tasked with controlling a system based on the current knowledge of its behaviour and to perturb it in order to minimise the uncertainty and make better predictions. By their nature, these objectives are conflicting. In this work, the adaptive dual control framework proposed in [22], is used.

This framework provides a solution to the control problem while also limiting the amount of overhead.

The Dual Control with Active Learning is a supervised learning technique. Even though Reinforcement Learning can also be qualified as a dual control method, it reaches a solution autonomously by determining a policy to follow through exploration. In this chapter, the GPR, which is also supervised learning, is used to model the behaviour of a user's channel quality. Because of this, the estimation of the loss due to the imperfect CQI prediction leverages the same GPR for robustness. Furthermore, the Active Learning component allows the agent to determine which part of the search space to explore in order to maximise impact, which is a strong feature of this technique.

Let's define a dynamic, non-linear, partially observable system described by:

$$y(t+1) = h\left(y(t), c(t)\right) + n(t), \tag{5.10}$$

where $y(t+1)$ is the value of the output system at time $t+1$, which is a function of the system behaviour $h(\cdot)$ given the past observation $y(t)$ and a control function $c(t)$. $n(t)$ is a zero-mean Gaussian noise. In this context, $h(\cdot)$ corresponds to the function to be estimated (f) in equation (5.1), according to the formalism of the previous section. Given a reference signal $r(t)$, the dual control problem consists in finding the best control strategy $\mu(t)$ such that

$$\mu(t) = \arg\min_{c(t)} \left\| y(t) - r(t) \right\|, \quad \forall t \quad . \tag{5.11}$$

Furthermore, it is possible to limit the amount of data collected by the controller by maximising the information collected. By steering the controller to sample in areas of higher uncertainty, it is possible to get a better understanding of the evolution of the system's dynamics If $\hat{h}$ is an estimate of the system dynamics h based on previous observations, the dual control with active learning problem consists in finding the optimal strategy $\mu(t)$ solving the following optimisation problem:

$$\max_{u(t)} \mathfrak{I}(\hat{h}, c(t)) \approx \arg\min_{c(t)} Var(\hat{h}, c(t)) \tag{5.12}$$

where $\mathfrak{I}$ represents the Shannon information of the dynamic system and Var is the variance [22]. The objectives of the active dual controller consist in partially identifying the dynamics of the system so that it can be kept as close as possible to the reference signal while sampling only in the points that minimize uncertainty for future predictions.

The dual control with active learning can be formally described as (Proposition 4 in [22]): Let the input-output relationship of a discrete-time dynamic system

be defined as in equation (5.10). Let $\hat{h}$ be the predicted estimate of the system's behaviour.The predicted future value $\hat{y}(t+1)$ can be inferred as:

$$\hat{y}(t+1) = \hat{h}\left(y(t), c(t)\right) + n(t). \tag{5.13}$$

The optimal strategy μ is then defined as

$$\mu(t) = \arg\min_{c(t)} w_a \left\|\hat{y}(t+1) - r(t)\right\| - w_e Var(\hat{y}(t+1), c(t)) \tag{5.14}$$

where w_a and w_e represent the *action* and *exploration* weights to steer the controller towards either steepest descent to the closest optimal solution ($w_e = 0$) or to a complete exploratory behaviour ($w_a = 0$). Generally the weights can be adjusted so that the controller behaves more exploratory at the beginning of the learning procedure and then moves to a more active controlling role. Figure 5.1 presents a block description of the dual control framework

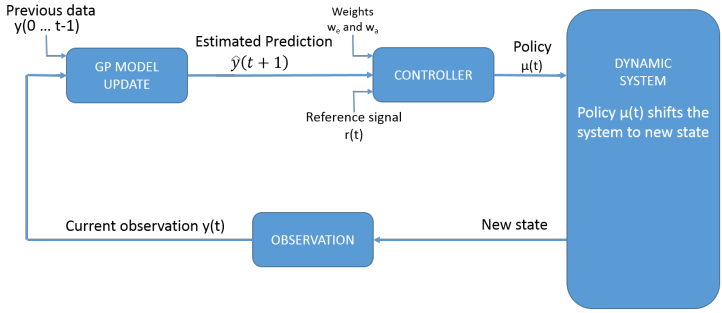

Figure 5.1: Dual control with active learning framework

5.3.2 Dual Control for Signalling Reduction

In the dual control framework for dynamic time window optimisation, the same GPR introduced for the CQI prediction is used (Algorithm 6) . In this case the GPR is used to predict the packet losses each user incurs when different time windows t_{w_u} are chosen for each user u. At time t_0 the eNB receives the CQI FB from each user u, then it chooses a time prediction window $t_{w_u}(t_0)$ and uses GPR to predict the CQI behaviour for the duration of such window. At the same time it uses GPR to predict the packet loss $\hat{L_u}(t_0+1, t_{w_u}(t_0))$ the user will experience given the current time window. The objective of the controller is then to solve, for every user u:

$$t_{w_u}(t_0+1) = \arg\min w_{a,u} \left\|\hat{L_u}(t_0+1) - r_{u,th}\right\| - w_{e,u} Var(\hat{L_u}(t_0+1), t_{w_u}(t_0)), \tag{5.15}$$

where $r_{u,th}$ is the reference packet loss for user u. At time $t_0 + t_{w_u}(t_0)$ the eNB measures the actual packet loss suffered by the user. The controller then corrects the CQI prediction window accordingly to provide better predictions and the process is repeated. Figure 5.2 presents a block description of the dual control framework for packet loss minimisation due to CQI prediction inaccuracy.

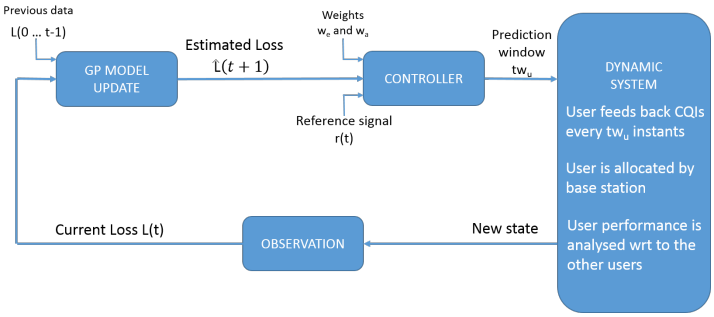

Figure 5.2: Dual control with active learning framework for packet loss minimisation

Algorithm 7 provides a concise view of the solution above.

Algorithm 7 Dual Control with Active Learning for Dynamic CQI FB assignment

1: **for** each user u **do**
2: **Initialization:** GP hyperparameters, objective weights $[w_a, w_e]$, reference signal $r_{u,th}$
3: **while** $t > t_0$ **do**
4: (1) Receive CQI FB from user and estimate the CQI behaviour using GPR.
5: (2) Estimate the system dynamics $\hat{L}$ using GPR.
6: (3) Determine the best time window $t_{w_u}(t+1)$ by solving (5.15) (employing Algorithm 6) and crop CQI prediction at selected time window $t_{w_u}(t+1)$.
7: (4) Schedule the user for the duration of the time window $t_{w_u}(t+1)$.
8: (4) Compute the variance $Var(L_u, t_{w_u})$.
9: (5) Update the dataset with the newly observed point $L_u(t)$.
10: **end while**
11: **end for**=0

5.4 Results

In this section, the simulation environment is first defined and then the results for the proposed models are provided.

5.4.1 Simulation Parameters

The system has been simulated using the open source VIENNA system level simulator [45]. An urban multi-cell environment has been considered to include the effects of multipath propagation and interference; 19 LTE macrocells are simulated with 30 users per cell, in which only the users in the most central cell are studied to reduce border effects. In order to model the effects of user mobility in a city-like environment, the users have an average speed of 5, 10 or 60 km/h. The propagation model is deterministic and based on the Winner Channel Model II [11]. The simulation parameters are included in table 5.1. The simulation environment differs slightly from the previous two chapters (for this chapter 19 macrocells are simulated, while previously the macro base stations were 7). This was done to have a bigger pool of simulated users for training of the GPR CQI estimation.

Parameters	Values
Number of Macrocells	19
Sectors per Macrocell	3
Inter-cell distance	500 m
Macro antenna gain	15 dB
Macro Transmit Power	46 dBm
Macro users per sector	2 to 100
Frequency	2.1 GHz
System Bandwidth	20 MHz
Number of PRBs	100
Access technology	OFDMA FDD
Number of antennae	1(Tx and Rx)
Channel model	Winner Channel Model II [11]
Block fading mean	0 dB
Block fading deviation	10 dB
Fast fading	10 dB
Thermal noise density	-174 dBm/Hz
Users speed	5 to 60 km/h

Table 5.1: System parameters for the LTE-A feedback reduction in time

5.4.2 Simulation Results

Firstly, the impact that the various frequency sampling schemes of the previous chapter have on the packet loss experienced by users is discussed in absence of prediction. The CQI FB messages are sampled at specific moments in time and the previously sampled value is used until the next sampling moment. Figure 5.3 shows the normalised goodput of a user moving at 10 km/h when the full feedback, subband-level, best-M and wideband schemes are employed.

It is visible that there is a loss in goodput when either the CSI frequency sampling methods are used or the CSI sampling time interval is increased. On the other hand, the effects of increasing the duration between sampling instants are less pronounced when the CQI information is quantized in frequency. This is particularly visible for the wideband FB scheme, where the initial goodput is just above one third of the full feedback but the loss in time is almost null. For large time sampling intervals, the three standard compliant FB schemes behave better than the full feedback. For the remainder of this work, the subband level method is employed, as it presents, for almost all the sampling delays considered, the highest goodput gain among the standard compliant schemes.

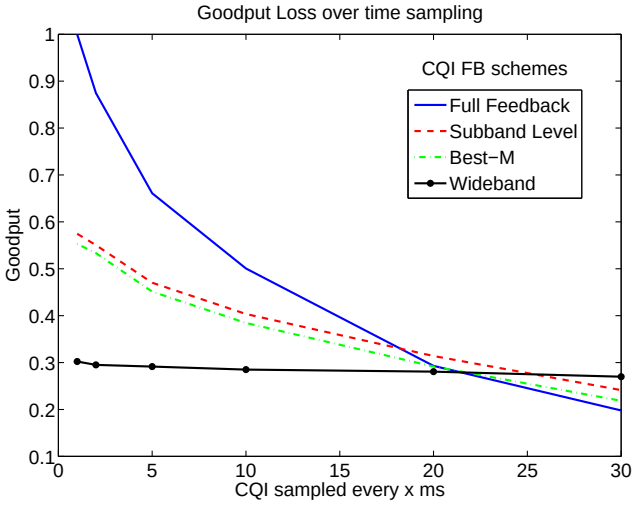

Figure 5.3: Goodput Loss of CQI FB frequency schemes over time delay

The effects of GPR CQI prediction for fixed CQI time sampling are presented in Figures 5.4 - 5.6 for users with speeds of 5, 10 and 60 km/h. The figures show the average packet loss seen by a user when either prediction or fixed time sampling are used. By fixed sampling, it is intended that the base station only uses the last received CQI value until a new one is sampled. For the first two plots, the GPR CQI prediction shows considerable gains over the alternative.

When users operate in high mobility, such as in Figure 5.6, the prediction remains valid only for a very small time duration. This is due to the fact the the fast varying channel does not allow for reliable estimation for extended time intervals. Nonetheless, it is possible to exploit the GPR estimation's gain over the sampling if short time windows are used.

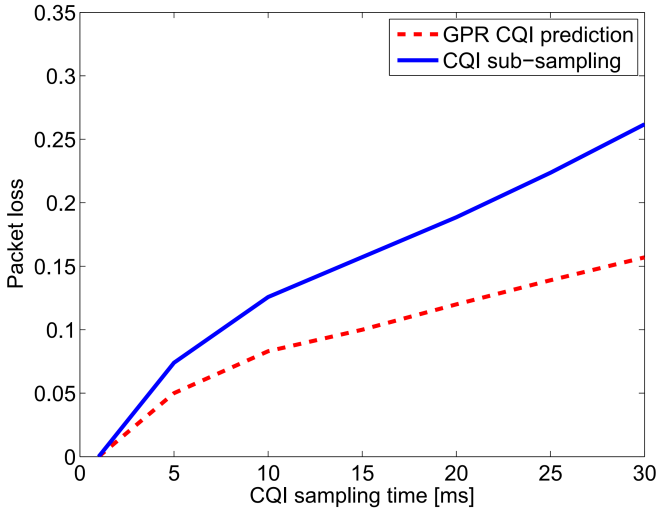

Figure 5.4: Packet loss for user moving at 5 km/h over time sampling intervals

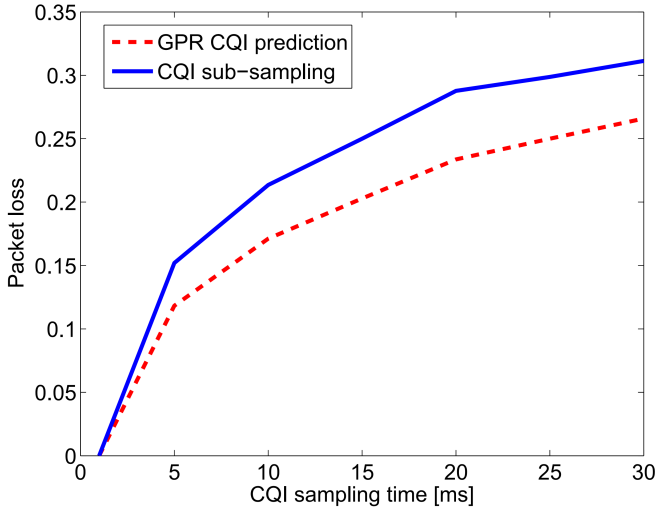

Figure 5.5: Packet loss for user moving at 10 km/h over time sampling intervals

Figure 5.7 shows a comparison between the real CQI values, measured every 2ms, and the estimated CQI values for a user moving at 10 km/h with a prediction window of 10 ms. There is good accordance between the predicted CQIs and the real values. The GPR is able to model the changes in the user's channel.

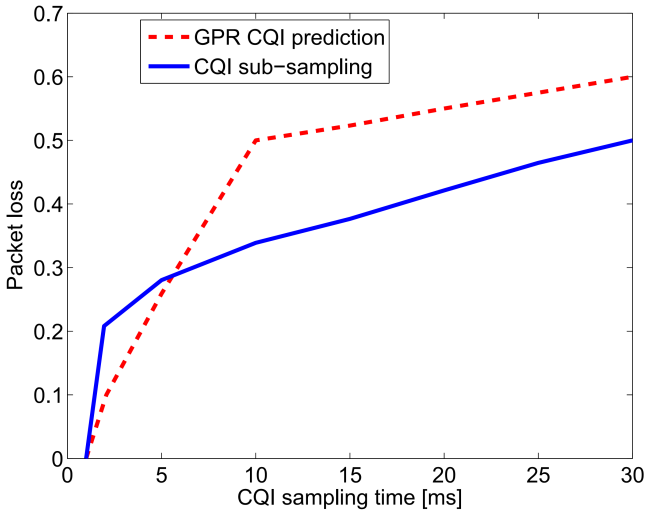

Figure 5.6: Packet loss for user moving at 60 km/h over time sampling intervals

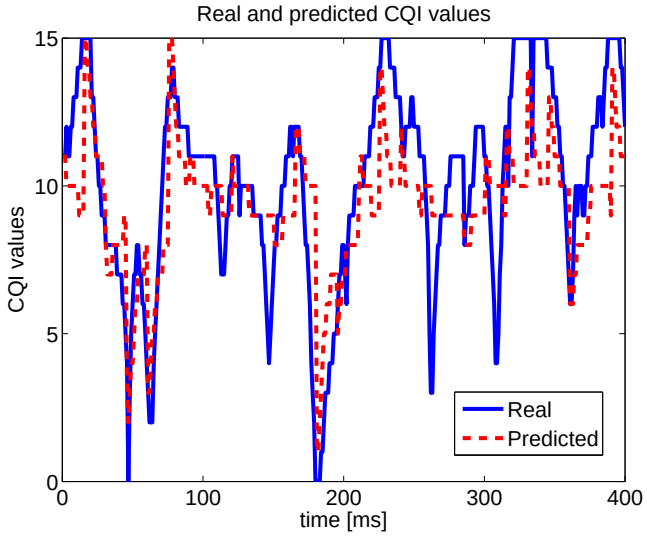

Figure 5.7: Estimated and real CQI values

Figure 5.8 shows the root mean square error (RMSE) of the GPR predictions for different training datasets. In case of users moving at 5 and 10 km/h, it is possible to see that convergence is reached and a large observation window allows

the GPR to make an accurate estimation. When users have high mobility, on the other hand, a large training can lead to more errors as the time correlation of the CQI values decreases as seen in Figure 5.8 (c).

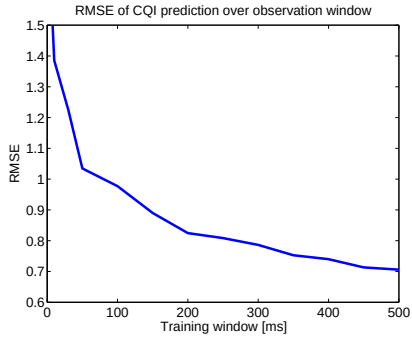

(a) User speed 5 km/h

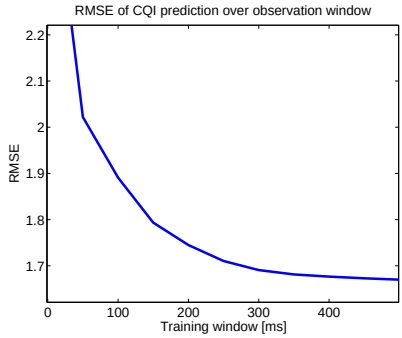

(b) User speed 10 km/h

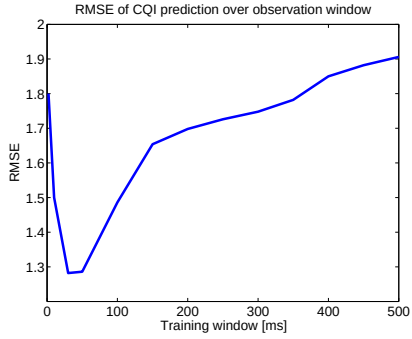

(c) User speed 60 km/h

Figure 5.8: RMSE for various observation windows and user mobility

The impact of different covariance functions on the CQI estimation process with GPR is presented in Figure 5.9. The Matérn function with smoothness $v = \frac{3}{2}$ behaves best. A detailed analysis of the various functions in the figure can be found in [147].

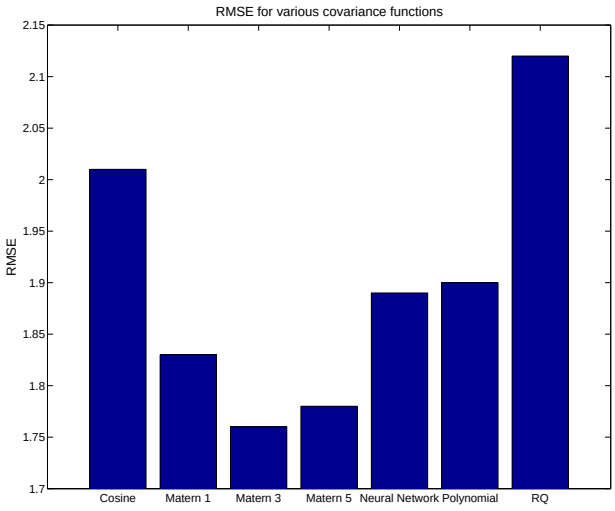

Figure 5.9: RMSE of different covariance functions

By using the dual control scheme, it is possible to set a maximum limit to the user's packet loss due to limited time feedback. If a user is selected to be scheduled by the eNB, then a predicted packet loss can be inferred with the proposed model and a decision is made based on equation (5.15).

In order to analyse a dynamic scenario, users with diverse requirements are simulated together; a total of 60 users are served within the cell, of which 30 have low mobility (5 km/h), 20 have average mobility (10 km/h) and 10 are high speed users (60 km/h). Table 5.2 shows the percentage of FB required by the system for various packet loss threshold values for both the proportional fair and best CQI schedulers after the model has converged to the optimal decision compared to the state of the art where no prediction is used and the CSI is sampled every 2 ms.

There are considerable gains for both schedulers but, as the PF maximises fairness, every user will be scheduled in the upcoming time slots and thus the time windows have to inferred so that the predicted packet loss is minimized. On the other hand, since the dual-control model has as input the packet loss of each user, if such user is not scheduled then the loss is null and a higher time window can be selected. For this reason the best CQI scheduler allows for much higher gains with an almost 94% reduction in FB signalling when the allowed packet loss is contained to only 5%.

PL threshold [%]	FB amount needed [%]	
	Proportional Fair	Best CQI
5	40	6.2
10	23	4
20	9.7	3.3
30	6.3	3.3

Table 5.2: Percentage FB necessary with dual-control

Figure 5.10 presents the behaviour of the proposed dual control method in Algorithm 2 for a single user. The packet loss at the sampling instants is indicated with the X markers while the square markers indicate the average sampled packet loss. The proposed solution then gradually builds a predicted packet loss behaviour, indicated in Figure 5.10 by the continuous curve. At each iteration, the model selects the next time window according to (5.15) with weights $w_a = 1$ and $w_e = 10$ and predicts the packet loss behaviour for the duration of the selected window. After the time window has passed, the eNB samples the packet loss again, corrects its prediction and determines the next prediction time window until it converges to the desired packet loss threshold. In this specific realization the packet loss threshold is imposed at 10% and the optimal inferred time window is 5 ms. It is important to notice that, because of the time varying nature of the channel, the measured loss can oscillate even if the time windows sampling is kept constant. The GPR takes this into account as measurement noise and is still able to approximate the system dynamics.

Figures 5.11 (a) and (b) show the prediction error calculated at each iteration and the variance of the prediction model; in both cases the proposed approach reaches the desired behaviour after only 5 iterations.

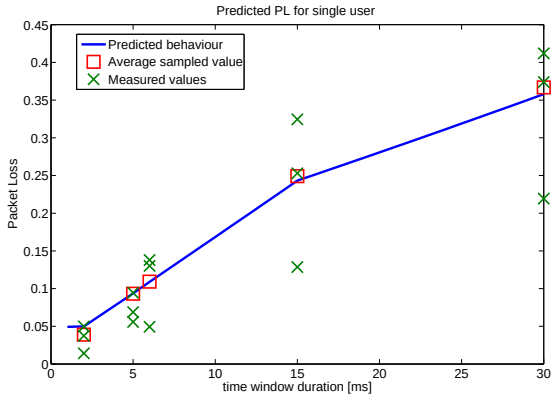

Figure 5.10: Predicted packet loss and measurements for different prediction time windows

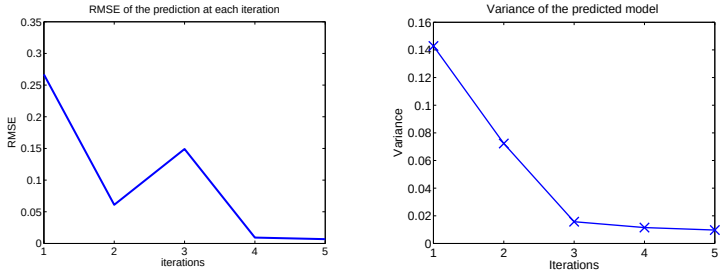

(a) Prediction error for every iteration

(b) Variance of the predicted model for every iteration

Figure 5.11: Prediction error and variance

In Figure 5.12 the packet loss threshold is 5%. In this case, the base station has to choose a very small prediction window of 2ms for a high mobility user with high packet loss.

Figures 5.13 (a) and (b) show the prediction error computed at each iteration and the variance of the prediction model. As in the previous case, convergence is attained after 5 iterations.

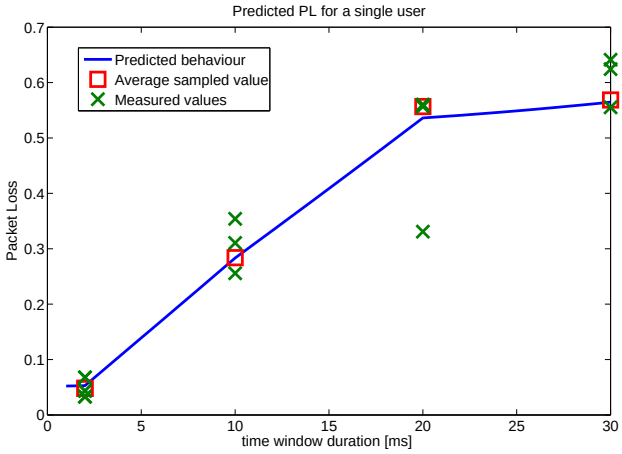

Figure 5.12: Predicted packet loss and measurements for different prediction time windows

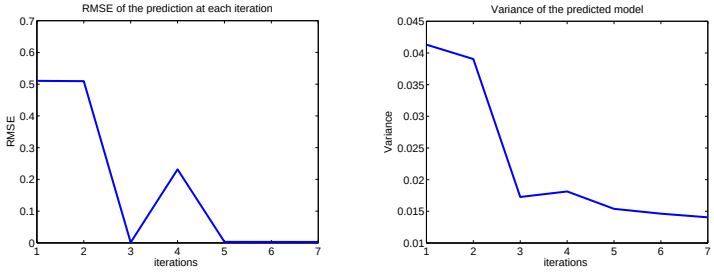

(a) Prediction error for every iteration

(b) Variance of the predicted model for every iteration

Figure 5.13: Prediction error and variance

The proposed model's behaviour in case of a low mobility user with a good channel is presented in Figure 5.14 where the packet loss threshold is imposed at 30%. In this case, the base station can choose a large prediction window of 27ms.

Figures 5.15 (a) and (b) show the prediction error committed at each iteration and the variance of the prediction model. In this case, convergence is attained after 3 iterations.

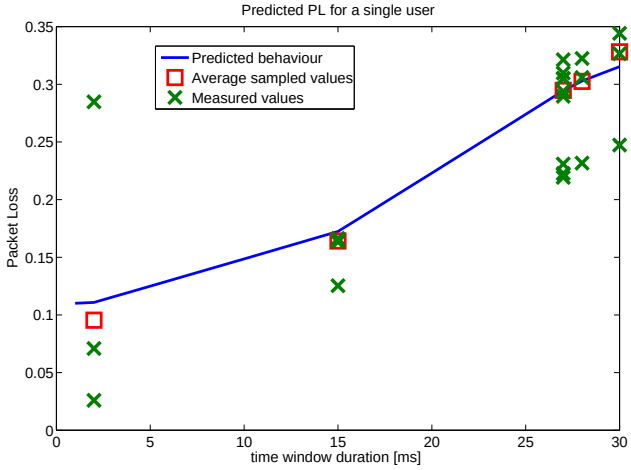

Figure 5.14: Predicted packet loss and measurements for different prediction time windows

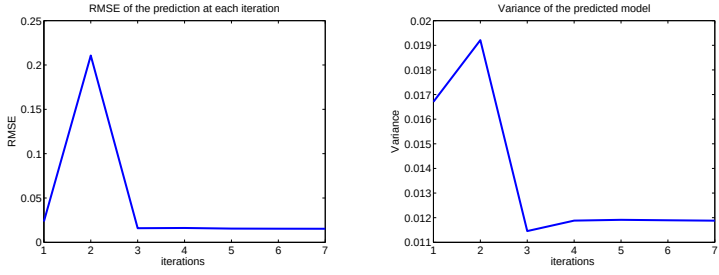

(a) Prediction error for every iteration

(b) Variance of the predicted model for every iteration

Figure 5.15: Prediction error and variance

5.5 Conclusion

In a previous chapter, it was shown that the feedback overhead cannot be overlooked as the number of connected devices keeps increasing. Some solutions are implemented in the frequency domain to limit the impact of this signalling information on the uplink bandwidth but additional restrictions in the time domain are also necessary.

An elegant GPR technique is proposed to predict the users' channel quality for various speeds limiting the loss incurred by increasing the time sampling period. The proposed CQI prediction method is able to estimate a user's channel with good accuracy.

Furthermore, a dual control method based on active learning was presented. Such method is able to determine the optimal prediction window given a packet loss threshold. The same method is also able to probe the system in such a way that an optimal solution is reached while also limiting the system's exploration by maximising the impact of the information collected. The proposed method shows gains of up to 94% in signalling reduction if best CQI scheduler is used when compared with state of the art if the packet loss is capped to 5%.

Chapter 6

Conclusions and Future Work

In this chapter the dissertation is concluded and the results are summarised. Firstly, an overall discussion on the achievements regarding the radio resource management problem in modern heterogeneous network is presented. Afterwards, analyses of the achievements obtained in each chapter are presented. Finally, prospectives on future work are discussed.

6.1 Conclusion

The main focus of this work has been on the design of practical, effective and implementable solutions to solve the RRM problem in a modern heterogeneous network, with an eye to future trends and their challenges. The main objectives of radio resource management are to allow a network to operate at the optimum of its capability and to shift to a new optimal point as the network's conditions vary. This entails a consistent monitoring of the overall network performance and a perfect knowledge of all the conditions and settings of any element within the network, from a mobile user to a base station and the controlling gateways. As the practical implementations of a cellular network impose limitations on the scope of monitoring and control, less general and more concrete questions have been the specific interest of this work.

The two main topics addressed in this dissertation have been on how to share resources in a full reuse network in way that maximises overall performance and, once a solution is found, how can the total amount of information overhead be limited without moving from the optimal point.

Both questions remain very relevant in modern networks and will become even more so in future technologies. The increase in heterogeneity and in connected devices will force the network operators in finding more efficacious dynamic solutions in place of the static ones used to day which stem from previous, less flexible cellular technologies.

All the solutions achieved in this work can be easily implemented in modern networks and adapted for future requirements. The solutions address the RRM problem from the intra-cell resource allocation to the inter-cell interference minimisation and address both channel prediction and the inherent trade-off present in the dichotomy between the desired data and the signalling information necessary to deliver such payload efficiently. Hereafter, the contributions of each chapter are exposed and the main achievements discussed.

6.1.1 Chapters discussion

The results obtained for each chapter are here discussed and a summary of each contribution is presented.

Chapter 2: SoA and challenges

The challenges present in the modern cellular networks and their state-of-the-art solutions have been discussed. The SoA analysis has painted a picture of the radio resource management as a large scale problem encompassing various layers of the LTE-A network, from the PHY to the transport layers at least. In this work, a general view of a downlink LTE-A network has been portrayed and aspects relative to internal resource allocation, inter-cell communication and signalling overhead have been specifically examined.

An analysis of resource allocation schedulers has been presented and the, usually not explored, aspect of energy efficiency has been analysed. One first interesting result is thus the presence of an energy-throughput-fairness trade-off, which is possible depending on the choice of scheduling algorithm. Furthermore, on top the SoA resource allocation mechanisms, a novel transport block aware scheduler has been conceived. This scheduler takes into consideration the practical limitations of an LTE base station and is able to increase performance (as in higher throughput and lower energy consumption) at no cost for the base station.

Finally, the chapter ended with a study of inter-cell communication and overhead reduction techniques which served as introduction for the works presented in later sections of this dissertation.

Chapter 3: ICIC and solutions for LTE-A

In this chapter a flexible, scalable solution to the interference coordination has been designed. The nature of high mobility in LTE-A forces the network controller to look for an interference management solution able to adapt to a varying environment where users connect and disconnect rapidly. Furthermore, such solution has to account for the different base station configurations and for the impact that the inter base station communication has on the ICIC.

The iterative Hungarian algorithm, as the basis of the proposed interference coordination method, was chosen as it allows for a good sub-optimal solution while keeping the complexity of the solution to an acceptable level. This way, each base station could reach an operating point in considerable less time than an optimal solution would require.

The distributed nature of the conceived solution also allowed the method to be scalable and to adapt to sudden changes. The information exchange protocol between base stations in a cluster, granted that the operational solution is very close to the network-wide optimum while requiring considerably less information than a centralised solution.

The properties of cognitive femtocells, lastly, have allowed the method to overcome the final hurdle of small cells unable to coordinate with the network. The cognitive femtocell was then able to sense the presence of nearby users and the amount of interference caused.

The solution presented in this chapter achieved gains of 45% for the combined macro and pico edge users at a very small cost for the cell center (less than than 4% loss) and has improved picocell users performance by 50% at a small cost for femtocell users (15%).

Chapter 4: Frequency domain quantization of the CSI information

In Chapter 4, a model to determine the impact of CSI signalling on the overall payload throughput has been presented. From such model it was possible to determine the trade-off between reducing the CSI overhead and having more spectral efficiency. The results show that it is indeed possible to limit the CSI information without loss, and with actual improvements, depending on the scheduling algorithm and the number of served users. Additional gains can be achieved by tailoring the mount of feedback to each user based on its requirements and contributions to the cell's throughput.

Two reinforcement learning solutions have been designed to allow a base station

to reach the optimal static (one FB allocation for all users) and dynamic (different FB allocation based on user's performance) operating points. The static method is able to reach its optimal solution while the dynamic one approximates its considerably well. The convergence of both methods was obtained with complexities well below the ones required by other standard operation performed in an LTE base station.

Additionally, the ICIC solution developed in Chapter 3 was incorporated within the signalling reduction framework. A clear improvement over SoA solutions was thus shown; it is indeed possible to double the cell edge throughput without any loss for the cell centre and only require half of the feedback information.

Chapter 5: CSI Time prediction and adaptive prediction window

Finally, the time domain analysis of the CSI behaviour and its impact on a user's performance were discussed in Chapter 5. A GR framework was presented as a channel quality estimation technique able to predict the CQI behaviour as an approximation of the SINR. Such method has shown itself to work quite well and possess the great advantages of being extremely flexible and requiring no a-priori choice of its parameters, except for the nature of the covariance function.

By using the GPR, it was possible to predict, with very good accuracy, the channel behaviour of users moving with low and average urban speeds of 5 and 10 km/h. The channel of users moving at 60 km/h was also estimated albeit with less preciseness.

A new dual control framework with active learning was also designed and implemented. Such method allowed the base station to tailor the CSI prediction window of each user based on the packet loss generated by erroneous estimation. In this way, the eNB could use very long prediction windows for users with extremely good channel conditions and, conversely, restrict the prediction if a user experiences poor channel or has very strict throughput requirements.

The solution is, in fact, able to limit the CSI information to only 40%, of the amount required by SoA if a proportional fair scheduler is used, and to about 6% of the respective SoA amount if Best CQI scheduling is employed.

6.1.2 Final conclusions

As it was discussed on the previous sections, only a relatively small part of the RRM was addressed in this work. The problems of inter-cell coordination

and overhead reduction are indeed very relevant but certainly not exhaustive. The results achieved show that it is possible to reach a very good operating point in a heterogeneous network and that overheads may be reduced without loss in performance, even with gains if transmission settings are tailored to the network's conditions. The choice of these two particular problems was dictated by the principle that future cellular networks will have to provide extremely high datarates for a very large set of devices [**?**]; extensive analysis in the industry has brought to the realisation that, of all the possible evolutions in technology, the biggest advantages will come from the increase in available spectrum, the densification of the networks and the introduction of small, low-power cells [152–154]. The topics here discussed are, then, particularly interesting seen the directions the community is taking. However, all these advancements do come at a cost. The increase of spectral bands will bring the development of more complex transceivers and the network densification comes at the great cost of risking to saturate the empty spaces by creating an interference ridden network [155], which in turn will force the design of interference aware mobile devices. There is thus no low hanging fruit available in the cellular network and trade-offs will have to be studied and manufactured.

Nonetheless, the results here achieved represent a good starting point for the study and, particularly, the development of future networks. The methods here conceived allow to be build upon as a the basis for future network design strategies.

6.2 Future Work

The RRM in modern, high throughput, low latency networks such as LTE-A is becoming an increasing limiting factor in high capacity, dense networks. This is particularly true today as the networks, with the tendency to move towards 5G become more complex and massive. The resource allocation, interference coordination and signalling overhead management problems tackled in this work are certainly not exhaustive in delivering a comprehensive solution. In the following two sections, future works based on this dissertation of this work are going to be discussed. The first section describes possible extensions of this work within the same scope of interests, while, in the second section, a broader analysis of the RRM beyond LTE-A is provided.

6.2.1 RRM: alternative views and other solutions

It would be very interesting, in the future, to analyse the RRM at every layer, from the physical to the application, and try to find a framework able to optimise a cellular network with information pertaining to all the layers. This idea, normally known as **cross-layer optimisation**, allows information to seep through between the, normally opaque, layers and to perform partial analysis of such data in order to optimise the performance at higher layers. This is no easy task as it is extremely difficult to determine which processes might benefit by this additional processing and where the trade-off might lay. The first step would then be to perform an extensive research on which information might be passed from a layer to the next and what impact it might have, machine learning tools, such as simulated annealing, could perform this task well.

On a more specific task, it could certainly be very interesting to extend the findings in this dissertation to a MIMO network. Both the ICIC and feedback overhead reduction have been performed in a SISO network. Although, in principle, the behaviour should remain largely the same, the presence of multiple streams increases the degrees of freedom and allows for extensions of this work in unexplored directions. Furthermore, the increase in antennas would also increase the amount of feedback required thus pushing the trade-off discussed in this work to an even more favourable point.

Another direct step from the results of this work would be to study and implement more learning techniques to the RRM problem. Such methods would allow, first, a direct comparison with the ones developed in this work and, secondly, could lead to a better understanding of complex network dynamics.

6.2.2 Beyond LTE-A: designing 5G

If attention is paid to the direction in which future networks seem to be going, another interesting extension of this work, especially in the context of cognitive radios, would be to implement machine to machine communication (M2M). M2M allows users to communicate directly with one another, in a peer to peer fashion, under a large umbrella transmission technology such as LTE. The objective of the mobile radio would then be communicate by causing the least interference possible to the nearby users connected to a base station. Conversely, a base station should be able to detect such radios, monitor their behaviour and schedule resources in a way that maximises overall performance.

Another very pressing point, given the tendency to move towards network densification, would be to build interference aware transceivers. This would

require the design of completely new PHY interfaces and communication protocols that do not treat interference as noise, but are able to either exploit it or cancel it completely [156].

The two more direct PHY changes being studied for future network include millimetre wave propagation and massive-MIMO. The former makes use of extremely high carrier frequencies (in the order of tens of GHz) to deliver very high throughputs. They can be extremely effective in a range optimal for urban small cells (such as 20 - 30 m) but require the design of new, efficient and steerable antennae and, more importantly, necessitate of good statistical propagation models for urban environments [157]. Massive-MIMO, instead, represents a new transmission technology in which a very large number of antennae is used to deliver an extremely directed beam towards a user. This allows for a very high gain at the receiver and for an uncomplicated transmitter thanks to the large antenna array [158]. On the other hand, massive-MIMO still requires intensive study of the practical implementation of thousands of antennae in a single array and of the compatibility of such technology in the context of a cellular network.

Generally speaking, it would very interesting to further study how machine learning and artificial intelligence techniques could be applied to a 5G cellular network in order to allow true self-organization capabilities. The true intelligent network should be able to recognize its local and global states and steer itself to an optimal operating point without the necessity of external input. Furthermore, the ideal self-managed network should be able to reach global optima by having only local information and assess or infer how this influences the whole network. If these are the properties of the ideal network, the reality of things is definitely a long way from this view. Nonetheless, the application of machine learning techniques could bridge the gap and, finally, bring the community to develop a network which is distributed, self-configuring, self-healing, not saturated with redundant data, energy efficient and, hopefully, accessible and fair.

Bibliography

[1] 3GPP TSG-RAN, "3GPP TR 36.300, Evolved Universal Terrestrial Radio Access (E-UTRA) and Evolved Universal Terrestrial Radio Access (E-UTRAN); Overall description;," April 2008.

[2] "Concepts of Orthogonal Frequency Division Multiplexing (OFDM) and 802.11 WLAN," http://rfmw.em.keysight.com/wireless/helpfiles/89600B/webhelp/subsystems/wlan-ofdm/Content/ofdm_basicprinciplesoverview.htm.

[3] Gabor Fodor, "Radio resource management for ofdm systems and long term evolution (lte)," Presentation by Ericsson at KTH.

[4] M. Rahman, H. Yanikomeroglu, and W. Wong, "Interference avoidance with dynamic inter-cell coordination for downlink lte system," in *Wireless Communications and Networking Conference, 2009. WCNC 2009. IEEE*, April 2009, pp. 1–6.

[5] 3GPP TSG-RAN, "3GPP TR 36.814, Evolved Universal Terrestrial Radio Access (E-UTRA); Further advancements for E-UTRA physical layer aspects," March 2010.

[6] E. Hossain, M. Rasti, H. Tabassum, and A. Abdelnasser, "Evolution toward 5g multi-tier cellular wireless networks: An interference management perspective," *Wireless Communications, IEEE*, vol. 21, no. 3, pp. 118–127, June 2014.

[7] H.-S. Jo, Y. J. Sang, P. Xia, and J. Andrews, "Heterogeneous cellular networks with flexible cell association: A comprehensive downlink sinr analysis," *Wireless Communications, IEEE Transactions on*, vol. 11, no. 10, pp. 3484–3495, October 2012.

[8] C. Kosta, B. Hunt, A. Quddus, and R. Tafazolli, "On interference avoidance through inter-cell interference coordination (icic) based on

ofdma mobile systems," *Communications Surveys Tutorials, IEEE*, vol. 15, no. 3, pp. 973–995, Third 2013.

[9] J. Fan, Q. Yin, G. Li, B. Peng, and X. Zhu, "Adaptive block-level resource allocation in ofdma networks," *Wireless Communications, IEEE Transactions on*, vol. 10, no. 11, pp. 3966–3972, November 2011.

[10] S. Tran and A. Eltawil, "Optimized scheduling algorithm for lte downlink system," in *Wireless Communications and Networking Conference (WCNC), 2012 IEEE*, April 2012, pp. 1462–1466.

[11] P. Kyösti, J. Meinilä, L. Hentilä, X. Zhao, T. Jämsä, C. Schneider, M. Narandzić, M. Milojević, A. Hong, J. Ylitalo, V.-M. Holappa, M. Alatossava, R. Bultitude, Y. de Jong, and T. Rautiainen, "WINNER II Channel Models," EC FP6, Tech. Rep., Sep. 2007. [Online]. Available: http://www.ist-winner.org/deliverables.html

[12] G. Auer, V. Giannini, C. Desset, I. Godor, P. Skillermark, M. Olsson, M. Imran, D. Sabella, M. Gonzalez, O. Blume, and A. Fehske, "How much energy is needed to run a wireless network?" *Wireless Communications, IEEE*, vol. 18, no. 5, pp. 40–49, October 2011.

[13] A. Chiumento, S. Pollin, C. Desset, L. Van der Perre, and R. Lauwereins, "Analysis of power efficiency of schedulers in LTE," in *Communications and Vehicular Technology in the Benelux (SCVT), 2012 IEEE 19th Symposium on*, Nov 2012, pp. 1–4.

[14] ——, "Exploiting transport-block constraints in lte improves downlink performance," in *Wireless Communications and Networking Conference (WCNC), 2014 IEEE*, April 2014, pp. 1398–1402.

[15] H. W. Kuhn, "The hungarian method for the assignment problem," *WNaval Research Logistics Quarterly*, vol. 2, pp. 83 –97, 1955.

[16] A. Chiumento, S. Pollin, C. Desset, L. Van der Perre, and R. Lauwereins, "Scalable lte interference mitigation solution for hetnet deployment," in *Wireless Communications and Networking Conference Workshops (WCNCW), 2014 IEEE*, April 2014, pp. 46–51.

[17] ——, "Scalable hetnet interference management and the impact of limited channel state information," *EURASIP Journal on Wireless Communications and Networking*, vol. 2015, no. 1, p. 74, 2015.

[18] A. Chiumento, L. Hollevoet, S. Pollin, F. Naessens, A. Dejonghe, and L. Van der Perre, "Diffs: A low power, multi-mode, multi-standard flexible digital front-end for sensing in future cognitive radios," *Journal*

of Signal Processing Systems, vol. 76, no. 2, pp. 109–120, 2014. [Online]. Available: http://dx.doi.org/10.1007/s11265-014-0908-x

[19] R. S. Sutton and A. G. Barto, *Introduction to Reinforcement Learning*, 1st ed. Cambridge, MA, USA: MIT Press, 1998.

[20] A. Chiumento, C. Desset, S. Pollin, L. Van der Perre, and R. Lauwereins, "The value of feedback for lte resource allocation," in *Wireless Communications and Networking Conference (WCNC), 2014 IEEE*, April 2014.

[21] A. Chiumento, S. Pollin, C. Desset, L. Van der Perre, and R. Lauwereins, ""Impact of CSI Feedback Strategies on LTE Downlink and Reinforcement Learning Solutions for Optimal Allocation," *Accepted for publication in Vehicular Technology, IEEE Transactions on*, 2015.

[22] T. Alpcan, "Dual control with active learning using gaussian process regression," *CoRR*, pp. –1–1, 2011.

[23] A. Chiumento, M. Bennis, C. Desset, A. Bourdoux, L. Van der Perre, and S. Pollin, "Gaussian process regression for csi and feedback estimation in lte," in *Communication Workshop (ICCW), 2015 IEEE International Conference on*, June 2015, pp. 1440–1445.

[24] A. Chiumento, M. Bennis, C. Desset, L. Van der Perre, and S. Pollin, "Adaptive CSI and Feedback Estimation in LTE and beyond: A Gaussian process regression approach," *submitted to EURASIP Journal on Wireless Communications and Networking*, vol. 2015, no. 1, p. 74, 2015.

[25] Alcatel-Lucent, "Alcatel-lucent evolved packet core solution: Delivering technical innovation for the new lte mobile core," Technology White Paper. [Online]. Available: http://lte.alcatel-lucent.com/locale/en_us/downloads/wp_mobile_core_technical_innovation.pdf

[26] L. Cimini, "Analysis and simulation of a digital mobile channel using orthogonal frequency division multiplexing," *Communications, IEEE Transactions on*, vol. 33, no. 7, pp. 665–675, Jul 1985.

[27] H. Holma and A. Toskala, *OFDMA and SC-FDMA Based Radio Access*. John Wiley & Sons, Ltd, 2009, pp. 1–11. [Online]. Available: http://dx.doi.org/10.1002/9780470745489.ch1

[28] D. Astely, E. Dahlman, A. Furuskar, Y. Jading, M. Lindstrom, and S. Parkvall, "Lte: the evolution of mobile broadband," *Communications Magazine, IEEE*, vol. 47, no. 4, pp. 44–51, April 2009.

[29] C. Mehlfuhrer, M. Wrulich, J. C. Ikuno, and D. Bosanska, "SIMULATING THE LONG TERM EVOLUTION PHYSICAL LAYER," *17th European Signal Processing Conference (EUSIPCO 2009)*, 2009.

[30] C. Xiong, G. Li, S. Zhang, Y. Chen, and S. Xu, "Csi feedback reduction for energy-efficient downlink ofdma," in *Wireless Communications and Networking Conference (WCNC), 2012 IEEE*, April 2012, pp. 1135–1139.

[31] 3GPP TSG-RAN, "3GPP TR 36.213, Physical Layer Procedures for Evolved UTRA (Release 10)," July 2012.

[32] S. Sesia, I. Toufik, and M. Baker, *LTE - the UMTS long term evolution : from theory to practice*. Chichester: Wiley, 2009.

[33] 3GPP TSG-RAN, "3GPP TR 36.300, Evolved Universal Terrestrial Radio Access (E-UTRA); physical channels and modulation;," January 2011.

[34] A. Ghosh, R. Ratasuk, B. Mondal, N. Mangalvedhe, and T. Thomas, "Lte-advanced: next-generation wireless broadband technology [invited paper]," *Wireless Communications, IEEE*, vol. 17, no. 3, pp. 10–22, June 2010.

[35] A. Damnjanovic, J. Montojo, Y. Wei, T. Ji, T. Luo, M. Vajapeyam, T. Yoo, O. Song, and D. Malladi, "A survey on 3gpp heterogeneous networks," *Wireless Communications, IEEE*, vol. 18, no. 3, pp. 10–21, June 2011.

[36] H. Mahmoud and I. Guvenc, "A comparative study of different deployment modes for femtocell networks," in *Personal, Indoor and Mobile Radio Communications, 2009 IEEE 20th International Symposium on*, Sept 2009, pp. 1–5.

[37] C. B. Networks, "Backhauling x2," Technology White Paper. [Online]. Available: http://cbnl.com/sites/all/files/userfiles/files/Backhauling-X2.pdf

[38] B. Soret and K. Pedersen, "Centralized and distributed solutions for fast muting adaptation in lte-advanced hetnets," *Vehicular Technology, IEEE Transactions on*, vol. 64, no. 1, pp. 147–158, Jan 2015.

[39] D. Lopez-Perez, A. Valcarce, G. de la Roche, and J. Zhang, "Ofdma femtocells: A roadmap on interference avoidance," *Communications Magazine, IEEE*, vol. 47, no. 9, pp. 41–48, September 2009.

[40] D. Lopez-Perez, I. Guvenc, G. de la Roche, M. Kountouris, T. Quek, and J. Zhang, "Enhanced intercell interference coordination challenges in

heterogeneous networks," *Wireless Communications, IEEE*, vol. 18, no. 3, pp. 22–30, June 2011.

[41] A. Ghosh, N. Mangalvedhe, R. Ratasuk, B. Mondal, M. Cudak, E. Visotsky, T. Thomas, J. Andrews, P. Xia, H. Jo, H. Dhillon, and T. Novlan, "Heterogeneous cellular networks: From theory to practice," *Communications Magazine, IEEE*, vol. 50, no. 6, pp. 54–64, June 2012.

[42] F. R. P. Cavalcanti and S. Andersson, *Optimizing Wireless Communication Systems*. SPRINGER, 2009.

[43] L. Tassiulas and S. Sarkar, "Maxmin fair scheduling in wireless networks," in *INFOCOM 2002. Twenty-First Annual Joint Conference of the IEEE Computer and Communications Societies. Proceedings. IEEE*, vol. 2, 2002, pp. 763 – 772 vol.2.

[44] G. Horvath and C. Vulkan, "Throughput analysis of the proportional fair scheduler in hsdpa," in *Wireless Conference, 2008. EW 2008. 14th European*, june 2008, pp. 1 –6.

[45] J. Ikuno, M. Wrulich, and M. Rupp, "System Level Simulation of Lte Networks," in *Vehicular Technology Conference (VTC 2010-Spring), 2010 IEEE 71st*, may 2010, pp. 1 –5.

[46] M. Rahman and H. Yanikomeroglu, "Enhancing cell-edge performance: a downlink dynamic interference avoidance scheme with inter-cell coordination," *Wireless Communications, IEEE Transactions on*, vol. 9, no. 4, pp. 1414 –1425, April 2010.

[47] R. Jain, D. Chiu, and W. Hawe, "A quantitative measure of fairness and discrimination for resource allocation in shared computer systems," *DEC Research Report TR-301*, 1984.

[48] D. Sabella, M. Caretti, and R. Fantini, "Energy efficiency evaluation of state of the art packet scheduling algorithms for lte," *Wireless Conference 2011 - Sustainable Wireless Technologies (European Wireless), 11th European*, pp. 1 –4, april 2011.

[49] 3GPP TSG-RAN, "3GPP TS 36.213, Physical Layer Procedures (Release 9)," June 2010.

[50] S. Donthi and N. Mehta, "An accurate model for eesm and its application to analysis of cqi feedback schemes and scheduling in lte," *Wireless Communications, IEEE Transactions on*, vol. 10, no. 10, pp. 3436–3448, October 2011.

[51] E. Dahlman, S. Parkvall, and J. Sköld, in *4G: LTE/LTE-Advanced for Mobile Broadband (Second Edition)*, second edition ed., E. D. P. Sköld, Ed. Oxford: Academic Press, 2014, pp. 1 – 15. [Online]. Available: http://www.sciencedirect.com/science/article/pii/B9780124199859000015

[52] R. Bosisio and U. Spagnolini, "Interference coordination vs. interference randomization in multicell 3gpp lte system," in *Wireless Communications and Networking Conference, 2008. WCNC 2008. IEEE*, March 2008, pp. 824–829.

[53] G. Boudreau, J. Panicker, N. Guo, R. Chang, N. Wang, and S. Vrzic, "Interference coordination and cancellation for 4g networks," *Communications Magazine, IEEE*, vol. 47, no. 4, pp. 74–81, April 2009.

[54] N. Himayat, S. Talwar, A. Rao, and R. Soni, "Interference management for 4g cellular standards [wimax/lte update]," *Communications Magazine, IEEE*, vol. 48, no. 8, pp. 86–92, August 2010.

[55] T. Novlan, R. Ganti, A. Ghosh, and J. Andrews, "Analytical evaluation of fractional frequency reuse for ofdma cellular networks," *Wireless Communications, IEEE Transactions on*, vol. 10, no. 12, pp. 4294–4305, December 2011.

[56] D. Bilios, C. Bouras, V. Kokkinos, A. Papazois, and G. Tseliou, "A performance study of fractional frequency reuse in ofdma networks," in *Wireless and Mobile Networking Conference (WMNC), 2012 5th Joint IFIP*, Sept 2012, pp. 38–43.

[57] I. Stiakogiannakis, G. Athanasiadou, G. Tsoulos, and D. Kaklamani, "Performance analysis of fractional frequency reuse for multi-cell wimax networks based on site-specific propagation modeling [wireless corner]," *Antennas and Propagation Magazine, IEEE*, vol. 54, no. 1, pp. 214–226, Feb 2012.

[58] R. Chang, Z. Tao, J. Zhang, and C.-C. Kuo, "A graph approach to dynamic fractional frequency reuse (ffr) in multi-cell ofdma networks," in *Communications, 2009. ICC '09. IEEE International Conference on*, June 2009, pp. 1–6.

[59] G. Fodor, C. Koutsimanis, A. Rácz, N. Reider, A. Simonsson, and W. Müller, "Intercell interference coordination in ofdma networks and in the 3gpp long term evolution system," *Journal of Communications*, vol. 4, no. 7, 2009.

[60] M. Rahman and H. Yanikomeroglu, "Enhancing cell-edge performance: a downlink dynamic interference avoidance scheme with inter-cell

coordination," *Wireless Communications, IEEE Transactions on*, vol. 9, no. 4, pp. 1414–1425, April 2010.

[61] D. González G, M. García-Lozano, S. Ruiz, and J. Olmos, "On the performance of static inter-cell interference coordination in realistic cellular layouts," in *Mobile Networks and Management*, ser. Lecture Notes of the Institute for Computer Sciences, Social Informatics and Telecommunications Engineering, K. Pentikousis, R. Agüero, M. García-Arranz, and S. Papavassiliou, Eds. Springer Berlin Heidelberg, 2011, vol. 68, pp. 163–176. [Online]. Available: http://dx.doi.org/10.1007/978-3-642-21444-8_15

[62] G. Koudouridis and C. Qvarfordt, "Exploration of capacity gains by inter-cell interference coordination based on user distribution," in *Communications Workshops (ICC), 2013 IEEE International Conference on*, June 2013, pp. 1078–1083.

[63] T. Quek, Z. Lei, and S. Sun, "Adaptive interference coordination in multi-cell ofdma systems," in *Personal, Indoor and Mobile Radio Communications, 2009 IEEE 20th International Symposium on*, Sept 2009, pp. 2380–2384.

[64] S. Das, H. Viswanathan, and G. Rittenhouse, "Dynamic load balancing through coordinated scheduling in packet data systems," in *INFOCOM 2003. Twenty-Second Annual Joint Conference of the IEEE Computer and Communications. IEEE Societies*, vol. 1, March 2003, pp. 786–796 vol.1.

[65] A. Gjendemsjo, D. Gesbert, G. Oien, and S. Kiani, "Optimal power allocation and scheduling for two-cell capacity maximization," in *Modeling and Optimization in Mobile, Ad Hoc and Wireless Networks, 2006 4th International Symposium on*, April 2006, pp. 1–6.

[66] R. Chang, Z. Tao, J. Zhang, and C.-C. Kuo, "Multicell ofdma downlink resource allocation using a graphic framework," *Vehicular Technology, IEEE Transactions on*, vol. 58, no. 7, pp. 3494–3507, Sept 2009.

[67] Y.-J. Chang, Z. Tao, J. Zhang, and C.-C. Kuo, "A graph-based approach to multi-cell ofdma downlink resource allocation," in *Global Telecommunications Conference, 2008. IEEE GLOBECOM 2008. IEEE*, Nov 2008, pp. 1–6.

[68] M. Necker, "A graph-based scheme for distributed interference coordination in cellular ofdma networks," in *Vehicular Technology Conference, 2008. VTC Spring 2008. IEEE*, May 2008, pp. 713–718.

[69] A. Hamza, S. Khalifa, H. Hamza, and K. Elsayed, "A survey on inter-cell interference coordination techniques in ofdma-based cellular networks," *Communications Surveys Tutorials, IEEE*, vol. 15, no. 4, pp. 1642–1670, Fourth 2013.

[70] G. Nardini, G. Stea, A. Virdis, M. Caretti, and D. Sabella, "Improving network performance via optimization-based centralized coordination of lte-a cells," in *Wireless Communications and Networking Conference Workshops (WCNCW), 2014 IEEE*, April 2014, pp. 18–22.

[71] S. Cicalo, V. Tralli, and A. Perez-Neira, "Centralized vs distributed resource allocation in multi-cell ofdma systems," in *Vehicular Technology Conference (VTC Spring), 2011 IEEE 73rd*, May 2011, pp. 1–6.

[72] I. Fraimis, V. Papoutsis, and S. Kotsopoulos, "A Decentralized Subchannel Allocation Scheme with Inter-Cell Interference Coordination (ICIC) for Multi-Cell OFDMA Systems," in *Global Telecommunications Conference (GLOBECOM 2010), 2010 IEEE*, Dec. 2010, pp. 1 –5.

[73] D. Kimura, Y. Harada, and H. Seki, "De-centralized dynamic icic using x2 interfaces for downlink lte systems," in *Vehicular Technology Conference (VTC Spring), 2011 IEEE 73rd*, May 2011, pp. 1–5.

[74] M. Qian, W. Hardjawana, Y. Li, B. Vucetic, J. Shi, and X. Yang, "Inter-cell interference coordination through adaptive soft frequency reuse in lte networks," in *Wireless Communications and Networking Conference (WCNC), 2012 IEEE*, April 2012, pp. 1618–1623.

[75] W. Huang, Y. Tang, and Z. Tu, "A novel intercell interference coordination algorithm based on x2 interface for lte system," in *Anti-Counterfeiting, Security and Identification (ASID), 2013 IEEE International Conference on*, Oct 2013, pp. 1–4.

[76] R. Combes, Z. Altman, M. Haddad, and E. Altman, "Self-optimizing strategies for interference coordination in ofdma networks," in *Communications Workshops (ICC), 2011 IEEE International Conference on*, June 2011, pp. 1–5.

[77] D. Ogata, A. Nagate, and T. Fujii, "Multi-bs cooperative interference control for lte systems," in *Vehicular Technology Conference (VTC Spring), 2012 IEEE 75th*, May 2012, pp. 1–5.

[78] A. Gopalan, C. Caramanis, and S. Shakkottai, "On the value of coordination and delayed queue information in multicellular scheduling," *Automatic Control, IEEE Transactions on*, vol. 58, no. 6, pp. 1443–1456, June 2013.

[79] A. Stolyar and H. Viswanathan, "Self-organizing dynamic fractional frequency reuse for best-effort traffic through distributed inter-cell coordination," in *IEEE INFOCOM 2009*, April 2009, pp. 1287–1295.

[80] S. Ko, H. Seo, H. Kwon, and B. G. Lee, "Distributed power allocation for efficient inter-cell interference management in multi-cell ofdma systems," in *Communications (APCC), 2010 16th Asia-Pacific Conference on*, Oct 2010, pp. 243–248.

[81] A. Feki and V. Capdevielle, "Autonomous resource allocation for dense lte networks: A multi armed bandit formulation," in *Personal Indoor and Mobile Radio Communications (PIMRC), 2011 IEEE 22nd International Symposium on*, Sept 2011, pp. 66–70.

[82] A. Al-Zahrani and F. Yu, "A game theory approach for inter-cell interference management in ofdm networks," in *Communications (ICC), 2011 IEEE International Conference on*, June 2011, pp. 1–5.

[83] L. Liang and G. Feng, "A game-theoretic framework for interference coordination in ofdma relay networks," *Vehicular Technology, IEEE Transactions on*, vol. 61, no. 1, pp. 321–332, Jan 2012.

[84] S. Khalifa, H. Hamza, and K. Elsayed, "Self-adaptive inter-cell interference coordination scheme for lte systems," in *Personal Indoor and Mobile Radio Communications (PIMRC), 2013 IEEE 24th International Symposium on*, Sept 2013, pp. 1779–1783.

[85] A. Adouane, L. Rodier, K. Khawam, J. Cohen, and S. Tohme, "Game theoretic framework for inter-cell interference coordination," in *Wireless Communications and Networking Conference (WCNC), 2014 IEEE*, April 2014, pp. 57–62.

[86] H. Hamza, S. Khalifa, and K. Elsayed, "Autonomous schemes for inter-cell interference coordination in the downlink of lte systems," *International Journal of Wireless Information Networks*, vol. 21, no. 3, pp. 181–195, 2014. [Online]. Available: http://dx.doi.org/10.1007/s10776-014-0243-y

[87] O. Fratu, A. Vulpe, R. Craciunescu, and S. Halunga, "Small cells in cellular networks: Challenges of future hetnets," *Wireless Personal Communications*, vol. 78, no. 3, pp. 1613–1627, 2014. [Online]. Available: http://dx.doi.org/10.1007/s11277-014-1906-9

[88] N. Saquib, E. Hossain, L. B. Le, and D. I. Kim, "Interference management in ofdma femtocell networks: issues and approaches," *Wireless Communications, IEEE*, vol. 19, no. 3, pp. 86–95, June 2012.

[89] X. Zhou, S. Feng, Y. Ding, Y. Liu, Y. Wang, and Y. Zhang, "Game-theoretical frequency reuse method for complex cognitive femto-cell network," in *Communications and Networking in China (CHINACOM), 2013 8th International ICST Conference on*, Aug 2013, pp. 318–322.

[90] S. Guruacharya, D. Niyato, D. I. Kim, and E. Hossain, "Hierarchical competition for downlink power allocation in ofdma femtocell networks," *Wireless Communications, IEEE Transactions on*, vol. 12, no. 4, pp. 1543–1553, April 2013.

[91] H. N. Vu and L. B. Le, "Distributed resource allocation for ofdma femtocell networks with macrocell protection," in *Wireless Communications and Networking Conference (WCNC), 2013 IEEE*, April 2013, pp. 440–445.

[92] X. Chen, H. Zhang, T. Chen, and J. Palicot, "Combined learning for resource allocation in autonomous heterogeneous cellular networks," in *Personal Indoor and Mobile Radio Communications (PIMRC), 2013 IEEE 24th International Symposium on*, Sept 2013, pp. 1061–1065.

[93] S. Shen and T. Lok, "Dynamic power allocation for downlink interference management in a two-tier ofdma network," *Vehicular Technology, IEEE Transactions on*, vol. 62, no. 8, pp. 4120–4125, Oct 2013.

[94] A. Adhikary, V. Ntranos, and G. Caire, "Cognitive femtocells: Breaking the spatial reuse barrier of cellular systems," in *Information Theory and Applications Workshop (ITA), 2011*, Feb 2011, pp. 1–10.

[95] L. Huang, G. Zhu, and X. Du, "Cognitive femtocell networks: an opportunistic spectrum access for future indoor wireless coverage," *Wireless Communications, IEEE*, vol. 20, no. 2, pp. 44–51, April 2013.

[96] H. Chamkhia, M. Hasna, and R. Bouallegue, "Capacity enhancement in cognitive radio wireless network with dynamic spectrum access," in *Information and Communication Technology Convergence (ICTC), 2014 International Conference on*, Oct 2014, pp. 99–104.

[97] T. Luan, F. Gao, Z. Yang, J. Li, and M. Lei, "Resource allocation and transmission optimization for mimo cognitive femtocells," in *Communications (ICC), 2014 IEEE International Conference on*, June 2014, pp. 4354–4359.

[98] C.-H. Lee and C.-Y. Shih, "Coverage analysis of cognitive femtocell networks," *Wireless Communications Letters, IEEE*, vol. 3, no. 2, pp. 177–180, April 2014.

[99] S. Sun, M. Kadoch, and T. Ran, "Adaptive son and cognitive smart lpn for 5g heterogeneous networks," *Mobile Networks and Applications*, pp. 1–11, 2015. [Online]. Available: http://dx.doi.org/10.1007/s11036-014-0563-2

[100] D. Love, R. Heath, V. Lau, D. Gesbert, B. Rao, and M. Andrews, "An overview of limited feedback in wireless communication systems," *Selected Areas in Communications, IEEE Journal on*, vol. 26, no. 8, pp. 1341–1365, October 2008.

[101] J. Chen, R. Berry, and M. Honig, "Limited feedback schemes for downlink ofdma based on sub-channel groups," *Selected Areas in Communications, IEEE Journal on*, vol. 26, no. 8, pp. 1451–1461, October 2008.

[102] S. Stefanatos and N. Dimitriou, "Downlink ofdma resource allocation under partial channel state information," in *Communications, 2009. ICC '09. IEEE International Conference on*, June 2009, pp. 1–5.

[103] M. George and R. Koilpillai, "Fairness-based resource allocation in ofdma downlink with imperfect csit," in *Wireless Communications Signal Processing (WCSP), 2013 International Conference on*, Oct 2013, pp. 1–6.

[104] S. Guharoy and N. Mehta, "Joint evaluation of channel feedback schemes, rate adaptation, and scheduling in ofdma downlinks with feedback delays," *Vehicular Technology, IEEE Transactions on*, vol. 62, no. 4, May 2013.

[105] R. Patachaianand and K. Sandrasegaran, "Link adaptation with multiple feedback thresholds," in *Personal Indoor and Mobile Radio Communications (PIMRC), 2012 IEEE 23rd International Symposium on*, Sept 2012, pp. 496–501.

[106] S. Sanayei and A. Nosratinia, "Opportunistic downlink transmission with limited feedback," *Information Theory, IEEE Transactions on*, vol. 53, no. 11, pp. 4363–4372, Nov 2007.

[107] Y. Xue and T. Kaiser, "Exploiting multiuser diversity with imperfect one-bit channel state feedback," *Vehicular Technology, IEEE Transactions on*, vol. 56, no. 1, pp. 183–193, Jan 2007.

[108] H. Alyazidi and I. Kostanic, "Ofdma feedback optimization in 4g-lte systems," in *Computer Aided Modeling and Design of Communication Links and Networks (CAMAD), 2012 IEEE 17th International Workshop on*, Sept 2012, pp. 70–74.

[109] S. Donthi and N. Mehta, "Performance analysis of subband-level channel quality indicator feedback scheme of lte," pp. 1–5, Jan 2010.

[110] S. Ananya and N. Mehta, "Performance of ofdm systems with best-m feedback, scheduling, and delays for uniformly correlated subchannels," *Wireless Communications, IEEE Transactions on*, vol. PP, no. 99, pp. 1–1, 2014.

[111] Y. Huang and B. D. Rao, "Performance analysis of heterogeneous feedback design in an ofdma downlink with partial and imperfect feedback." *IEEE Transactions on Signal Processing*, vol. 61, no. 4, pp. 1033–1046, 2013.

[112] M. Diallo, M. Helard, and L. Cariou, "A limited and efficient quantized feedback for ieee 802.11n evolution," in *Telecommunications (ICT), 2013 20th International Conference on*, May 2013, pp. 1–5.

[113] I. Wong and B. Evans, "Optimal resource allocation in the ofdma downlink with imperfect channel knowledge," *Communications, IEEE Transactions on*, vol. 57, no. 1, pp. 232–241, January 2009.

[114] Y. Hu and A. Ribeiro, "Optimal wireless communications with imperfect channel state information," *Signal Processing, IEEE Transactions on*, vol. 61, no. 11, pp. 2751–2766, June 2013.

[115] Y. Sun, C. Koksal, K.-H. Kim, and N. Shroff, "Scheduling of multicast and unicast services under limited feedback by using rateless codes," in *INFOCOM, 2014 Proceedings IEEE*, April 2014, pp. 1671–1679.

[116] X. Hou and C. Yang, "How much feedback overhead is required for base station cooperative transmission to outperform non-cooperative transmission?" in *Acoustics, Speech and Signal Processing (ICASSP), 2011 IEEE International Conference on*, May 2011, pp. 3416–3419.

[117] S. Kim, D. Kim, and Y. Lee, "Limited channel feedback for coordinated beamforming under sinr requirements," in *Communications Workshops (ICC), 2013 IEEE International Conference on*, June 2013, pp. 431–435.

[118] Y. He and S. Dey, "Power allocation in spectrum sharing cognitive radio networks with quantized channel information," *Communications, IEEE Transactions on*, vol. 59, no. 6, pp. 1644–1656, June 2011.

[119] S. Akoum and R. Heath, "Interference coordination: Random clustering and adaptive limited feedback," *Signal Processing, IEEE Transactions on*, vol. 61, no. 7, pp. 1822–1834, April 2013.

[120] M. Goldenbaum, R. Akl, S. Valentin, and S. Stanczak, "On the effect of feedback delay in the downlink of multiuser ofdm systems," in *Information Sciences and Systems (CISS), 2011 45th Annual Conference on*, March 2011, pp. 1–6.

[121] M. Maddah-Ali and D. Tse, "Completely stale transmitter channel state information is still very useful," *Information Theory, IEEE Transactions on*, vol. 58, no. 7, pp. 4418–4431, July 2012.

[122] R. Akl, S. Valentin, G. Wunder, and S. Stanczak, "Compensating for cqi aging by channel prediction: The lte downlink," in *Global Communications Conference (GLOBECOM), 2012 IEEE*, Dec 2012, pp. 4821–4827.

[123] M. Ni, X. Xu, and R. Mathar, "A channel feedback model with robust sinr prediction for lte systems," in *Antennas and Propagation (EuCAP), 2013 7th European Conference on*, April 2013, pp. 1866–1870.

[124] M. Awal and L. Boukhatem, "Dynamic cqi resource allocation for ofdma systems," in *Wireless Communications and Networking Conference (WCNC), 2011 IEEE*, March 2011, pp. 19–24.

[125] ——, "Opportunistic periodic feedback mechanisms for ofdma systems under feedback budget constraint," in *Vehicular Technology Conference (VTC Spring), 2011 IEEE 73rd*, May 2011, pp. 1–5.

[126] L. Sivridis and J. He, "A strategy to reduce the signaling requirements of cqi feedback schemes," *Wireless Personal Communications*, vol. 70, no. 1, pp. 85–98, 2013. [Online]. Available: http://dx.doi.org/10.1007/s11277-012-0680-9

[127] "LTE-Advanced: A Practical Systems Approach to Understanding 3GPP LTE Releases 10 and 11 Radio Access Technologies," S. Ahmadi, Ed. Academic Press, 2014, pp. i – iii. [Online]. Available: http://www.sciencedirect.com/science/article/pii/B9780124051621000162

[128] C. H. Papadimitriou and K. Steiglitz, *Combinatorial Optimization: Algorithms and Complexity*. Upper Saddle River, NJ, USA: Prentice-Hall, Inc., 1982.

[129] M. R. Garey and D. S. Johnson, *Computers and Intractability: A Guide to the Theory of NP-Completeness (Series of Books in the Mathematical Sciences)*. W. H. Freeman & Co Ltd, Jan. 1979.

[130] C. Buchheim, A. Caprara, and A. Lodi, "An effective branch-and-bound algorithm for convex quadratic integer programming," in *Integer Programming and Combinatorial Optimization*, ser. Lecture Notes in Computer Science, F. Eisenbrand and F. Shepherd, Eds. Springer Berlin Heidelberg, 2010, vol. 6080, pp. 285–298.

[131] J. Oksanen, J. Lunden, and V. Koivunen, "Resource minimization driven spectrum sensing policy," in *Acoustics, Speech and Signal Processing*

(ICASSP), 2012 IEEE International Conference on, March 2012, pp. 3657–3660.

[132] M. Bkassiny, S. Jayaweera, Y. Li, and K. Avery, "Optimal and low-complexity algorithms for dynamic spectrum access in centralized cognitive radio networks with fading channels," in *Vehicular Technology Conference (VTC Spring), 2011 IEEE 73rd*, May 2011, pp. 1–5.

[133] I. Comsa, M. Aydin, S. Zhang, P. Kuonen, and J. F. Wagen, "Reinforcement learning based radio resource scheduling in lte-advanced," in *Automation and Computing (ICAC), 2011 17th International Conference on*, Sept 2011, pp. 219–224.

[134] M. ul Islam and A. Mitschele-Thiel, "Reinforcement learning strategies for self-organized coverage and capacity optimization," in *Wireless Communications and Networking Conference (WCNC), 2012 IEEE*, April 2012, pp. 2818–2823.

[135] M. Simsek, M. Bennis, and A. Czylwik, "Dynamic inter-cell interference coordination in hetnets: A reinforcement learning approach," in *Global Communications Conference (GLOBECOM), 2012 IEEE*, Dec 2012, pp. 5446–5450.

[136] D. Kumar, N. Kanagaraj, and R. Srilakshmi, "Harmonized q-learning for radio resource management in lte based networks," in *ITU Kaleidoscope: Building Sustainable Communities (K-2013), 2013 Proceedings of*, April 2013, pp. 1–8.

[137] H. Wang and R. Song, "Distributed q-learning for interference mitigation in self-organised femtocell networks: Synchronous or asynchronous?" *Wireless Personal Communications*, vol. 71, no. 4, pp. 2491–2506, 2013. [Online]. Available: http://dx.doi.org/10.1007/s11277-012-0950-6

[138] C. J. C. H. Watkins, "Learning from delayed rewards," Ph.D. dissertation, King's College, Cambridge, UK, May 1989.

[139] S. Kapetanakis and D. Kudenko, "Improving on the reinforcement learning of coordination in cooperative multi-agent systems," 2002.

[140] A. L. Strehl, L. Li, E. Wiewiora, J. Langford, and M. L. Littman, "Pac model-free reinforcement learning," in *In: ICML-06: Proceedings of the 23rd international conference on Machine learning*, 2006, pp. 881–888.

[141] M. Jabbarihagh and F. Lahouti, "A decentralized approach to network coding based on learning," in *Information Theory for Wireless Networks, 2007 IEEE Information Theory Workshop on*, July 2007, pp. 1–5.

[142] A. Galindo-Serrano, L. Giupponi, and M. Majoral, "On implementation requirements and performances of Q-Learning for self-organized femtocells," in *GLOBECOM Workshops (GC Wkshps), 2011 IEEE*, Dec 2011, pp. 231–236.

[143] M. Wiering, *Reinforcement learning state-of-the-art*. Berlin New York: Springer, 2012.

[144] A. Galindo-Serrano and L. Giupponi, "Distributed Q-Learning for Aggregated Interference Control in Cognitive Radio Networks," *Vehicular Technology, IEEE Transactions on*, vol. 59, no. 4, pp. 1823–1834, May 2010.

[145] 3GPP TSG-RAN, "3GPP TS 36.413, Evolved Universal Terrestrial Radio Access Network (E-UTRAN); S1 Application Protocol (S1AP)," September 2014.

[146] M. Osborne and S. J. Roberts, "Gaussian processes for prediction," Department of Engineering Science, University of Oxford, Tech. Rep. PARG-07-01, 2007.

[147] C. E. Rasmussen and C. K. I. Williams, *Gaussian Processes for Machine Learning (Adaptive Computation and Machine Learning)*. Cambridge, Massachusetts: The MIT Press, 2005.

[148] S. M. L., *Statistical Interpolation of Spatial Data: Some Theory for Kriging*. New York: Springer, 1999.

[149] J. A. Hoeting, R. A. Davis, A. A. Merton, and S. E. Thompson, "Model selection for geostatistical models," *Ecological Applications*, vol. 16, no. 1, pp. 87–98, feb 2006. [Online]. Available: http://dx.doi.org/10.1890/04-0576

[150] F. Perez-Cruz and J. Murillo-Fuentes, "Gaussian processes for digital communications," in *Acoustics, Speech and Signal Processing, 2006. ICASSP 2006 Proceedings. 2006 IEEE International Conference on*, vol. 5, May 2006, pp. V–V.

[151] M. Rumney, Ed., *LTE and the Evolution to 4G Wireless: Design and Measurement Challenges*. Agilent Technologies: Wiley, 2013.

[152] QUALCOMM, "The 1000x Mobile Data Challenge: More Small Cells, More Spectrum, Higher Efficiency (white paper)," 2013.

[153] Nokia, "Enhance mobile networks to deliver 1,000 times more capacity by 2020 (white paper)," 2013.

[154] N. Bhushan, J. Li, D. Malladi, R. Gilmore, D. Brenner, A. Damnjanovic, R. Sukhavasi, C. Patel, and S. Geirhofer, "Network densification: the dominant theme for wireless evolution into 5g," *Communications Magazine, IEEE*, vol. 52, no. 2, pp. 82–89, February 2014.

[155] X. Zhang and J. Andrews, "Downlink cellular network analysis with multi-slope path loss models," *Communications, IEEE Transactions on*, vol. 63, no. 5, pp. 1881–1894, May 2015.

[156] F. Boccardi, R. Heath, A. Lozano, T. Marzetta, and P. Popovski, "Five disruptive technology directions for 5g," *Communications Magazine, IEEE*, vol. 52, no. 2, pp. 74–80, February 2014.

[157] T. Rappaport, S. Sun, R. Mayzus, H. Zhao, Y. Azar, K. Wang, G. Wong, J. Schulz, M. Samimi, and F. Gutierrez, "Millimeter wave mobile communications for 5g cellular: It will work!" *Access, IEEE*, vol. 1, pp. 335–349, 2013.

[158] E. Larsson, O. Edfors, F. Tufvesson, and T. Marzetta, "Massive mimo for next generation wireless systems," *Communications Magazine, IEEE*, vol. 52, no. 2, pp. 186–195, February 2014.

FACULTY OF ENGINEERING
DEPARTMENT OF ELECTRICAL ENGINEERING
ESAT
Kasteelpark Arenberg 10 Box 2440
B-3001 Leuven